AD_____

Award Number: DAMD17-99-1-9481

TITLE: Protein Kinase Pathways that Regulate Neuronal Survival and Death

PRINCIPAL INVESTIGATOR: Kim A. Heidenreich, Ph.D.

CONTRACTING ORGANIZATION: University of Colorado Health Sciences Center
Denver, Colorado 80291-0238

REPORT DATE: August 2002

TYPE OF REPORT: Annual

PREPARED FOR: U.S. Army Medical Research and Materiel Command
Fort Detrick, Maryland 21702-5012

DISTRIBUTION STATEMENT: Approved for Public Release;
Distribution Unlimited

REPORT DOCUMENTATION PAGE

Form Approved
OMB No. 074-0188

1. AGENCY USE ONLY (Leave blank)	2. REPORT DATE	3. REPORT TYPE AND DATES COVERED
	August 2002	Annual (1 Aug 01 - 31 Jul 02)

4. TITLE AND SUBTITLE
Protein Kinase Pathways that Regulate Neuronal Survival and Death

5. FUNDING NUMBERS
DAMD17-99-1-9481

6. AUTHOR(S)
Kim A. Heidenreich, Ph.D.

7. PERFORMING ORGANIZATION NAME(S) AND ADDRESS(ES)
University of Colorado Health Sciences Center
Denver, Colorado 80291-0238

kim.heidenreich@uchsc.edu

8. PERFORMING ORGANIZATION REPORT NUMBER

9. SPONSORING / MONITORING AGENCY NAME(S) AND ADDRESS(ES)
U.S. Army Medical Research and Materiel Command
Fort Detrick, Maryland 21702-5012

10. SPONSORING / MONITORING AGENCY REPORT NUMBER

11. SUPPLEMENTARY NOTES
report contains color

12a. DISTRIBUTION / AVAILABILITY STATEMENT
Approved for Public Release; Distribution Unlimited

12b. DISTRIBUTION CODE

13. Abstract ***(Maximum 200 Words)*** *(abstract should contain no proprietary or confidential information)*
Loss of post-mitotic neurons from the adult brain underlies the pathology of neurodegenerative diseases and neurotoxin exposure. Neuronal cell death occurs by two mechanisms: necrosis and apoptosis. Apoptosis is a process whereby developmental cues and environmental stimuli activate a genetic program to implement a series of steps that culminate in cell death. An important aspect of apoptosis is that it can be halted and such interventions may rescue dying neurons. The overall goal of this project is to identify key protein kinases involved in regulating neuronal survival and apoptosis. The aims for the this year of funding as described in the Statement of Work were to: 1) Continue studies on protein kinase cascades that regulate neuronal survival, 2) Modulate the protein kinase cascades regulated by neurotrophic factors and determine the consequence on neuronal survival and death, and 3) Begin studies examining the cross-talk in pro-apoptotic and anti-apoptotic protein kinase signaling cascades. The progress made in these areas has resulted in 4 published manuscripts (plus 2 submitted articles) and 9 abstracts presented at national and international scientific meetings in 2002.

14. SUBJECT TERMS
neurodegeneration, apoptosis, neurons, MEF2, IGF-I, lithium, death receptors, Bim, intrinsic death pathway

15. NUMBER OF PAGES
86

16. PRICE CODE

17. SECURITY CLASSIFICATION OF REPORT	18. SECURITY CLASSIFICATION OF THIS PAGE	19. SECURITY CLASSIFICATION OF ABSTRACT	20. LIMITATION OF ABSTRACT
Unclassified	Unclassified	Unclassified	Unlimited

Table of Contents

Introduction

Loss of post-mitotic neurons from the adult brain underlies the pathology of neurodegenerative diseases and neurotoxin exposure. Neuronal cell death occurs by two mechanisms: necrosis and apoptosis. Apoptosis is a process whereby developmental cues and environmental stimuli activate a genetic program to implement a series of steps that culminate in cell death. An important aspect of apoptosis is that it can be halted and such interventions may rescue dying neurons. The overall goal of this project is to identify key protein kinases involved in regulating neuronal survival and apoptosis. The aims for the this year of funding as described in the Statement of Work were to: 1) Continue studies on protein kinase cascades that regulate neuronal survival, 2) Modulate the protein kinase cascades regulated by neurotrophic factors and determine the consequence on neuronal survival and death, and 3) Begin studies examining the cross-talk in pro-apoptotic and anti-apoptotic protein kinase signaling cascades. The progress made in these areas, described below, has resulted in 4 published manuscripts (plus 2 submitted manuscripts) and 9 abstracts presented at national and international scientific meetings.

Task #1. The first task is to identify protein kinase cascades that regulate neuronal survival.

As described in our progress report last year, we identified MEF2 as a transcription factor downstream of a depolarization-dependent, calcium-regulated pathway that controls neuronal survival. These results were published in the Journal of Neuroscience last year. We have extended these studies during the current year by examining whether GSK-3β is the kinase regulating this pathway in dying neurons. To investigate a potential role for GSK-3β in MEF2D phosphorylation, we examined the effects of lithium, an uncompetitive inhibitor of GSK-3β, on MEF2D in granule neurons induced to undergo apoptosis. Lithium inhibited caspase-3 activation and DNA condensation and fragmentation induced by removal of depolarizing potassium and serum. Lithium suppressed the hyperphosphorylation and caspase-mediated degradation of MEF2D. Moreover, lithium sustained MEF2 DNA binding and transcriptional activity in the absence of depolarization. Unexpectedly, MEF2D hyperphosphorylation was not blocked by either forskolin, insulin-like growth factor-I, or valproate, three mechanistically distinct inhibitors of GSK-3β. These results suggest that lithium targets a novel kinase, different from GSK-3β, that phosphorylates and inhibits the pro-survival function of MEF2D in cerebellar granule neurons. Future studies will be aimed at identifying the protein kinase that induces

hyperphosphorylation and degradation of MEF2. These initial results have been submitted to the Journal of Biochemistry.

Task #2 The second task is to determine whether activation or inhibition of the neurotrophin- regulated kinases is necessary or sufficient to influence neuronal survival.

Another area that we've made progress in is understanding how neurotrophin signaling, in particular IGF-I, impacts on the intrinsic death machinery in neurons. Over the last year, we identified the intrinsic (mitochondrial) death pathway as a principal target of IGF-I action in cerebellar granule neurons. Cerebellar granule neurons depend on insulin-like growth factor-I (IGF-I) for their survival. However, the mechanism underlying the neuroprotective effects of IGF-I is presently unclear. Studies in the the last year have indicated that IGF-I protects granule neurons by suppressing key elements of the intrinsic (mitochondrial) death pathway. IGF-I blocked activation of the executioner caspase-3 and the intrinsic initiator caspase-9 in primary cerebellar granule neurons deprived of serum and depolarizing potassium. IGF-I inhibited cytochrome C release from mitochondria and prevented its redistribution to neuronal processes. The effects of IGF-I on cytochrome C release were not mediated by blockade of the mitochondrial permeability transition pore since IGF-I failed to inhibit mitochondrial swelling or depolarization. In contrast, IGF-I blocked induction of the BH3-only Bcl-2 family member, Bim, a mediator of Bax-dependent cytochrome C release. The suppression of Bim expression by IGF-I did not involve inhibition of the c-Jun transcription factor. Instead, IGF-I prevented activation of the forkhead family member, FKHRL1, another transcriptional regulator of Bim. Finally, adenoviral-mediated expression of dominant-negative AKT activated FKHRL1 and induced expression of Bim. These data suggest that IGF-I signaling via AKT promotes survival of cerebellar granule neurons by blocking the FKHRL1-dependent transcription of Bim, a principal effector of the intrinsic death signaling cascade. These results are in press (The Journal of Neuroscience).

Task #3 The third task is to determine whether there is cross-talk between pro-apoptotic and anti-apoptotic signaling pathways.

In other experiments this year, we examined the involvement of death receptor signaling in granule neuron apoptosis by expressing adenoviral, AU1-tagged, dominant-negative Fas-associated death domain (Ad-AU1–ΔFADD). Ad-AU1–ΔFADD decreased apoptosis of granule neurons from 65±5% to 27±2% (n=7, $p<0.01$). Unexpectedly, immunocytochemical staining for

AU1 revealed that <5% of granule neurons expressed ΔFADD. In contrast, ΔFADD was expressed in >95% of calbindin-positive Purkinje neurons (~2% of the cerebellar culture). Granule neurons in proximity to ΔFADD-expressing Purkinje cells demonstrated markedly increased survival. Both granule and Purkinje neurons expressed insulin-like growth factor-I (IGF-I) receptors and ΔFADD-mediated survival of granule neurons was inhibited by an IGF-I receptor blocking antibody. These results demonstrate that the selective suppression of death receptor signaling in Purkinje neurons is sufficient to rescue neighboring granule neurons that depend on Purkinje cell-derived IGF-I. Thus, the extrinsic death pathway has a profound, but indirect, effect on the survival of cerebellar granule neurons. These results have been published in the Journal of Biochemistry. **Appendix 1.**

Key Research Accomplishments

Our key research accomplishments over the last year lie in several areas. One is identifying protein kinases and phosphatases that regulate transcription factors controlling neuronal survival and death. We have also examined the intrinsic and extrinsic death machinery in cerebellar neurons and the protein kinases that impact on the death process. Perhaps, the most exciting finding over the last year is the discovery that different types of neurons use distinct molecular mechanisms to die.

Reportable Outcomes

Manuscripts (2002)

1. Linseman, DA, ML McClure, RJ Bouchard, TA Laessig, D Brenner, and **KA Heidenreich**. Suppression of death receptor signaling in cerebellar Purkinje neurons protects neighboring granule neurons form apoptosis. J. Biol. Chem 277:24546-24553, 2002.

2. Allen, MP, DA Linseman, H Udo, M Xu, B Varnum, ER Kandel, **KA Heidenreich**, and ME Wierman. A novel mechanism for GnRH neuron migration involving Gas6/Ark signaling to p38 MAP kinase. Mol. Cell. Biol. 22 (2): 599-613, 2002

3. Linseman, DA, RA Phelps, RJ Bouchard, TA Laessig, SS Le, and **KA Heidenreich**. Insulin-like growth factor-I blocks Bim induction and intrinsic death signaling in cerebellar granule neurons. J, Neuroscience, in press.

4. Allen, MP, M Xu, DA Linseman, JE Pawlowski, GM Bokoch, **KA Heidenreich**, and ME Wierman Adhesion related kinase (ARK) repression of gonadotropin releasing hormone

(GnRH) gene expression requires Rac activation of the extracellular signal-regulated kinase (ERK) pathway. J. Biol. Chem., in press.

5. Linseman, DA, BJ Cornejo, SS Le, MK Meintzer,, TA Laessig , RJ Bouchard, and **KA Heidenreich.** A novel mechanism for lithium neuroprotection involving suppression of myocyte enhancer factor 2D hyperphosphorylation and degradation. (submitted, J.Biol. Chem.).

Abstracts (2002)

1. Linseman, DA, ML McClure, RA Phelps, RJ Bouchard, TA Laessig, SS Le, F Ahmadi, and **KA Heidenreich**. Extrinsic and intrinsic death signaling in cerebellar neuronal apoptosis: the IGF-I connection. 8th International Conference on Neural Transplantation and Repair, Keystone, CO 2002.

2. Jones, SM, MK Meintzer, CR Freed, **KA Heidenreich**, and Zawada, WM. SC68376, a novel inhibitor of p38 MAP kinase rescues rat and human dopaminergic neurons from apoptotic cell death. 8th International Conference on Neural Transplantation and Repair, Keystone, CO 2002

3. Ahmadi, F., S. Doolin, NR Zahniser, MP McGrogan**, KA Heidenreich**, and MW Zawada. Effects of serum withdrawal and MPP+ on the HNT-neurons. 8th International Conference on Neural Transplantation and Repair, Keystone, CO 2002.

4. Linseman, DA, RA Phelps, RJ Bouchard, TA Laessig, SS Le, F Ahmadi, and **KA Heidenreich.** IGF-I inhibits Bim induction and the intrinsic death signaling cascade in cerebellar granule neurons. Keystone Symposium, Mitochondria and Pathogenesis, Copper, CO 2002.

5. McClure, ML, DA Linseman, RJ Bouchard, TA Laessig, FA Ahmadi, and **KA Heidenreich**, Suppression of death receptor signaling in cerebellar Purkinje neurons protects neighboring granule neurons from apoptosis via an IGF-I dependent mechanism. The Endocrine Society's 84th Annual Meeting, 2002.

6. Linseman, DA, RA Phelps, RJ Bouchard, TA Laessig, SS Le, and **KA Heidenreich**. Insulin-like growth factor-I rescues cerebellar granule cerebellar neurons from apoptosis by blocking Bim induction and mitochondrial death signaling. The Endocrine Society's 84th Annual Meeting, 2002.

7. McClure ML, D A Linseman, R Bouchard, T A Laessig, M K Meintzer, S S Le and **K A Heidenreich**. Identification of an autophagic death pathway in cerebellar Purkinje neurons downstream of death receptor signaling.. Society for Neuroscience 2002.

8. Ahmadi, F., DA Linseman, RJ Bouchard, S Jones, CR Freed, **KA Heidenreich**, and MW Zawada. Rotenone induces death of primary dopamine neurons by a caspase-dependent mechanism. Soc. for Neuroscience Annual meeting, 2002.

9. Linseman, DA, CM Bartley, MK Meintzer, SS Le, TA Laessig, RJ Bouchard, and **KA Heidenreich.** Ca2+/Calmodulin-dependent Protein kinase II Promotes Neuronal Survival by Inhibiting HDAC Repression of MED2D. The American Society for Cell Biology, 2002.

Invited talks

2001 Danish Society for Neuroscience and Danish Society for Biochemistry and Molecular Biology, Symposium on Molecular Mechanisms in Neuronal Degeneration, Copenhagen, Denmark

2002 Plenary talk, New York Academy of Science Symposium " PD: Life Cycle of the Dopamine Neuron", Princeton, N.J.

Conclusions

The scope of research over the last year has been to continue experiments outlined in Task#1, Task#2, and Task #3 of our original research proposal. Towards this goal, we have identified a number protein kinase cascades and effectors that regulate neuronal survival and apoptosis. In cultured rat cerebellar granule neurons, a good model for studying apoptosis in primary differentiated neurons, we have studied various aspects of 2 different pathways that regulate neuronal survival, an IGF-I–regulated protein kinase pathway involving PI-3 kinase and Akt and a Ca++ sensitive pathway regulating the activity of a family of transcription factors that signal survival. The major contribution of these studies is the discovery that IGF-I signaling via AKT promotes survival of cerebellar granule neurons by blocking the FKHRL1-dependent transcription of Bim, a principal effector of the intrinsic death signaling cascade. We will continue to examine other components of the intrinsic death pathway, i.e. Bax and determine how they interact to promote cell death. Experiments are also planned to continue studying the regulation of MEF2s in neurons and identify the genes that are transcriptionally modified by this family of transcription factors. We plan on using a proteomics approach to identify prosurvival proteins.

References NONE

Appendices: _3 MANUSCRIPTS attached

_8 ABSTRACTS attached

THE JOURNAL OF BIOLOGICAL CHEMISTRY

Vol. 277, No. 27, Issue of July 5, pp. 24546–24553, 2002
Printed in U.S.A.

Suppression of Death Receptor Signaling in Cerebellar Purkinje Neurons Protects Neighboring Granule Neurons from Apoptosis via an Insulin-like Growth Factor I-dependent Mechanism*

Received for publication, February 1, 2002, and in revised form, April 3, 2002
Published, JBC Papers in Press, April 18, 2002, DOI 10.1074/jbc.M201098200

Daniel A. Linseman‡, Maria L. McClure‡, Ron J. Bouchard, Tracey A. Laessig, Ferogh A. Ahmadi, and Kim A. Heidenreich§

From the Department of Pharmacology, University of Colorado Health Sciences Center and the Denver Veterans Affairs Medical Center, Denver, Colorado 80220

Neuronal apoptosis contributes to the progression of neurodegenerative disease. Primary cerebellar granule neurons are an established *in vitro* model for investigating neuronal death. After removal of serum and depolarizing potassium, granule neurons undergo apoptosis via a mechanism that requires intrinsic (mitochondrial) death signals; however, the role of extrinsic (death receptor-mediated) signals is presently unclear. Here, we investigate involvement of death receptor signaling in granule neuron apoptosis by expressing adenoviral, AU1-tagged, dominant-negative Fas-associated death domain (Ad-AU1-ΔFADD). Ad-AU1-ΔFADD decreased apoptosis of granule neurons from 65 ± 5 to 27 ± 2% (n = 7, p < 0.01). Unexpectedly, immunocytochemical staining for AU1 revealed that <5% of granule neurons expressed ΔFADD. In contrast, ΔFADD was expressed in >95% of calbindin-positive Purkinje neurons (~2% of the cerebellar culture). Granule neurons in proximity to ΔFADD-expressing Purkinje cells demonstrated markedly increased survival. Both granule and Purkinje neurons expressed insulin-like growth factor-I (IGF-I) receptors, and ΔFADD-mediated survival of granule neurons was inhibited by an IGF-I receptor blocking antibody. These results demonstrate that the selective suppression of death receptor signaling in Purkinje neurons is sufficient to rescue neighboring granule neurons that depend on Purkinje cell-derived IGF-I. Thus, the extrinsic death pathway has a profound but indirect effect on the survival of cerebellar granule neurons.

Apoptosis is a type of programmed cell death characterized by a cascade of proteolytic events orchestrated by the caspase family of cysteine proteases (1). There are two principal pathways leading to apoptotic cell death. These include the "extrinsic" or death receptor-initiated pathway and the "intrinsic" or mitochondrial pathway (2). The extrinsic pathway originates with binding of death-promoting ligands (*e.g.* FasL) to their cognate death receptors (*e.g.* Fas) (3). Ligand binding induces oligomerization of death receptors and promotes their association with adapter molecules like Fas-associated death domain protein (FADD)[1] (4). The receptor-FADD interaction occurs via a protein-protein binding motif known as the death domain (5). The initiator caspase, pro-caspase 8, is then recruited to the death-inducing signaling complex via binding to the death effector domain of FADD (6). The resulting proximity of multiple pro-caspase 8 molecules facilitates their autocatalytic cleavage to the active protease caspase 8 (7). The intrinsic pathway is initiated by release of cytochrome *c* from mitochondria and its subsequent association with apoptosis-activating factor 1 and pro-caspase 9 (8). This large protein complex (the apoptosome) promotes activation of caspase 9 (9). The intrinsic pathway is regulated by both pro- and anti-apoptotic members of the Bcl-2 family (10). Each of the above initiator caspases, 8 and 9, cleave downstream executioner caspases such as caspase 3 from the pro-form to the active protease, thus resulting in the cleavage of critical cellular proteins and apoptosis (11, 12).

Neuronal apoptosis plays an essential role in the normal development of the central nervous system (13). Developmental neuronal cell death requires activation of a caspase cascade as evidenced by the substantial hyperplasia observed in many areas of the brain in caspase 3 knock-out mice (14). Aberrant apoptotic mechanisms are thought to contribute significantly to many neurodegenerative disorders including Alzheimer's and Parkinson's disease (15). Therefore, elucidation of the apoptotic signaling pathways underlying neurodegeneration is critical to enhance current therapies for these disorders. Recent findings indicate that components of both the extrinsic (death receptors or their ligands) and intrinsic (Bcl-2 family members) death pathways are regulated at the level of expression during neurodegeneration or neuronal injury *in vivo* (16, 17). Moreover, transgenic animal models or spontaneously occurring mutants of specific death receptor-signaling molecules or Bcl-2 family members provide further evidence that these pathways are involved in neuronal injury (18, 19).

To examine the signal transduction mechanisms underlying neuronal apoptosis, primary neuronal cultures have been extensively utilized. Primary cerebellar granule neurons isolated from early postnatal rats are a well characterized model system

* This work was supported by a Department of Veterans Affairs Merit Award (to K. A. H.), Department of Defense Grant DAMD17-99-1-9481 (to K. A. H.), National Institutes of Health Grant NS38619-01A1 (to K. A. H.), and a Veterans Affairs Research Enhancement Award Program (to K. A. H. and D.A.L.). The costs of publication of this article were defrayed in part by the payment of page charges. This article must therefore be hereby marked "*advertisement*" in accordance with 18 U.S.C. Section 1734 solely to indicate this fact.

‡ These authors contributed equally to this work.

§ To whom correspondence should be addressed: University of Colorado Health Sciences Center Dept. of Pharmacology (C236) 4200 E. Ninth Ave. Denver, CO 80262. Tel.: 303-399-8020 (ext. 3891); Fax: 303-393-5271; E-mail: Kim.Heidenreich@UCHSC.edu.

[1] The abbreviations used are: FADD, Fas-associated death domain protein; IGF-I, insulin-like growth factor-I; ΔFADD, Fas-associated death domain protein lacking a death effector domain; DAPI, 4,6-diamidino-2-phenylindole; m.o.i., multiplicity of infection; PBS, phosphate-buffered saline; Ad-AU1-ΔFADD, adenoviral, AU1-tagged, dominant-negative Fas-associated death domain; 25k + Ser, control medium containing serum and 25 mM potassium; 5k−Ser, apoptotic medium lacking serum and containing 5 mM potassium.

for investigating neuronal apoptosis (20). These cell cultures are highly homogeneous, with greater than 95% of the isolated cells being granule neurons (21). The remaining cells include glial cells and other neuronal cells such as Purkinje neurons, which demonstrate an interdependent relationship with granule neurons both *in vivo* and *in vitro* (22, 23). Cerebellar granule neurons require activity-dependent signals (membrane depolarization) and serum for their survival *in vitro* (20, 21, 24). After removal of serum and lowering of extracellular potassium from 25 to 5 mM (trophic factor withdrawal), granule neurons undergo rapid apoptotic cell death characterized by caspase activation and nuclear condensation and fragmentation (21). Cerebellar granule neuron apoptosis is attenuated by neurotrophic growth factors, including insulin-like growth factor-I (IGF-I) (20, 21, 24–26), or by inhibitors of the stress-activated protein kinases, c-Jun-NH_2-terminal kinase or p38 mitogen-activated protein kinase (27). Significantly, both neurotrophins and stress-activated protein kinase inhibitors also rescue neurons from apoptosis *in vivo*, thus validating the results obtained in cerebellar granule neurons *in vitro* (28, 29).

Several studies indicate that the intrinsic death pathway plays a critical role in cerebellar granule neuron apoptosis. For example, granule neurons display a rapid translocation of the pro-apoptotic Bcl-2 family member, Bax, to mitochondria and release of cytochrome *c* after trophic factor withdrawal (30). Moreover, cerebellar granule neurons isolated from Bax knockout mice exhibit a significant reduction in apoptosis in response to serum and potassium deprivation (31). In addition, expression of the BH3-only, pro-apoptotic Bcl-2 family member, Bim, is markedly increased in granule neurons during trophic factor withdrawal (32). In contrast to the above findings, relatively little is known about the involvement of the extrinsic death pathway in promoting cerebellar granule neuron apoptosis. Le-Niculescu *et al.* (33) show that FasL mRNA is induced after trophic factor withdrawal in cerebellar granule neurons, and furthermore, sequestration of FasL with FasFc attenuates granule neuron apoptosis. However, additional data supporting a role for the extrinsic death pathway in cerebellar granule neuron apoptosis have not been forthcoming.

In the present study, we examined the involvement of death receptor signaling in cerebellar granule neuron apoptosis by expressing a dominant-negative mutant of FADD (ΔFADD) in primary cultures of cerebellar granule neurons using adenoviral vectors. Our results show that adenoviral ΔFADD was expressed almost exclusively in cerebellar Purkinje cells, yet it effectively rescued granule neurons from apoptosis. The ΔFADD-mediated survival of granule neurons was dependent on their proximity to ΔFADD-expressing Purkinje cells and required Purkinje cell-derived IGF-I. These data indicate that the extrinsic death pathway significantly, but indirectly, influences the survival of cerebellar granule neurons.

EXPERIMENTAL PROCEDURES

Materials—Adenoviral-AU1-ΔFADD (34) was kindly provided by Dr. David Brenner and the adenoviral core at the University of North Carolina (Chapel Hill, NC). Dr. Sylvia Christakos at the University of Medicine and Dentistry of New Jersey (Newark, NJ) kindly provided rabbit polyclonal antibodies raised against rat calbindin D28K (35). Monoclonal antibodies to the AU1 epitope tag were purchased from Berkley Antibody Co. (Richmond, CA). Neutralizing monoclonal antibodies against the IGF-I receptor were purchased from Oncogene (Boston, MA). Fluorescein isothiocyanate- and Cy3-conjugated secondary antibodies were obtained from Jackson Immunoresearch (West Grove, PA). Hoechst dye 33258 and DAPI (4,6-diamidino-2-phenylindole) were purchased from Sigma.

Cell Culture—Primary rat cerebellar granule neurons were isolated from 7-day-old Sprague-Dawley rat pups as described previously (36). Briefly, cells were plated at a density of 2.0×10^6 cells/ml in basal modified Eagle's medium containing 10% fetal bovine serum, 25 mM KCl, 2 mM L-glutamine, and penicillin (100 units/ml)-streptomycin (100 μg/ml) (Invitrogen). Cytosine arabinoside (10 μM) was added to the culture medium 24 h after plating to limit the growth of non-neuronal cells. Experiments were performed after 7 days in culture. Apoptosis was induced by removing the plating medium and replacing it with serum-free medium containing 5 mM KCl.

Adenoviral AU1-ΔFADD Infection—The ΔFADD adenovirus was purified by cesium chloride gradient ultracentrifugation. The viral titer (multiplicity of infection (m.o.i.) was determined by measuring the absorbance at 260 nm (where 1.0 absorbance units = 1×10^{12} particles/ml), and infectious particles were verified by plaque assay. Five days after plating, neuronal cultures were infected with Ad-AU1-ΔFADD at a m.o.i. ranging from 5 to 50. After infection, cells were returned to the incubator for 48 h at 37 °C and 10% CO_2. On day 7, neurons were induced to undergo apoptosis. Twenty-four hours later, the cells were fixed for quantification of apoptosis and/or immunocytochemistry as described below (under "Experimental Procedures").

Quantitation of Apoptosis—Neuronal cultures were fixed with 4% paraformaldehyde in phosphate-buffered saline (PBS, pH 7.4) for 30 min at room temperature and washed with PBS, and nuclei were stained with either Hoechst dye or DAPI. Cells were scored as apoptotic if their nuclei were condensed or fragmented. In general, ~500 cells from at least 2 fields of a 35-mm well were counted. However, some experiments were performed on glass coverslips, and granule neuron apoptosis was quantified in relation to their proximity to AU1-positive, ΔFADD-expressing Purkinje cells. For these experiments, two techniques were utilized to prevent selective bias in defining the anti-apoptotic effect of ΔFADD and the spatial association between surviving granule neurons and ΔFADD-expressing Purkinje cells. First, 40× fields were randomly scanned under the Cy3 filter for AU1-positive Purkinje cells (see "Immunocytochemistry" in this section, below). Fields were randomly selected that contained from 0 to 4 Purkinje cells per field (where "0" Purkinje cells implied no AU1 immunoreactivity apparent in the 40× field, an area of ~100,000 μm^2). After identification of the above fields, the filter was changed to DAPI, and granule neuron apoptosis was quantified within each given field. The second technique utilized to prevent selective counting bias was that random fields were selected by two independent researchers. Ten fields containing on average 30 granule neurons per field were counted per condition from a total of three independent experiments. Data are presented as the percentage of cells in a given treatment group, which were scored as apoptotic. All experiments were performed at least in triplicate.

Immunocytochemistry—Cerebellar cultures were plated on polyethyleneimine-coated glass cover slips at a density of $\sim 1.0 \times 10^5$ cells/coverslip. Five days after plating, cells were infected with Ad-AU1-ΔFADD and subsequently induced to undergo apoptosis 48 h post-infection as described above. After treatment, cells were fixed with 4% paraformaldehyde and then permeabilized and blocked in PBS containing 0.2% Triton X-100 and 5% bovine serum albumin. Cells were then incubated overnight at 4 °C with either mouse-anti-AU1 (1:1000), rabbit-anti-calbindin (1:5000), or mouse-anti-IGF-I receptor (1 μg/ml) diluted in PBS containing 0.2% Triton X-100 and 2% bovine serum albumin. The primary antibody was aspirated, and cells were washed five times with PBS. Cells were then incubated with the appropriate Cy3-conjugated or fluorescein isothiocyanate-conjugated secondary antibody (diluted 1:500) and DAPI for 1 h at room temperature. The cells were then washed 5 times with PBS, and coverslips were adhered to glass slides with mounting medium (0.1% *p*-phenylenediamine in 75% glycerol in PBS). Fluorescence imaging was performed on a Zeiss Axioplan 2 microscope equipped with a Cooke Sensicam deep-cooled CCD camera, and images were analyzed and subjected to digital deconvolution using the Slidebook software program (Intelligent Imaging Innovations Inc., Denver, CO).

Data Analysis—Results shown represent the means ± S.E. for the number (n) of independent experiments performed. Statistical differences between the means of unpaired sets of data were evaluated using one-way analysis of variance followed by a *post hoc* Dunnett's test (54). A p value of <0.01 was considered statistically significant.

RESULTS

Adenoviral ΔFADD Attenuates Apoptosis of Cerebellar Granule Neurons Induced by Trophic Factor Withdrawal—To investigate if death receptor signaling is involved in the apoptotic cell death of primary cerebellar granule neurons subjected to trophic factor withdrawal, cerebellar cell cultures were infected with increasing titers of adenoviral, AU1-tagged, dominant-negative FADD (Ad-AU1-ΔFADD). ΔFADD is a truncated pro-

tein that lacks the death effector domain and, therefore, inhibits coupling of liganded death receptors to the initiator caspase 8 (34, 37). Forty-eight hours after infection, cells were switched from control medium containing serum and 25 mM potassium to apoptotic medium lacking serum and containing 5 mM potassium. After an additional 24-h incubation, cells were fixed, and nuclei were stained with Hoechst dye. Granule neurons containing condensed and/or fragmented nuclei were scored as apoptotic. As shown in Fig. 1*A*, uninfected granule neurons maintained in control medium throughout the experiment demonstrated a low amount of basal apoptosis (6 ± 1%, $n = 7$). Apoptosis in uninfected granule neurons switched to apoptotic medium for 24 h measured 65 ± 5% ($n = 7$). Infection with a negative control adenovirus (Ad-cytomegalovirus (*CMV*)) at a m.o.i. of 50 had no effect on granule neuron apoptosis (69 ± 5%, $n = 7$), whereas infection with ΔFADD resulted in a significant reduction in granule neuron apoptosis to 27 ± 2% ($n = 7$, $p < 0.01$) at a m.o.i. of 50. At the adenoviral titers used in this series of experiments (m.o.i. of from 5 to 50) there was no detectable dose dependence of ΔFADD on granule neuron apoptosis (Fig. 1*A*). When granule neuron apoptosis was carefully analyzed on a field-by-field basis, it was evident that the protection observed with ΔFADD was not uniformly distributed throughout the cell culture (Fig. 1*B*). Like the apoptosis observed in uninfected cultures (Fig. 1*B*, compare the *upper right panel* (apoptotic) to *upper left panel* (control)), there were some fields in the ΔFADD-infected cultures that contained a similar high percentage of apoptotic granule neurons (Fig. 1*B*, *Field A*). However, other fields in the ΔFADD-infected cultures displayed a marked reduction in cerebellar granule neuron apoptosis (Fig. 1*B*, *Field B*). Interestingly, this localized effect of ΔFADD on granule neuron survival was invariably associated with the presence of one or more large and irregularly shaped nuclei within the field of protected granule neurons (Fig. 1*B*, *Field B*, see the nuclei indicated by the *arrows*).

The Survival of Granule Neurons Is Dependent on Their Proximity to ΔFADD-expressing Purkinje Cells—The cerebellar cell cultures utilized in this study have been extensively characterized and are deemed highly homogeneous with greater than 95% of the culture being granule neurons (21). Of the remaining cells, the most prevalent are Purkinje neurons, which display an interdependent relationship with granule neurons both *in vivo* and *in vitro* (22, 23). The calcium-binding protein, calbindin, has been utilized as a marker for Purkinje cells in the cerebellum (38). Immunocytochemical staining of our cerebellar cell cultures for calbindin revealed that the large, irregularly shaped nuclei described above in Fig. 1*B* (*Field B*) were those of Purkinje neurons (Fig. 2*A*). The identified Purkinje neurons demonstrated a classical morphology characterized by an expansive dendritic tree (39). Further immunocytochemical analysis demonstrated that Purkinje cells were very efficiently infected with Ad-AU1-ΔFADD as shown by their marked staining with anti-AU1 (Fig. 2*B*). On average, Purkinje neurons made up ~2% of the entire cerebellar cell culture, and greater than 95% of identified Purkinje cells were AU1-positive after infection with Ad-AU1-ΔFADD at a m.o.i. of from 5 to 50. The lack of concentration dependence for ΔFADD expression in Purkinje neurons over this range of adenoviral titers correlated with the lack of dose dependence for ΔFADD inhibition of granule neuron apoptosis (see Fig. 1*A*), suggesting that the protection observed was dependent on ΔFADD expression in Purkinje neurons.

As described above, the ability of ΔFADD to rescue granule neurons from trophic factor withdrawal-induced death was unevenly distributed throughout the cell culture, and the protected granule neurons were near Purkinje cells (Fig. 1*B*, *Field B*). To further examine this effect, granule neuron apoptosis was analyzed on a field-by-field basis as described in Fig. 1*B*; however, infected cultures were stained with both DAPI (to

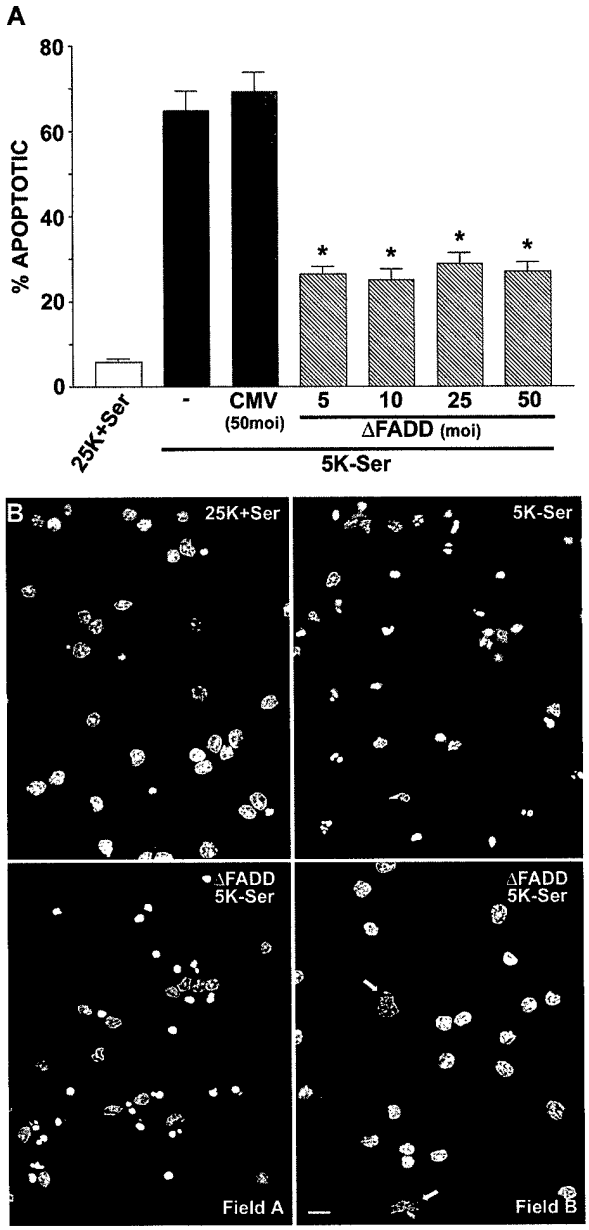

FIG. 1. **Adenoviral infection with ΔFADD attenuates cerebellar granule neuron apoptosis induced by trophic factor withdrawal; the protective effects of ΔFADD are localized.** *A*, cerebellar granule neurons were infected with either a negative control adenovirus (Ad-cytomegalovirus (*CMV*)) or Ad-AU1-ΔFADD at the m.o.i. shown on day 5 in culture. On day 7, cells were incubated in either control (*25K+Ser*) or apoptotic (*5K-Ser*) medium for 24 h. After incubation, granule neurons were fixed, and nuclei were stained with Hoechst dye. Cells containing condensed and/or fragmented chromatin were scored as apoptotic. For each experiment, at least 2 fields of ~500 granule neurons/field were counted per condition. The results shown represent data obtained from seven independent experiments. *, statistically different from 5K-Ser alone ($p < 0.01$). *B*, uninfected granule neurons (*top panels*) or granule neurons infected with ΔFADD at a m.o.i. = 50 (*bottom panels*) were incubated in either control (*25K+Ser*) or apoptotic (*5K-Ser*) medium for 24 h, and nuclei were then stained with DAPI. Nuclei with condensed and/or fragmented chromatin were abundant in uninfected granule neurons incubated in 5K-Ser medium and in some fields of granule neurons infected with ΔFADD (*Field A*). However, other fields of granule neurons infected with ΔFADD did not display a significant number of apoptotic nuclei (*Field B*). These latter fields invariably contained one or more larger and irregularly shaped nuclei (indicated by the *arrows*). *Scale bar* = 10 μm.

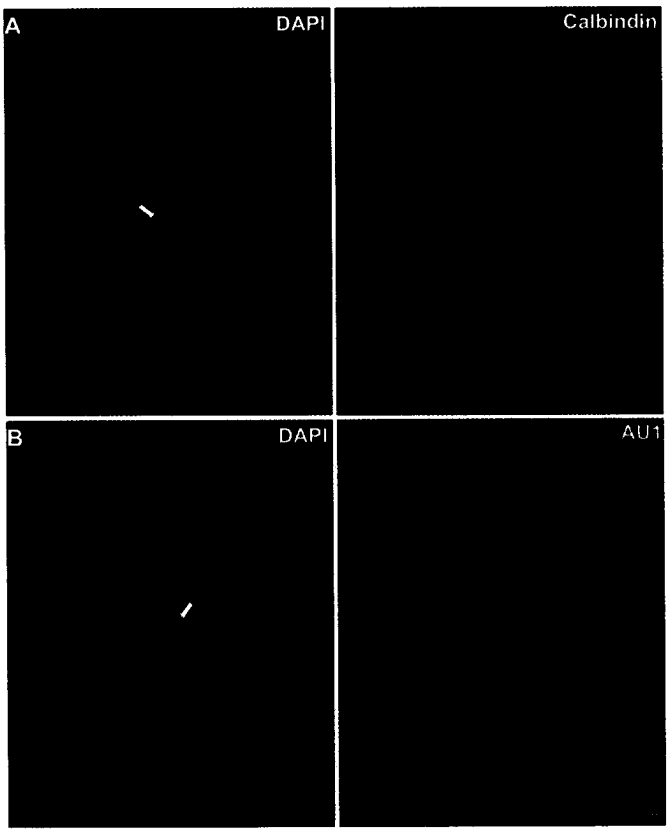

FIG. 2. **Ad-AU1-ΔFADD is expressed in calbindin-positive Purkinje neurons.** *A*, cerebellar cell cultures were maintained in control (25K+Ser) medium for 7 days. After fixation, cells were stained with DAPI (*left panel*) and anti-calbindin (*right panel*) to identify Purkinje neurons. The small nuclei are granule neurons, whereas the large irregularly shaped nucleus (identified by the *arrow*) is that of a calbindin-positive Purkinje cell. *B*, cerebellar cell cultures were infected with Ad-AU1-ΔFADD at a m.o.i. = 50 on day 5 in culture. On day 7, the cells were fixed and stained with DAPI (*left panel*) and anti-AU1 (*right panel*) to identify ΔFADD-infected cells. The small nuclei are granule neurons, whereas the large irregularly shaped nucleus (identified by the *arrow*) is that of a ΔFADD-infected Purkinje cell. *Scale bar* = 20 μm.

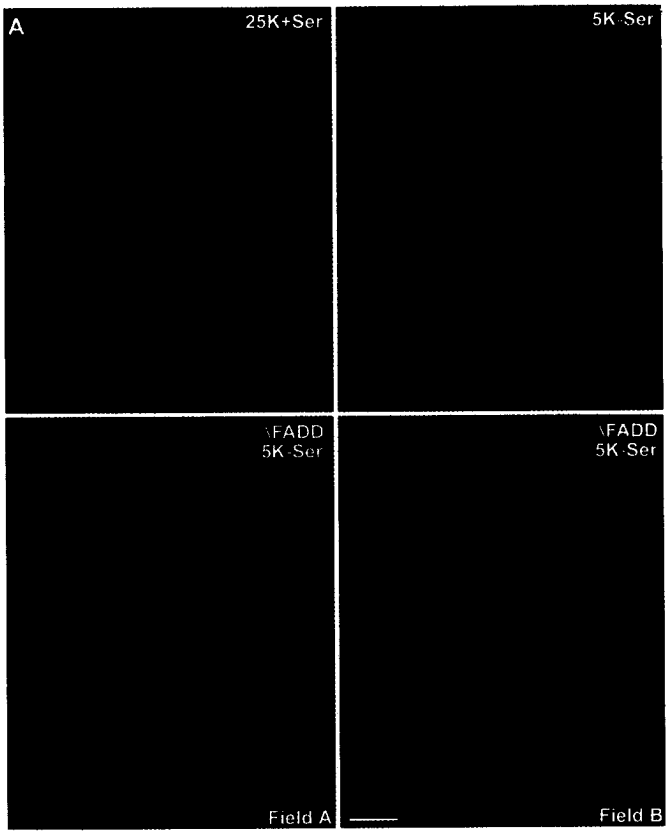

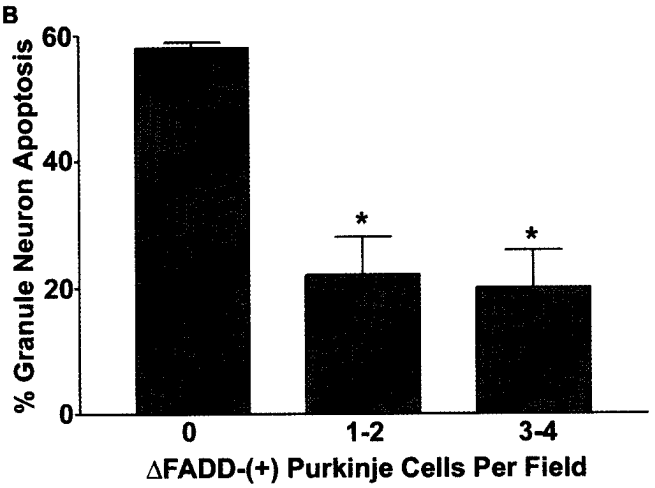

FIG. 3. **Granule neurons in proximity to ΔFADD-expressing Purkinje cells demonstrate increased survival.** *A*, uninfected granule neurons (*top panels*) or granule neurons infected with Ad-AU1-ΔFADD at a m.o.i. = 50 (*bottom panels*) were incubated in either control (*25K+Ser*) or apoptotic (*5K-Ser*) medium for 24 h and then stained with DAPI and anti-AU1. Condensed and/or fragmented nuclei were abundant in uninfected granule neurons incubated in 5K-Ser medium. Apoptotic granule neurons were also plentiful in fields infected with ΔFADD that did not contain any ΔFADD-expressing Purkinje cells (*Field A*). In contrast, fields infected with ΔFADD that contained one or more ΔFADD-positive Purkinje cells displayed a significant decrease in the number of apoptotic granule neurons after trophic factor withdrawal (*Field B*). *Scale bar* = 20 μm. *B*, ΔFADD-infected cerebellar cell cultures were incubated in apoptotic medium and stained for DAPI and AU1, as described in *A*. After staining, the number of healthy *versus* apoptotic granule neurons were counted in fields containing either 0, 1–2, or 3–4 ΔFADD-expressing Purkinje cells per field. Ten fields containing an average of 30 granule neurons/field were counted per condition. The results shown represent data obtained from three independent experiments. *, statistically different from "0" ΔFADD-(+) Purkinje cells per field ($p < 0.01$).

assess nuclear morphology) and anti-AU1 to identify ΔFADD-expressing cells. Uninfected cells displayed the expected high amount of granule neuron apoptosis after trophic factor withdrawal (Fig. 3*A*, compare the *upper right panel* (apoptotic) to the *upper left panel* (control)). Similarly, fields of infected cultures that did not contain any ΔFADD-positive Purkinje cells also exhibited significant granule neuron death after trophic factor withdrawal (Fig. 3*A*, *Field A*). In contrast, fields of infected cells that contained at least one ΔFADD-expressing Purkinje neuron displayed a marked reduction in granule neuron apoptosis (Fig. 3*A*, *Field B*). To quantitate this effect, the number of healthy *versus* apoptotic granule neurons was counted per 40× field in ΔFADD-infected cultures that were incubated in apoptotic medium for 24 h. The granule neuron apoptosis results were then subdivided into three data sets based on the number of ΔFADD-positive Purkinje cells (0, 1–2, or 3–4) identified per field by AU1 staining. As shown in Fig. 3*B*, fields of granule neurons in infected cultures that did not contain any ΔFADD-positive Purkinje cells exhibited 58 ± 1% apoptosis (n = 3 experiments, 10 fields/experiment), a value similar to that observed in uninfected cerebellar cultures. However, fields that contained either 1–2 or 3–4 ΔFADD-expressing Purkinje cells demonstrated a significant decrease in granule neuron apoptosis to 22 ± 6 or 20 ± 6%, respectively (n = 3, $p < 0.01$). These results indicate that the ΔFADD-mediated

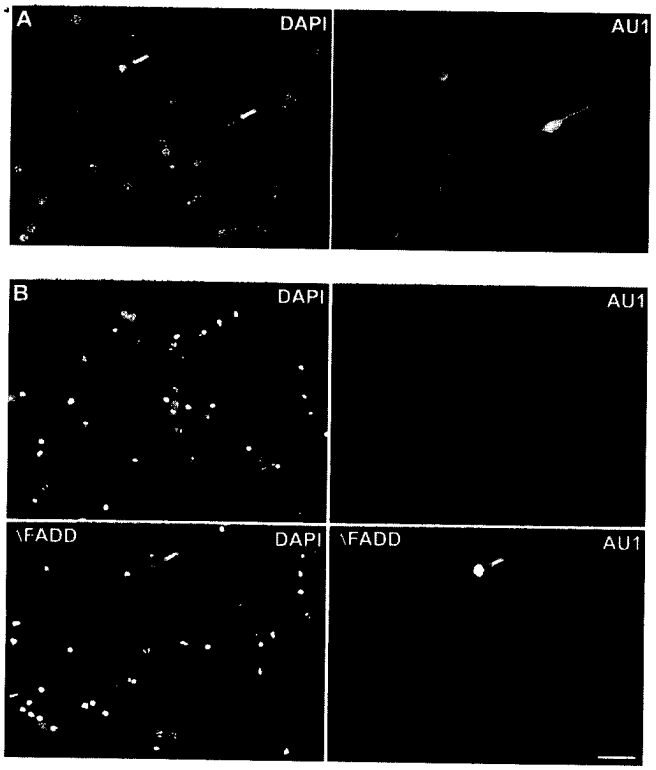

FIG. 4. **Cerebellar granule neurons do not efficiently express Ad-AU1-ΔFADD.** *A*, cerebellar cell cultures were infected on day 5 with Ad-AU1-ΔFADD at a m.o.i. = 50. On day 7, cells were fixed and stained with DAPI (*left panel*) and anti-AU1 (*right panel*). AU1 staining revealed that less than 5% of granule neurons expressed ΔFADD (identified by the *arrows*). *B*, uninfected granule neurons (*top panels*) or AU1-ΔFADD-infected granule neurons (*bottom panels*) were incubated in apoptotic (5K-Ser) medium for 24 h, fixed, and stained with DAPI (*left panels*) and AU1 (*right panels*). Trophic factor withdrawal induced a similar apoptotic response in uninfected cells and infected cells in close association with granule neurons expressing AU1-ΔFADD (indicated by the *arrow*). *Scale bar* = 20 μm.

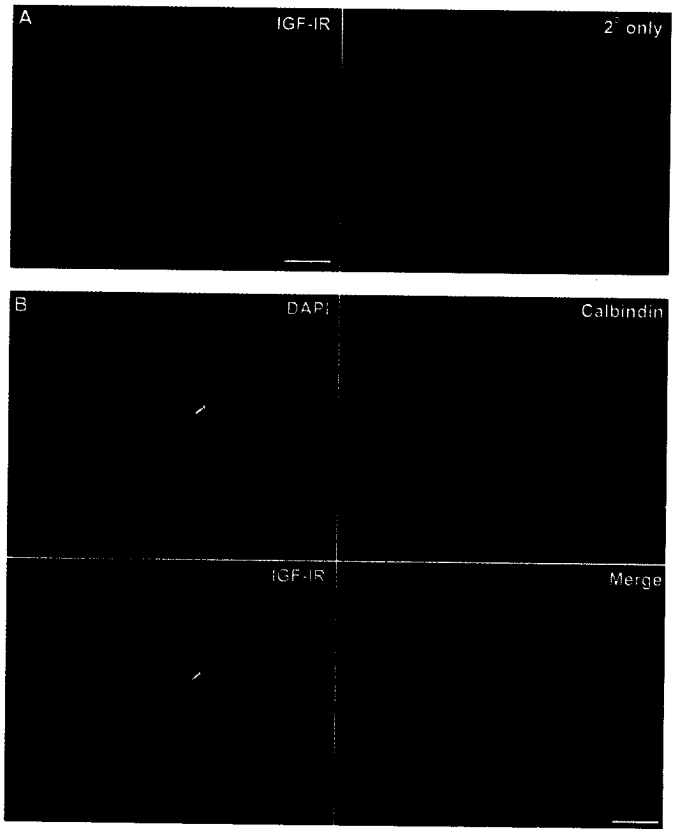

FIG. 5. **Cerebellar granule neurons and Purkinje neurons express IGF-I receptors on their cell surfaces.** *A*, cerebellar granule neurons were fixed and stained with a monoclonal antibody that recognizes the IGF-I receptor (*IGF-IR*). After incubation with a Cy3-conjugated secondary antibody, IGF-I receptors were identified by fluorescence microscopy. IGF-I receptors were expressed primarily at the cell membrane (*left panel*). Incubation with the secondary antibody alone (2° only) did not produce any positive staining (*right panel*). *B*, cerebellar cell cultures were stained as described in *A* but, in addition, calbindin-positive Purkinje cells were identified using a polyclonal antibody to calbindin D28K and a fluorescein isothiocyanate-conjugated secondary. Both granule neurons and calbindin-positive Purkinje neurons showed immunoreactivity for IGF-I receptors. Note the *overlapping yellow staining* indicative of IGF-I receptor and calbindin colocalization in Purkinje cells (*lower right panel*). *Scale bar* = 20 μm.

protection of cerebellar granule neurons from trophic factor withdrawal-induced apoptosis depends on the proximity of granule neurons to ΔFADD-expressing Purkinje cells.

Ad-AU1-ΔFADD Is Not Efficiently Expressed in Granule Neurons—Although Purkinje neurons demonstrated marked expression of Ad-AU1-ΔFADD (Fig. 2*B*), most granule neurons were devoid of AU1 staining (Fig. 4*A*). Quantitatively, when more than 2000 granule neurons were visualized from cerebellar cell cultures infected with Ad-AU1-ΔFADD (m.o.i. = 50), less than 100 stained positively for the AU1 epitope tag at 48 h post-infection (4.4 ± 0.7%, data pooled from 3 independent experiments). These results indicate that granule neurons do not efficiently express AU1-ΔFADD after adenoviral infection. Furthermore, fields of infected cultures that contained one or more AU1-ΔFADD-positive granule neurons displayed a similar amount of apoptotic granule neuron death after trophic factor withdrawal as was observed in uninfected cultures (Fig. 4*B*). This latter result further demonstrates that the ability of ΔFADD to rescue granule neurons from apoptosis is not mediated by proximity to the very few granule neurons actually expressing ΔFADD. However, it is noteworthy that essentially all of the granule neurons that were AU1-ΔFADD-positive were protected from trophic factor withdrawal-induced death regardless of their proximity to Purkinje neurons.

ΔFADD-mediated Cerebellar Granule Neuron Survival Is Dependent on IGF-I—The above data indicate that inhibition of death receptor signaling in Purkinje cells (via infection with Ad-AU1-ΔFADD) not only maintains the Purkinje neurons during trophic factor withdrawal but also results in the protection of closely neighboring granule neurons that require Purkinje cell-derived survival signals. One potent neurotrophin known to rescue cerebellar granule neurons from apoptosis is the growth factor IGF-I (20, 21, 24–26). *In situ* mRNA hybridization studies show that the principal source of IGF-I in the developing cerebellum is the Purkinje cell (40). To investigate a potential role of IGF-I in granule neuron survival, we first analyzed the expression of IGF-I receptors in the cerebellar cell cultures. Immunocytochemical staining with an antibody to the IGF-I receptor demonstrated that cerebellar granule neurons expressed IGF-I receptors primarily at the cell membrane (Fig. 5*A*, *left panel*). Incubation with the Cy3-conjugated secondary antibody alone did not produce any positive staining (Fig. 5*A*, *right panel*). When cerebellar cultures were co-immunostained for both IGF-I receptors and calbindin, both granule neurons and calbindin-positive Purkinje neurons showed immunoreactivity for IGF-I receptors on their cell surfaces (Fig. 5*B*, *lower right panel*, see the *yellow overlapping staining* for co-localized IGF-I receptors and calbindin in a representative Purkinje neuron; the surrounding cells are granule neurons).

Next, the effect of an IGF-I receptor blocking antibody on the ΔFADD-mediated protection of cerebellar granule neurons was

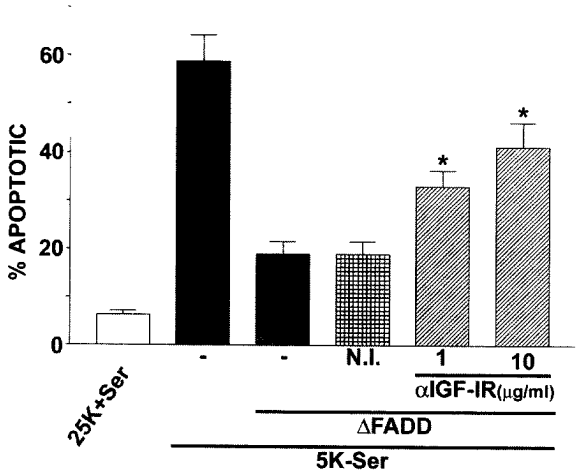

FIG. 6. **ΔFADD-mediated granule neuron survival is inhibited by an IGF-I receptor blocking antibody.** Cerebellar cell cultures were either uninfected or infected with Ad-AU1-ΔFADD (m.o.i. = 50) on day 5. On day 7, cells were incubated in either control (25K+Ser) or apoptotic (5K-Ser) medium alone or containing either an anti-IGF-I receptor blocking antibody (αIGF-IR, 1 or 10 μg/ml) or a non-immune (*N.I.*) control IgG (10 μg/ml) for 24 h. After incubation, cells were fixed, and nuclei were stained with Hoechst dye. Cells containing condensed and/or fragmented nuclei were scored as apoptotic. For each experiment, at least 2 fields of ~500 granule neurons/field were counted per condition. The results shown represent data obtained from seven independent experiments. *, statistically different from ΔFADD alone ($p < 0.01$).

assessed (Fig. 6). Ad-AU1-ΔFADD decreased apoptosis of granule neurons from 59 ± 5% ($n = 7$) to 19 ± 3% ($n = 7$, $p < 0.01$). Incubation with a non-immune IgG control had no effect on the ability of ΔFADD to decrease granule neuron apoptosis (19 ± 3% apoptosis, $n = 7$), whereas inclusion of a neutralizing antibody that binds to the extracellular domain of the IGF-I receptor significantly attenuated the protective effect of ΔFADD in a dose-dependent manner (41 ± 5% apoptosis at an antibody concentration of 10 μg/ml, $n = 7$, $p < 0.01$ compared with ΔFADD alone). Finally, radioimmunoassay of serum-free media obtained from cerebellar cell cultures revealed that the concentration of IGF-I was below the limits of detection (≥6 ng/ml), further confirming that the protection by IGF-I was localized in nature. Collectively, these results suggest that ΔFADD-mediated survival of cerebellar granule neurons requires local secretion of Purkinje cell-derived IGF-I.

DISCUSSION

In the present study, we investigated a role for the extrinsic death pathway in the apoptotic cell death of primary cerebellar granule neurons subjected to trophic factor withdrawal. Adenoviral expression of dominant-negative FADD (ΔFADD) rescued a significant percentage of granule neurons from trophic factor withdrawal-induced death. Initially, this result suggested that death receptor signaling may play a direct role in cerebellar granule neuron apoptosis. However, immunocytochemical analysis revealed that adenoviral ΔFADD was not efficiently expressed in granule neurons but, instead, showed marked expression in the small number of Purkinje neurons found in these cerebellar cell cultures. Moreover, the ability of adenoviral ΔFADD to rescue granule neurons from apoptosis was dependent on their proximity to ΔFADD-expressing Purkinje cells and required IGF-I. Two major conclusions can be drawn from the above results. First, although the data do not support a direct role for the extrinsic death pathway in cerebellar granule neuron apoptosis, the results are the first to demonstrate that death receptor signaling in Purkinje neurons indirectly influences the survival of granule neurons. Second, selective suppression of the extrinsic death pathway in Purkinje cells is sufficient to rescue neighboring granule neurons that depend on Purkinje cell-derived trophic support including IGF-I.

Previous studies have implicated the intrinsic death pathway in the apoptosis of cerebellar granule neurons. For example, trophic factor withdrawal-induced death of granule neurons requires the pro-apoptotic Bcl-2 family members Bax and Bim (30–32). Bim is a BH3-only Bcl-2 family member that acts in a concerted manner with Bax to promote apoptosis (41). Similar results have also been observed *in vivo* in inherited animal models of cerebellar neuronal death. The lurcher mutant mouse is characterized by a gain-of-function mutation in the Δ2 glutamate receptor that results in the death of cerebellar Purkinje cells (22). Subsequent to the loss of their target Purkinje cells, granule neurons die secondarily via an apoptotic mechanism (22). Targeted deletion of Bax has only a minor effect on Purkinje neuron death but essentially abolishes the secondary death of granule neurons in lurcher mutant mice (42, 43). Thus, Bcl-2 family members regulate cerebellar granule neuron apoptosis both *in vitro* and *in vivo*, strongly suggesting that the intrinsic death pathway plays a principal role in granule neuron apoptosis.

However, much less is known about the involvement of extrinsic death signaling in cerebellar granule neurons. Previous work illustrated that trophic factor withdrawal induces an increase in the mRNA for FasL in primary cerebellar granule neurons, and furthermore, granule neurons isolated from FasL-deficient mice (*gld* mice) demonstrate a significant decrease in their susceptibility to trophic factor withdrawal-induced death (33). Although these results suggest that the extrinsic pathway may be involved in granule neuron apoptosis, our data indicate that disruption of death receptor signaling in cerebellar Purkinje neurons is sufficient to significantly decrease apoptosis in neighboring granule neurons. Thus, the conclusions that were originally drawn from the *gld* mice may actually reflect a loss of the extrinsic death machinery in Purkinje cells that normally make up a small component of cerebellar cell cultures. Yet, it should be noted that our data do not absolutely exclude a direct role for the extrinsic death pathway in granule neuron apoptosis. In fact we observed that the small number of granule neurons that did express ΔFADD were rescued from apoptosis regardless of their proximity to Purkinje cells. However, recent data indicate that specific inhibitors of caspase 8 (an extrinsic initiator caspase) fail to rescue granule neurons from trophic factor withdrawal-induced death, whereas selective caspase 9 (an intrinsic initiator caspase) inhibitors block apoptosis (44). Although the relative selectivities of synthetic caspase inhibitors are not absolute, these findings support an intrinsic-dependent but extrinsic-independent mode of cell death in granule neurons.

The putative role of extrinsic and intrinsic death signaling in the apoptosis of Purkinje neurons is much less well defined than in granule neurons. As described above, Bax deletion did not significantly affect Purkinje neuron survival in lurcher mutant mice (42, 43). In contrast, normal mice in which Bax is knocked out show a significant increase in Purkinje cell number in the cerebellum (45). A similar increase in the number of cerebellar Purkinje cells is also observed in mice overexpressing a human Bcl-2 transgene, suggesting that the intrinsic death pathway influences the developmental death of Purkinje neurons (46). In addition, the spontaneous apoptotic death of Purkinje cells observed *in vitro* in murine cerebellar organotypic cultures is reduced in tissue isolated from Bcl-2 transgenic mice (47). This latter result indicates that the intrinsic

death pathway may also play a role in Purkinje neuron apoptosis induced by stress associated with *in vitro* culture conditions. However, a more detailed analysis of the mechanism underlying Purkinje cell death is currently lacking. Our data suggest that one important function of Purkinje neurons (*i.e.* to provide trophic support to neighboring granule neurons) is compromised after the withdrawal of trophic factors from cerebellar cell cultures. Moreover, expression of ΔFADD, an inhibitor of extrinsic death signaling, maintains Purkinje cell function during trophic factor withdrawal. Thus, extrinsic death signals in addition to intrinsic signals play a significant role in Purkinje neuron loss-of-function and ultimately death.

Finally, the ability of ΔFADD-expressing Purkinje cells to rescue neighboring granule neurons from apoptosis was inhibited by an IGF-I receptor-blocking antibody, suggesting involvement of IGF-I in the neuroprotection. Previous work has shown that Purkinje cells are the principal source of IGF-I production in the developing cerebellum *in vivo* (40), and IGF-I is a potent neurotrophin for cerebellar granule neurons *in vitro* (20, 21, 24–26). *In vivo* studies demonstrate that Purkinje-derived trophic support, including IGF-I, is essential for the proper development of cerebellar granule neurons (22, 48). For example, in Purkinje cell degeneration (*pcd*) mice, in which Purkinje cells die spontaneously before adulthood, cerebellar IGF-I mRNA expression decreases significantly as the Purkinje neurons degenerate (49). After the death of Purkinje cells in *pcd* mice, granule neurons undergo apoptosis resulting from the loss of Purkinje cell-derived IGF-I. Our cerebellar cultures were isolated from postnatal day 7 rats, and Purkinje neurons from this stage of development exhibit maximal IGF-I secretion *in vivo* (50). In addition, IGF-I secretion by Purkinje neurons is highly correlated with the differentiated phenotypes of both granule neurons and Purkinje cells, as is observed in our cultures (50–52). Collectively, the above findings are consistent with an important role for Purkinje cell-derived IGF-I in promoting the survival of cerebellar granule neurons.

Precisely how ΔFADD expression influences Purkinje cell IGF-I production or secretion is presently unclear. It may be that ΔFADD simply blocks extrinsic death signaling in Purkinje neurons and, therefore, sustains their normal function of secreting trophic factors like IGF-I. Alternatively, it is possible that ΔFADD expression somehow enhances IGF-I synthesis or secretion. Further experiments will be necessary to identify the exact mechanism underlying the regulation of Purkinje cell-derived IGF-I by death receptor signaling molecules. In addition, the molecular mechanism that mediates the neuroprotective effects of IGF-I is unclear. Recently, we have shown that exogenous IGF-I rescues cerebellar granule neurons by inhibiting the intrinsic death pathway.[2] Moreover, in transgenic mice overexpressing IGF-I, there was a marked increase in the expression of Bcl-2 in cerebellar Purkinje neurons (53). This finding indicates that Purkinje-derived IGF-I may not only promote the survival of neighboring granule neurons via a paracrine mechanism but may also support Purkinje cells directly via an autocrine mechanism, perhaps by suppressing intrinsic death signals at the mitochondria.

In conclusion, we have shown that adenoviral ΔFADD infection of cerebellar cell cultures results in the restricted expression of ΔFADD in Purkinje neurons. ΔFADD-expressing Purkinje cells rescue neighboring granule neurons from trophic factor withdrawal-induced apoptosis via secretion of IGF-I. The dependence of cerebellar granule neuron survival on Purkinje cell-derived trophic support mimics that found *in vivo* during cerebellar development. The results are the first to show that the extrinsic death pathway in Purkinje neurons indirectly but significantly influences the survival of cerebellar granule neurons.

[2] D. A. Linseman, R. A. Phelps, R. J. Bouchard, T. A. Laessig, S. S. Le, and K. A. Heidenreich, manuscript in preparation.

REFERENCES

1. Nunez, G., Benedict, M. A., Hu, Y., and Inohara, N. (1998) *Oncogene* **17,** 3237–3245
2. Green, D. R. (1998) *Cell* **94,** 695–698
3. Pinkoski, M. J., and Green, D. R. (1999) *Cell Death Differ.* **6,** 1174–1181
4. Chinnaiyan, A. M., O'Rourke, K., Tewari, M., and Dixit, V. M. (1995) *Cell* **81,** 505–512
5. Feinstein, E., Kimichi, A., Wallach, D., Boldin, M., and Varfolomeev, E. (1995) *Trends Biochem. Sci.* **20,** 342–344
6. Muzio, M., Chinnaiyan, A. M., Kischkel, F. C., O'Rourke, K., Shevchenko, A., Ni, J., Scaffidi, C., Bretz, J. D., Zhang, M., Gentz, R., Mann, M., Krammer, P. H., Peter, M. E., and Dixit, V. M. (1996) *Cell* **85,** 817–827
7. Muzio, M., Stockwell, B. R., Stennicke, H. R., Salvesen, G. S., and Dixit, V. M. (1998) *J. Biol. Chem.* **273,** 2926–2930
8. Cai, J., Yang, J., and Jones, D. P. (1998) *Biochim. Biophys. Acta* **1366,** 139–149
9. Zou, H., Li, Y., Liu, X., and Wang, X. (1999) *J. Biol. Chem.* **274,** 11549–11556
10. Tsujimoto, Y. (1998) *Genes Cells* **3,** 697–707
11. Stennicke, H. R., Jurgensmeier, J. M., Shin, H., Deveraux, Q., Wolf, B. B., Yang, X., Zhou, Q., Ellerby, H. M., Ellerby, L. M., Bredesen, D., Green, D. R., Reed, J. C., Froelich, C., and Salvesen, G. S. (1998) *J. Biol. Chem.* **273,** 27084–27090
12. Pan, G., Humke, E. W., and Dixit, V. M. (1998) *FEBS Lett.* **426,** 151–154
13. Nijhawan, D., Honarpour, N., and Wang, X. (2000) *Annu. Rev. Neurosci.* **23,** 73–87
14. Kuida, K., Zheng, T. S., Na, S., Kuan, C., Yang, D., Karasuyama, H., Rakic, P., and Flavell, R. A. (1996) *Nature* **384,** 368–372
15. Yuan, J., and Yankner, B. A. (2000) *Nature* **407,** 802–809
16. Kitamura, Y., Shimohama, S., Kamoshima, W., Ota, T., Matsuoka, Y., Nomura, Y., Smith, M. A., Perry, G., Whitehouse, P. J., and Taniguchi, T. (1998) *Brain Res.* **780,** 260–269
17. Felderhoff-Mueser, U., Taylor, D. L., Greenwood, K., Kozma, M., Stibenz, D., Joashi, U. C., Edwards, A. D., and Mehmet, H. (2000) *Brain Pathol.* **10,** 17–29
18. Martin-Villalba, A., Herr, I., Jeremias, I., Hahne, M., Brandt, R., Vogel, J., Schenkel, J., Herdegen, T., and Debatin, K. M. (1999) *J. Neurosci.* **19,** 3809–3817
19. Parsadanian, A. S., Cheng, Y., Keller-Peck, C. R., Holtzman, D. M., and Snider, W. D. (1998) *J. Neurosci.* **18,** 1009–1019
20. Galli, C., Meucci, O., Scorziello, A., Werge, T. M., Calissano, P., and Schettini, G. (1995) *J. Neurosci.* **15,** 1172–1179
21. D'Mello, S. R., Galli, C., Ciotti, T., and Calissano, P. (1993) *Proc. Natl. Acad. Sci. U. S. A.* **90,** 10989–10993
22. Selimi, F., Doughty, M., Delhaye-Bouchaud, N., and Mariani, J. (2000) *J. Neurosci.* **20,** 992–1000
23. Baptista, C. A., Hatten, M. E., Blazeski, R., and Mason, C. A. (1994) *Neuron* **12,** 243–260
24. Miller, T. M., Tansey, M. G., Johnson, E. M., Jr., and Creedon, D. J. (1997) *J. Biol. Chem.* **272,** 9847–9853
25. Gleichmann, M., Weller, M., and Schulz, J. B. (2000) *Neurosci. Lett.* **282,** 69–72
26. D'Mello, S. R., Borodetz, K., and Soltoff, S. P. (1997) *J. Neurosci.* **17,** 1548–1560
27. Harada, J., and Sugimoto, M. (1999) *Jpn. J. Pharmacol.* **79,** 369–378
28. Clarkson, E. D., Zawada, W. M., Bell, K. P., Esplen, J. E., Choi, P. K., Heidenreich, K. A., and Freed, C. R. (2001) *Exp. Neurol.* **168,** 183–191
29. Zawada, W. M., Meintzer, M. K., Rao, P., Marotti, J., Wang, X., Esplen, J. E., Clarkson, E. D., Freed, C. R., and Heidenreich, K. A. (2001) *Brain Res.* **891,** 185–196
30. Desagher, S., Osen-Sand, A., Nichols, A., Eskes, R., Montessuit, S., Lauper, S., Maundrell, K., Antonsson, B., and Martinou, J.-C. (1999) *J. Cell Biol.* **144,** 891–901
31. Miller, T. M., Moulder, K. L., Knudson, C. M., Creedon, D. J., Deshmukh, M., Korsmeyer, S. J., and Johnson, E. M., Jr. (1997) *J. Cell Biol.* **139,** 205–217
32. Putcha, G. V., Moulder, K. L., Golden, J. P., Bouillet, P., Adams, J. A., Strasser, A., and Johnson, E. M., Jr. (2001) *Neuron* **29,** 615–628
33. Le-Niculescu, H., Bonfoco, E., Kasuya, Y., Claret, F. X., Green, D. R., and Karin, M. (1999) *Mol. Cell. Biol.* **19,** 751–763
34. Streetz, K., Leifeld, L., Grundmann, D., Ramakers, J., Eckert, K., Spengler, U., Brenner, D. A., Manns, M., and Trautwein, C. (2000) *Gastroenterology* **119,** 446–460
35. Christakos, S., Rhoten, W. B., and Feldman, S. C. (1987) *Methods Enzymol.* **139,** 534–551
36. Li, M., Wang, X., Meintzer, M. K., Laessig, T., Birnbaum, M. J., and Heidenreich, K. A. (2000) *Mol. Cell. Biol.* **20,** 9356–9363
37. Bradham, C. A., Qian, T., Streetz, K., Trautwein, C., Brenner, D. A., and Lemasters, J. J. (1998) *Mol. Cell. Biol.* **18,** 6353–6364
38. Hockberger, P. E., Yousif, L., and Nam, S. C. (1994) *Neuroimage* **1,** 276–287
39. Vogel, M. W., and Prittie, J. (1995) *J. Neurobiol.* **26,** 537–552
40. Bartlett, W. P., Li, X. -S., Williams, M., and Benkovic, S. (1991) *Dev. Biol.* **147,** 239–250
41. Zong, W. X., Lindsten, T., Ross, A. J., MacGregor, G. R., and Thompson, C. B. (2001) *Genes Dev.* **15,** 1481–1486
42. Doughty, M. L., De Jager, P. L., Korsmeyer, S. J., and Heintz, N. (2000) *J. Neurosci.* **20,** 3687–3694
43. Selimi, F., Vogel, M. W., and Mariani, J. (2000) *J. Neurosci.* **20,** 5339–5345
44. Gerhardt, E., Kugler, S., Leist, M., Beier, C., Berliocchi, L., Volbracht, C.,

Weller, M., Bahr, M., Nicotera, P., and Schulz, J. B. (2001) *Mol. Cell. Neurosci.* **17,** 717–731
45. Fan, H., Favero, M., and Vogel, M. W. (2001) *J. Comp. Neurol.* **436,** 82–91
46. Zanjani, H. S., Vogel, M. W., Delhaye-Bouchaud, N., Martinou, J.-C., and Mariani, J. (1996) *J. Comp. Neurol.* **374,** 332–341
47. Ghoumari, A. M., Wehrle, R., Bernard, O., Sotelo, C., and Dusart, I. (2000) *Eur. J. Neurosci.* **12,** 2935–2949
48. Andersson, I. K., Edwall, D., Norstedt, G., Rozell, B., Skottner, A., and Hansson, H.-A. (1988) *Acta Physiol. Scand.* **132,** 167–173
49. Zhang, W., Ghetti, B., and Lee, W.-H. (1997) *Brain Res. Dev. Brain Res.* **98,** 164–176
50. Bondy, C. A. (1991) *J. Neurosci.* **11,** 3442–3455
51. Lin, X., and Bulleit, R. F. (1997) *Brain Res. Dev. Brain Res.* **99,** 234–242
52. Torres-Aleman, I., Pons, S., and Arevalo, M. A. (1994) *J. Neurosci. Res.* **39,** 117–126
53. Baker, N. L., Carlo Russo, V., Bernard, O., D'Ercole, A. J., and Werther, G. A. (1999) *Brain Res. Dev. Brain Res.* **118,** 109–118
54. Ludbrook, J. (1998) *Clin. Exp. Pharmacol. Physiol.* **25,** 1032–1037

MOLECULAR AND CELLULAR BIOLOGY, Jan. 2002, p. 599–613 Vol. 22, No. 2
0270-7306/02/$04.00+0 DOI: 10.1128/MCB.22.2.599–613.2002

Novel Mechanism for Gonadotropin-Releasing Hormone Neuronal Migration Involving Gas6/Ark Signaling to p38 Mitogen-Activated Protein Kinase

Melissa P. Allen,[1,2] Daniel A. Linseman,[2,3] Hiroshi Udo,[4] Mei Xu,[1,2] Jerome B. Schaack,[5] Brian Varnum,[6] Eric R. Kandel,[4] Kim A. Heidenreich,[2,3] and Margaret E. Wierman[1,2,7]*

Departments of Medicine,[1] Pharmacology,[3] Microbiology,[5] and Physiology and Biophysics,[7] University of Colorado Health Sciences Center, and Research Service, Veterans Affairs Medical Center,[2] Denver, Colorado; Amgen, Inc., Thousand Oaks, California[6]; and Howard Hughes Medical Institute, Center for Neurobiology and Behavior, Columbia University, New York, New York[4]

Received 1 June 2001/Returned for modification 2 August 2001/Accepted 16 October 2001

Gonadotropin-releasing hormone (GnRH) is the central regulator of the reproductive axis. Normal sexual maturation depends on the migration of GnRH neurons from the olfactory placode to the hypothalamus during development. Previously, we showed restricted expression of the membrane receptor adhesion-related kinase (Ark) in immortalized cell lines derived from migratory but not postmigratory GnRH neurons. In addition, Ark and GnRH transcripts were detected along the GnRH neuron migratory route in the E13 mouse cribriform plate. In the present study, we examined the role of Ark and its ligand, Gas6 (encoded by growth arrest-specific gene 6), in GnRH neuron migration. Gas6 stimulated lamellipodial extension, membrane ruffling, and chemotaxis of immortalized NLT GnRH neuronal cells via the Ark receptor. Gas6/Ark signaling promoted activation of the Rho family GTPase Rac, and adenoviral-mediated expression of dominant negative N17Rac abolished Gas6/Ark-induced actin cytoskeletal reorganization and migration of GnRH neuronal cells. In addition, p38 MAPK was activated downstream of Ark and Rac, and inhibition of p38 MAPK with either SB203580 or adenoviral dominant negative p38α also blocked Gas6/Ark-mediated migration. Finally, downstream of Rac and p38 mitogen-activated protein kinase (MAPK), Gas6/Ark signaling promoted activation of MAPK-activated protein kinase 2 and induced phosphorylation of HSP25, a known regulator of cortical actin remodeling. The data are the first to demonstrate a migratory signaling pathway downstream of Ark/Axl family receptors and suggest a previously unidentified role for p38 MAPK in neuronal migration. Furthermore, these studies support a potential role for Ark in the regulation of GnRH neuronal migration.

The acquisition of reproductive competence relies on a hierarchy of events initiated by gonadotropin-releasing hormone (GnRH). Neurons producing GnRH are unique, originating in the olfactory placode and migrating into the central nervous system during development (59, 66). Traveling in association with vomeronasal nerve fibers, the GnRH neurons migrate through the nasal septum, cross the cribriform plate (the nasal-brain border), and continue along vomeronasal nerve fibers until they reach the preoptic area and hypothalamus (67, 70). After completing the journey, GnRH neurons project axons toward the median eminence, establishing contacts with pituitary portal vessels. GnRH release is tightly regulated and occurs in a pulsatile manner to stimulate pituitary gonadotropin production (60).

In humans, X-linked Kallmann's syndrome, arising from mutations in the *KAL-1* gene, results in aberrant olfactory and GnRH neuron migration (11, 24, 32, 58). *KAL-1* encodes a cell adhesion molecule, anosmin-1, that is believed to be required for olfactory nerve migration (58, 62). Since the GnRH neurons travel in association with olfactory nerves, the defect in olfactory nerve migration is thought to disrupt the GnRH neuron pathway, resulting in loss of GnRH neuronal migration. Although the path of the GnRH neurons from the olfactory placode to the forebrain during development has been well characterized, the cellular signaling mechanisms that directly govern GnRH neuron motility are unknown.

Because primary GnRH neurons are extremely limited in number (~800 neurons in the mouse, several thousand in the primate) (54, 66), studies of their development and differentiation have been difficult. We and others have utilized immortalized GnRH neuronal cell lines as a model system to identify factors potentially involved in GnRH neuronal physiology. Simian virus 40 T-antigen-targeted tumorigenesis was used to establish GnRH neuronal cell lines at two distinct developmental phases, migratory and postmigratory (39, 49). GN10, GN11, and NLT GnRH neuronal cells were isolated from an olfactory tumor of migration-arrested GnRH neurons (49), while GT-1 cells (and subclones GT1-1, GT1-3, and GT1-7) were derived from a postmigratory hypothalamic tumor (39). Characterization of these cell lines has provided evidence that many GnRH neuronal attributes were retained during the immortalization process. For example, GT-1 cells secrete GnRH in a pulsatile fashion similarly to GnRH neurons in vivo (39, 65) and can restore reproductive function when implanted into the brains of hypogonadal mice (61). Furthermore, the GT cells resemble GnRH neurons found in vivo displaying perikarya and neurites and express neuron-specific transcripts,

* Corresponding author. Mailing address: Veterans Affairs Medical Center, 1055 Clermont St., Box 111H, Denver, CO 80220. Phone: (303) 399-8020, ext. 3137. Fax: (303) 393-5271. E-mail: Margaret.Wierman@uchsc.edu.

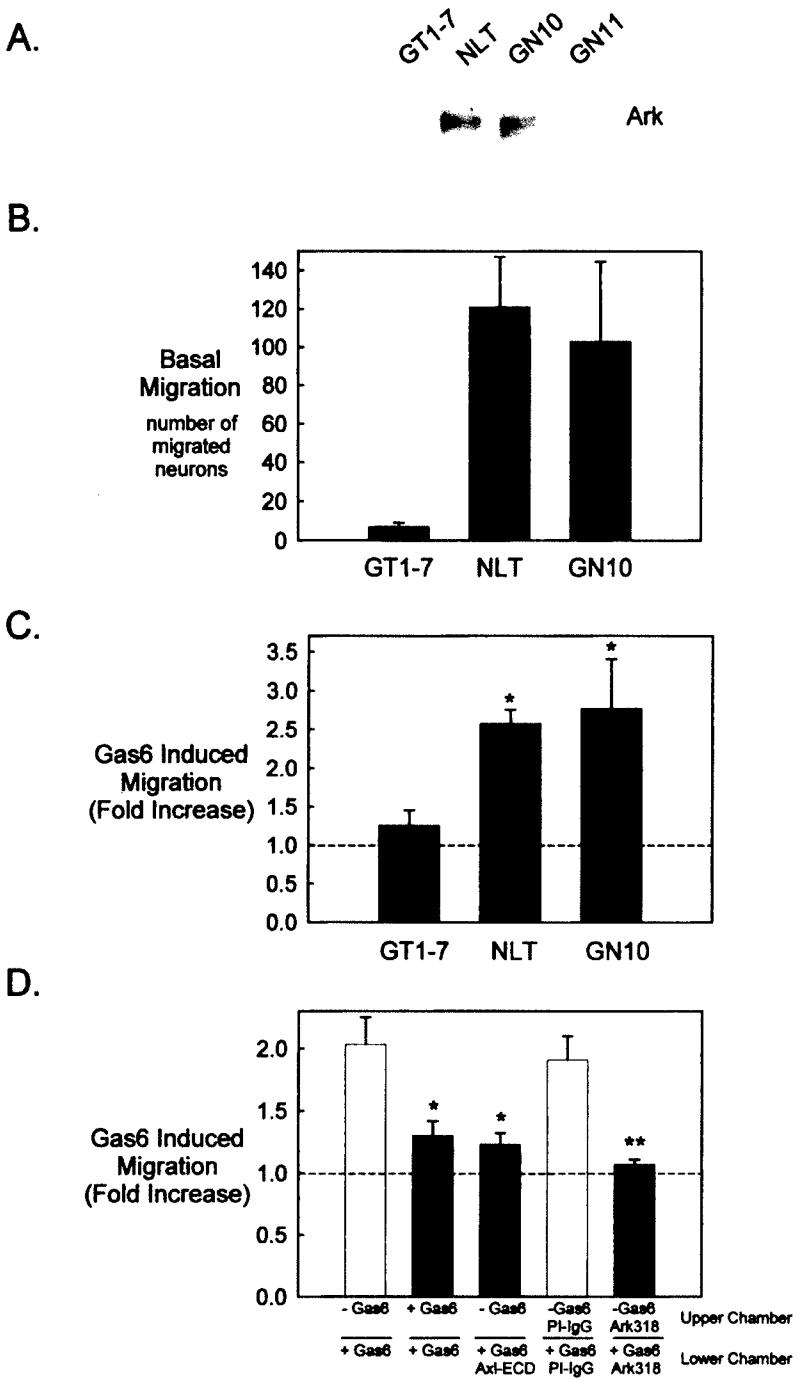

FIG. 1. Gas6 stimulates migration of Ark-expressing GnRH neuronal cell lines. (A) GT1–7, NLT, GN10, and GN11 cell lysates (20 μg) were analyzed by immunoblotting with Ark318 IgG. (B to D) The migratory behavior of the cells was examined with a Boyden chamber system as described in Materials and Methods. (B) Twenty-four-hour migration in the presence of 0.5% FBS in the lower chamber. Values are as follows: GT1-7, 7 ± 2 (n = 4); NLT, 121 ± 26 (n = 4); GN10, 103 ± 42 (n = 6). (C) Twenty-four-hour migration in the presence of Gas6 (400 ng/ml) in the lower chamber (n = 4 for GT1-7 and n = 6 for NLT and GN10). *, statistically significant by the t test: $P < 0.01$ for NLT and $P < 0.05$ for GN10. (D) Effects of Gas6, recombinant Axl ECD (800 ng/ml), Ark318 IgG (10 μg/ml), and PI IgG (10 μg/ml) on migration (24 h). *, statistically significantly different from the control (Gas6 in the lower chamber only) by the Tukey-Kramer multiple comparisons test, $P < 0.05$ (n = 3). **, statistically different from the control (PI IgG in the upper and lower chambers) by the t test. $P < 0.05$ (n = 3).

FIG. 2. Gas6 stimulates Ark-dependent formation of lamellipodia and membrane ruffles in NLT GnRH neuronal cells. (A) NLT cells were incubated with Gas6 (400 ng/ml) for the indicated times. Following fixation, F-actin was visualized with rhodamine phalloidin. Arrows indicate lamellipodia and membrane ruffles. The data are representative of three independent experiments (see Materials and Methods for quantitation of actin cytoskeletal remodeling). Bar = 20 μm. (B) NLT cells were pretreated (4 h) with the Axl ECD (800 ng/ml), Ark318 IgG (10 μg/ml), or PI IgG (10 μg/ml) followed by a 10-min stimulation with Gas6 (400 ng/ml). F-actin was visualized as in panel A. The partial effectiveness of the Ark318 IgG at blocking the Gas6 effect is indicated by the arrow. The data are representative of two independent experiments. Bar = 20 μm.

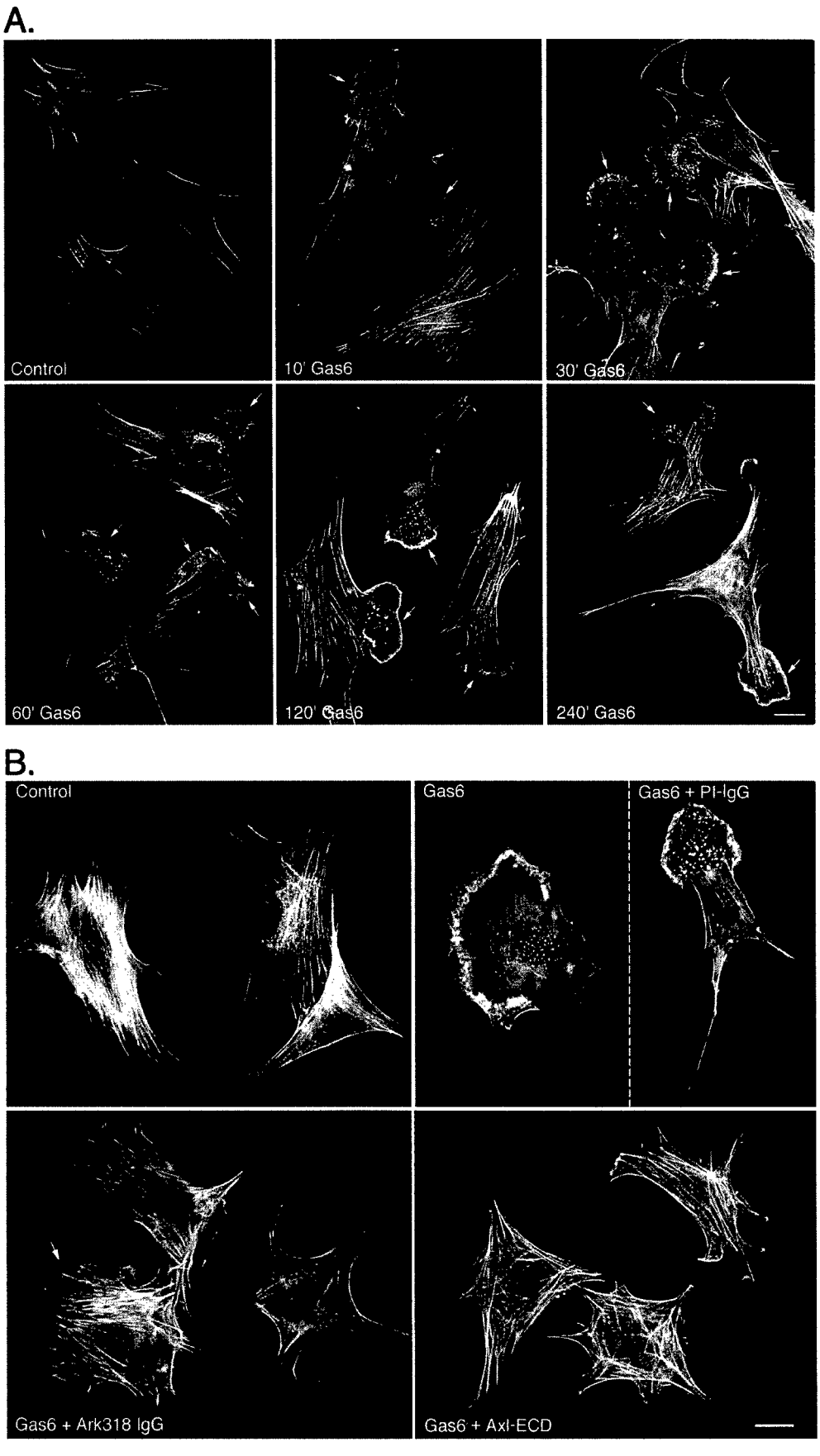
A.
Control
10' Gas6
30' Gas6
60' Gas6
120' Gas6
240' Gas6
B.
Control
Gas6
Gas6 + PI-IgG
Gas6 + Ark318 IgG
Gas6 + Axl-ECD

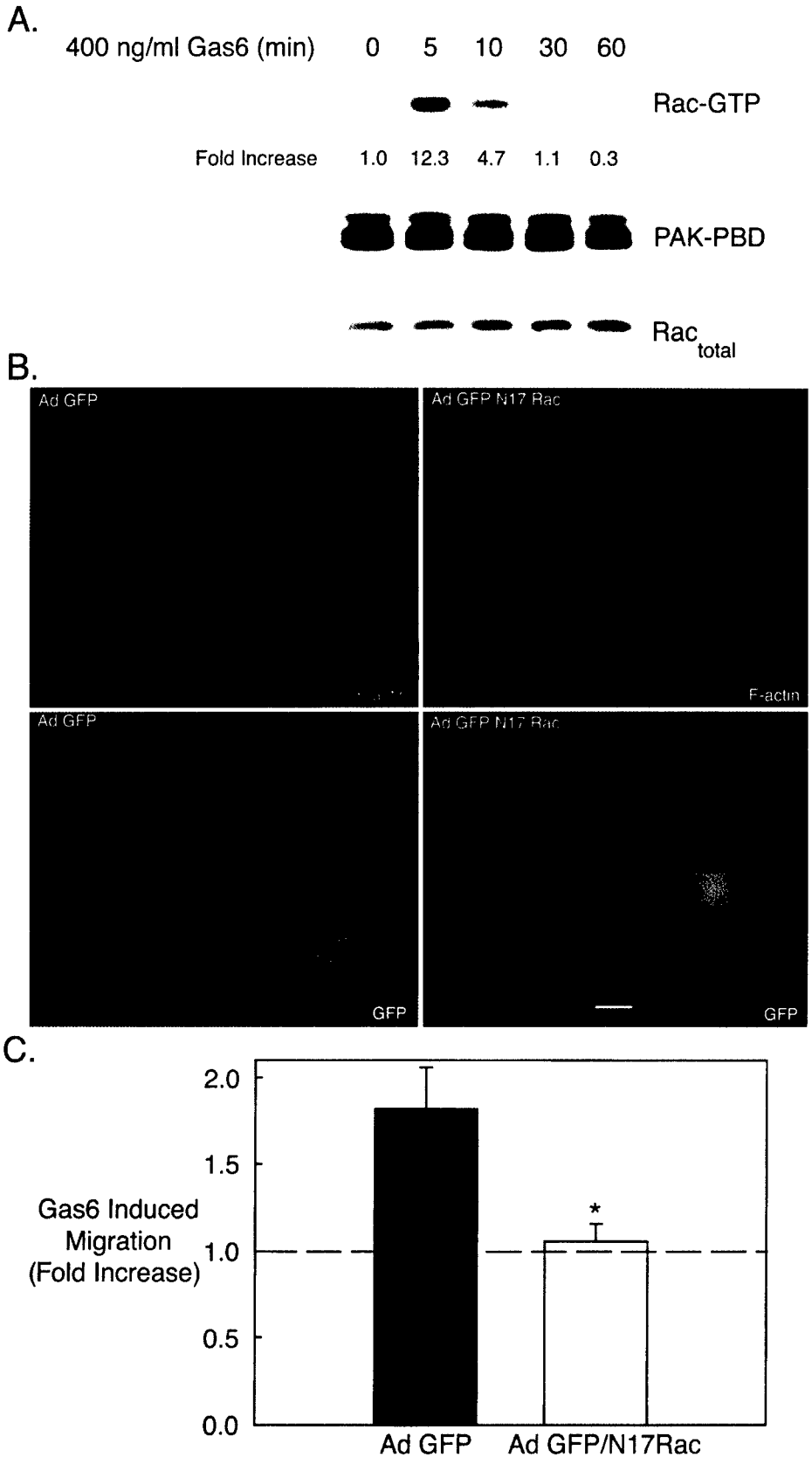

FIG. 3. Gas6/Ark-stimulated NLT migration and cytoskeletal reorganization requires the Rho family GTPase Rac. (A) NLT cells were treated with Gas6 (400 ng/ml) for the indicated times followed by a Rac activation assay. Briefly, GTP-bound Rac (Rac-GTP) was precipitated with PAK-PBD agarose, and GTP-bound Rac was visualized by Rac immunoblotting. Equal amounts of PAK-PBD were used to precipitate Rac-GTP (PAK-PBD blot), and each sample contained a similar amount of Rac protein (for the Rac_{total} blot, 1/20 of each sample was loaded). The data

including neuron-specific enolase and the 68-kDa neurofilament protein (39). Although the GN/NLT cell lines have not been as well characterized, they synthesize GnRH, albeit at a much lower level than the GT clones, and express neuron-specific proteins, including tau and microtubule-associated peptide 2 (49, 72). Furthermore, recent studies have indicated that the GN/NLT neuronal cells are intrinsically motile like GnRH neurons found in the olfactory placode in vivo (36; M. P. Allen et al., 30th Ann. Meet. Soc. Neurosci., abstr. 225.2, 2000). Thus, the immortalized cell lines provide excellent models that mimic both the migratory and postmigratory phenotypes of in vivo GnRH neurons.

To elucidate factors that may regulate GnRH neuron motility, differential display was used to compare the gene expression profiles of postmigratory GT1-7 and migratory GN10 neuronal cell lines (10). One candidate gene that was differentially expressed in the GN10 GnRH cells encoded adhesion-related kinase (Ark), a unique membrane receptor consisting of an extracellular domain akin to cell adhesion molecules and a cytoplasmic tyrosine kinase domain (10). Ark is the murine homolog of the human protein Axl (also known as UFO and Tyro7) (23, 28, 45, 52) and belongs to a novel receptor family that includes Tyro3 (also known as etk2, Dtk, brt, Rse, Sky, and tif) and Mer (also known as Tyro12, eyk, and Nyk) (reviewed in reference 8). Members of this family are expressed in the central nervous system as well as other tissues (28, 47, 52). Ark/Axl family receptors have been shown to promote cell growth and survival (2, 5, 12, 15, 16, 33, 35), adhesion (4, 38), and migration (13) via binding to a common ligand, Gas6 (encoded by growth arrest-specific gene 6) (42, 64). Gas6 is also expressed in the brain, suggesting that Gas6/Ark signaling may play a role in central nervous system physiology (48).

Previous studies from our laboratory demonstrated that Gas6 promotes survival of Ark-expressing migratory GnRH neuronal cells (2). More recent findings have shown that Ark regulates GnRH gene expression (1). Moreover, Ark and GnRH transcripts were detected along the GnRH neuron migratory route in mouse E13 cribriform plate RNA (1). Given the differential expression of Ark in cell lines derived from migratory but not postmigratory GnRH neurons and Ark expression in the cribriform plate during embryogenesis, we explored a role for Gas6/Ark signaling in GnRH neuron motility. In migratory GnRH neuronal cells, Gas6 stimulates Ark-dependent actin cytoskeletal reorganization and chemotaxis via activation of the Rho family GTPase, Rac. Although Rac has previously been implicated in neuronal migration, its downstream targets in neurons remain largely undefined (73). The results illustrate that p38 mitogen-activated protein kinase (MAPK), a protein previously implicated in neuronal apoptosis (68), is required downstream of Rac in Gas6/Ark-induced GnRH neuronal-cell motility. The data are the first to describe an Ark/Axl receptor-mediated migratory signaling pathway. In addition, the data support a novel function for p38 MAPK in regulating neuronal migration.

MATERIALS AND METHODS

Reagents. Recombinant human Gas6 was generated as described previously (64). Ark318 immunoglobulin G (IgG) and preimmune (PI) IgG were generously provided by Claudio Basilico and Paola Bellosta (New York University) (5). PD98059, SB203580, and protein A/G agarose were purchased from Calbiochem (San Diego, Calif.). Rhodamine phalloidin was obtained from Molecular Probes (Eugene, Oreg.). Rabbit polyclonal antibodies that recognize the Tyr/Thr-dually phosphorylated (active) forms of p38 and ERK1/2 were purchased from New England Biolabs (Beverly, Mass.) and Promega (Madison, Wis.), respectively. Polyclonal heat shock protein 25 (HSP25) antibody was obtained from Stressgen (Victoria, Canada). Monoclonal (M2) Flag antibody was from Sigma (St. Louis, Mo.). Polyclonal antibodies to ERK2 and p38 were obtained from Santa Cruz (Santa Cruz, Calif.). Rac activation and MAPK-activated protein (MAPKAP) kinase 2 activation kits were purchased from Upstate Biotechnology (Lake Placid, N.Y.). Purified collagen was purchased from Worthington (Freehold, N.J.). Transwell migration chambers (6.5-mm diameter, 8-μm pore size) were obtained from Costar (Corning, N.Y.). The bicinchoninic acid protein assay kit was purchased from Pierce (Rockford, Ill.). The complete protease inhibitor cocktail was from Boehringer Mannheim (Indianapolis, Ind.). Hybond polyvinylidene difluoride (PVDF) blotting membranes, enhanced chemiluminescence reagents, and horseradish peroxidase-conjugated secondary antibodies were purchased from Amersham (Piscataway, N.J.). Dulbecco's modified Eagle's medium (DMEM) and antibiotics were from Life Technologies (Rockville, Md.), and fetal calf serum was from Gemini Bio-Products (Calabasas, Calif.). The DiffQuik staining kit was from Dade Behring (Newark, Del.). Glass coverslips (12-mm circles) were purchased from Fisher Scientific (Pittsburgh, Pa.).

Cell culture. GN10, GN11, NLT (49), and GT1-7 (39) GnRH neuronal cell lines were grown in DMEM supplemented with 10% fetal calf serum, 100 U of penicillin per ml, 100 μg of streptomycin per ml, and 0.25 μg of amphotericin B per ml at 37°C in humidified 5% CO_2-95% air.

Boyden chamber migration assays. Neuronal cells were rinsed once in PBS and incubated for 16 to 18 h in DMEM supplemented with 0.5% fetal calf serum, 100 U of penicillin per ml, 100 μg of streptomycin per ml, and 0.25 μg of amphotericin B per ml at 37°C in humidified 5% CO_2-95% air. The cells were removed from cell culture plates by trypsin digestion, pelleted by centrifugation at 2,000 × *g* for 5 min, and resuspended in migration medium (DMEM, 0.5% fetal bovine serum [FBS], 0.5% bovine serum albumin, 4 mM $MgCl_2$, 4 mM $CaCl_2$). A total of 30,000 cells were plated into the upper chamber of collagen (0.1 mg/ml)-coated Transwells and allowed to migrate for 24 h at 37°C in humidified 5% CO_2-95% air. For determination of basal migration rates, migration medium was included in the lower Transwell chamber. For chemotaxis experiments, vehicle or Gas6 (400 ng/ml) was added to the lower chamber containing the migration medium. For blocking experiments, the Axl extracellular domain (ECD) was added to the lower chamber at a final concentration of 800 ng/ml. For experiments using PD98059 (30 μM), SB203580 (30 μM), PI IgG (10 μg/ml), and Ark318 IgG (10 μg/ml), the reagents were added to both the upper and lower compartments of the Transwell. For adenoviral experiments, NLT cells were infected for 24 to 48 h and then incubated for 16 to 18 h in low-serum medium (0.5% FBS) like uninfected cells prior to setting up the migration assay. Following the 24-h migration, the cells were fixed and stained by using a DiffQuik kit. The number of migrating cells for each condition was determined by counting cells in four different fields on each membrane.

Immunoblotting. Neuronal cells were washed once in PBS at 4°C and lysed in 0.1 ml of cell lysis buffer containing 20 mM HEPES (pH 7.4), 1% Triton X-100, 50 mM NaCl, 1 mM EGTA, 20 mM sodium orthovanadate, and 50 mM sodium fluoride and supplemented with complete protease inhibitors. Cell debris was removed by centrifugation at 14,000 × *g* for 15 min at 4°C. The protein concentration of the supernatant was determined with a bicinchoninic acid protein assay kit. Protein (20 to 50 μg) was resolved by sodium dodecyl sulfate-polyacrylamide

are representative of three independent experiments. The increase in Rac-GTP was calculated by dividing the Rac-GTP density by the Rac_{total} density at each time point and setting the value at the zero time point to 1. (B) NLT cells were infected with Ad GFP or Ad GFP/N17Rac (see Materials and Methods), stimulated for 10 min with Gas6 (400 ng/ml), and stained with rhodamine phalloidin. Actin is shown in red and GFP is in green. The data are representative of two independent experiments. Bar = 20 μm. (C) NLT cells infected with Ad GFP or GFP/N17Rac were tested in the Boyden chamber migration assay with or without Gas6. *, statistically different from the Ad GFP value by the *t* test, $P < 0.05$ ($n = 5$).

gel electrophoresis (SDS-PAGE) on 7.5 to 12% gels and transferred to PVDF. The membranes were blocked in 5% nonfat milk–TBS-T buffer (137 mM NaCl, 0.1% Tween-20, 20 mM Tris-Cl; pH 7.6) for 1 h at room temperature (RT) or overnight at 4°C. Membranes were incubated for 1 h in primary antibody and washed three times in TBS-T for 15 min. The membranes were incubated in horseradish peroxidase-linked secondary antibody for 30 to 60 min, washed three times in TBS-T for 15 min, and incubated in enhanced chemiluminescence immunodetection reagents according to the manufacturer's instructions. Antibodies to the following proteins were used at the indicated dilutions: phospho-ERK1/2, 1:5,000; ERK2, 1:1,000; phospho-p38, 1:1,000; p38, 1:2,000; Ark318, 1:1,000; HSP25, 1:2,000; and Flag, 1 μg/ml. The Rac activation assay and the MAPKAP kinase 2 activation assay were performed according to the manufacturer's instructions. For adenoviral experiments, NLT cells were infected for 48 h, incubated in low-serum medium (0.5% FBS) for 16 h, and then stimulated with Gas6 (400 ng/ml) for different lengths of time. Following incubation, cell lysates were resolved by SDS-PAGE and immunoblotted for the appropriate proteins as described above. Densitometry analysis was performed with the Bio-Rad Fluor-S multi-imager and Quantity One software.

Actin localization. NLT cells (15,000) were seeded onto sterile glass coverslips. On the following day, the cells were washed once in PBS and incubated for 16 to 18 h in DMEM supplemented with 0.5% fetal calf serum, 100 U of penicillin per ml, 100 μg of streptomycin per ml, and 0.25 μg of amphotericin B per ml at 37°C in humidified 5% CO_2–95% air. For blocking experiments including the Axl ECD (800 ng/ml), PI IgG (10 μg/ml), Ark318 IgG (10 μg/ml), PD98059 (30 μM), and SB203580 (30 μM), the cells were pretreated for 4 h and then stimulated with 400 ng of Gas6 per ml for 10 min. Following Gas6 treatment, the cells were rinsed once in PBS and fixed in 4% paraformaldehyde–PBS for 30 min at RT followed by two additional PBS rinses. The cells were permeabilized in 5% bovine serum albumin–0.2% Triton X-100–PBS for 30 min at RT. F-actin was stained with 25 μl of rhodamine phalloidin per ml in the permeabilization solution for 30 min at RT. The cells were rinsed three times with PBS, mounted on slides, and viewed with a Zeiss Axioskop II microscope. For adenoviral experiments, the cells were infected for 24 to 48 h, trypsinized, and replated at 15,000 cells/coverslip as described above for uninfected cells. To quantitate the percentage of cells that displayed membrane ruffles and/or lamellipodia, cells in three fields were counted on each coverslip. For statistical analysis, n is the number of fields counted.

Adenoviruses. The wild-type p38α, dominant negative p38α (p38αDN), and constitutively active MKK6 (MKK6CA) plasmids were generously provided by Roger Davis (University of Massachusetts Medical School). p38αDN contains two mutations, Thr-180 to Ala and Tyr-182 to Phe (50). In the MKK6CA mutant, Ser-207 and Thr-211 were replaced by Glu (51). Adenoviruses containing p38α, p38αDN, and MKK6CA were generated by subcloning the various cDNAs into the shuttle plasmid pACCMV (14) followed by overlap recombination with the adenoviral vector Ad5*dl*327$_{RSV}$β-gal (57). Large-scale virus stocks were purified by cesium chloride gradient centrifugation, and titers were determined by plaque assays in 293 cells.

To construct Rac1 adenoviruses, Rac1 was cloned from a mouse cDNA library, and mutations (Rac1G12V and Rac1T17N) were generated by PCR-based site-directed mutagenesis. The adenoviral green fluorescent protein (GFP), GFP/N17Rac, and GFP/V12Rac were generated with the AdEasy system (19). The Rac adenoviruses coexpress GFP and the respective mutant Rac protein. For immunoblotting experiments, GFP-, GFP/N17Rac-, and GFP/V12Rac-expressing adenoviruses were used at a multiplicity of infection (MOI) of 40 PFU per cell, and the MKK6CA- and wild-type-p38α-bearing adenoviruses were used at an MOI of 100 PFU/cell. For migration experiments, GFP and GFP/N17Rac were used at 10 to 20 PFU/cell, and the p38αDN adenovirus was used at 50 PFU/cell. The empty adenovirus (Ad-CMV) was used at the same MOI as others in the respective experiment and served as a negative control. For actin localization, GFP, GFP/N17Rac, and GFP/V12Rac were used at 40 to 80 PFU/cell, and MKK6CA and p38α were used at 100 PFU/cell.

^{32}P incorporation into HSP25. NLT cells were incubated overnight in DMEM containing 0.5% FBS. The cells were then incubated for 4 h in phosphate-free DMEM–0.5% FBS and 2 mCi of $^{32}P_i$. Subsequently, the cells were washed twice in phosphate-free medium and stimulated with Gas6 (400 ng/ml) for 10 to 30 min. Cells were lysed (see "Immunoblotting" above), and the lysate was incubated with anti-HSP25 antibody for 2 h at 4°C with constant mixing. Protein A/G agarose was added to the lysate, and incubation was continued for another 2 h. The protein A/G agarose was washed three times in cold lysis buffer, and the samples were boiled and loaded onto a SDS–12.5% PAGE gel. The proteins were transferred to PVDF, and the membrane was exposed to film for 4 h at RT to detect phosphorylated HSP25. Subsequently, the membrane was probed with anti-HSP25 antibody to detect the total HSP25 protein present.

RESULTS

Gas6 promotes migration of Ark-expressing GnRH neuronal cell lines. Previous differential display analysis demonstrated Ark expression in migratory (GN10) but not postmigratory (GT1-7) GnRH neuronal cells (10). In addition to the GN10 cells, two other cell lines were established from simian virus 40 T-antigen immortalized migratory GnRH neurons, the GN11 and NLT lines (49). Immunoblot analysis with a polyclonal Ark antibody (Ark318) revealed the restricted expression of Ark in all three cell lines derived from migratory GnRH neurons (GN10, GN11, and NLT) but not GT1-7 cells (Fig. 1A). However, Ark expression was substantially lower in the GN11 subclone than in the GN10 and NLT cells. Therefore, the GN11 cell line was not further investigated in this study.

Because the GN10 and NLT GnRH neuronal cells were isolated during migration, we suspected that they retained motile characteristics that had been lost by the postmigratory GT1-7 cells. To test this hypothesis, a Boyden chamber system was utilized to examine the migratory behavior of the cell lines. A Boyden chamber consists of an upper porous membrane on which the cells of interest are seeded and a lower chamber containing a chemoattractant. In a typical assay, cells migrate through the pores and attach to the lower side of the membrane, and subsequently the number of migrated cells is determined. As predicted, the GN10 and NLT GnRH neuronal cells were intrinsically migratory, unlike the GT1-7 cells (Fig. 1B).

To examine a role for Ark in GnRH neuronal-cell motility, Gas6, the Ark ligand, was included as the chemoattractant in the migration assay. As shown in Fig. 1C, Gas6 (400 ng/ml) potentiated NLT and GN10 migration 2.6-fold ($n = 4$, $P < 0.01$) and 2.7-fold ($n = 6$, $P < 0.05$), respectively, while having no significant effect on Ark-negative GT1-7 cells (1.2-fold increase; $n = 4$, $P = 0.36$). Inclusion of Gas6 in both the upper and lower compartments effectively attenuated NLT migration, indicating that the effect was chemotactic rather than chemokinetic (Fig. 1D). Moreover, the Axl ECD and the polyclonal anti-Ark318 IgG antagonized NLT migration, demon-

FIG. 4. The ERK pathway is not essential for development of the motile phenotype induced by Gas6/Ark signaling. (A) NLT cells were treated for the indicated times with Gas6 (400 ng/ml) and immunoblotted for phospho-ERK1/2 and total ERK2. In the last lane, cells were pretreated for 4 h with PD98059 (PD) (30 μM) and then stimulated with Gas6 for 10 min. The data are representative of two independent experiments. The increase in phospho-ERK1/2 was calculated by dividing the phospho-ERK1/2 density by the total ERK2 density at each time point and then setting the zero time point value to 1. (B) NLT cells were pretreated for 4 h with PD (30 μM), stimulated with Gas6 (10 min), and then stained with rhodamine phalloidin. The data are representative of four independent experiments. Bar = 20 μm. (C) NLT cells were subjected to the migration assay in the presence of vehicle (DMSO) or PD (30 μM) as described in Materials and Methods. The data are the fold increase in migration in the presence of Gas6 (400 ng/ml). *, $P = 0.05$ ($n = 5$, t test).

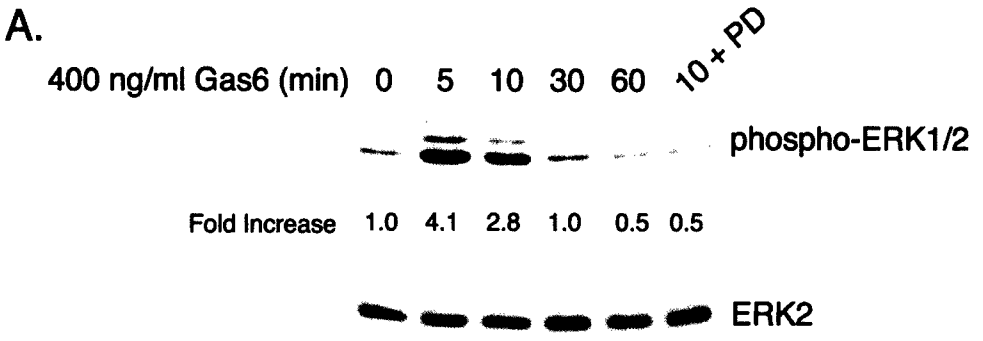
A.
400 ng/ml Gas6 (min) 0 5 10 30 60 10+PD
phospho-ERK1/2
Fold Increase 1.0 4.1 2.8 1.0 0.5 0.5
ERK2

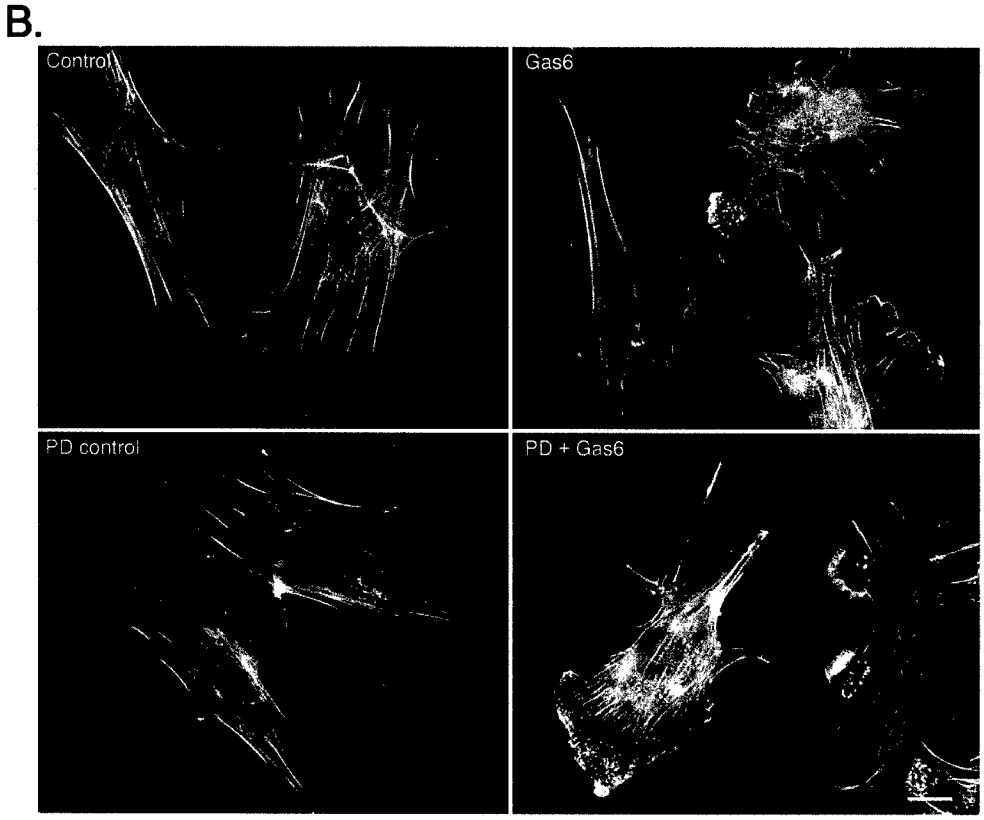
B.
Control
Gas6
PD control
PD + Gas6

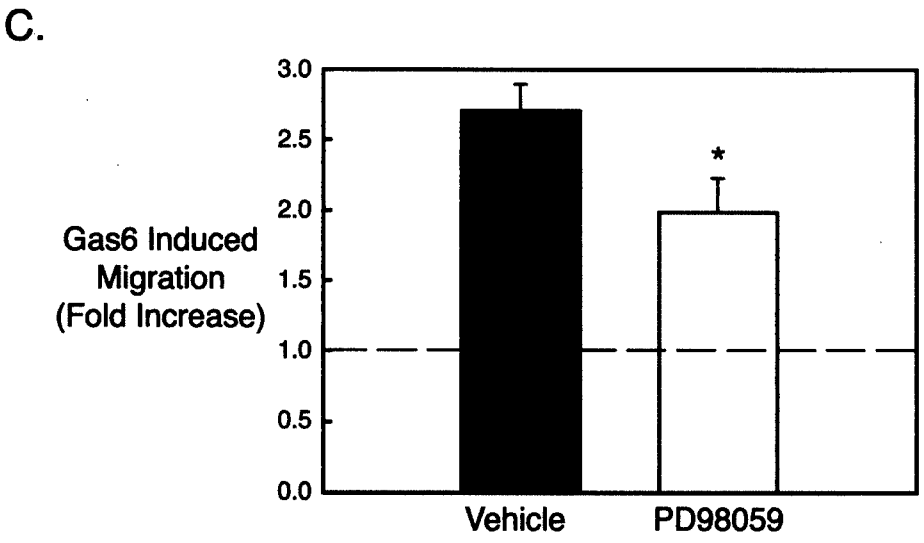
C.
Gas6 Induced Migration (Fold Increase)
3.0
2.5
2.0
1.5
1.0
0.5
0.0
*
Vehicle
PD98059

strating that the effect was both ligand and receptor dependent, respectively (Fig. 1D). Since similar results were obtained with the GN10 neuronal cell line (data not shown), in the remainder of the studies we utilized the NLT cell line as representative of migratory GnRH neurons.

Gas6 stimulates actin cytoskeletal remodeling and migration of NLT GnRH neuronal cells via Ark and the small G protein Rac. A morphological hallmark of cellular motility is the development of membrane ruffles and lamellipodia that are readily visualized by staining cellular filamentous actin (F-actin). Examination of unstimulated NLT cells revealed an intense actin stress fiber network (Fig. 2A). Gas6 treatment (400 ng/ml) resulted in dramatic reorganization of the NLT actin cytoskeleton to a motile phenotype that occurred within 10 min and persisted for at least 4 h (Fig. 2A). In this assay, 9% ± 1.5% of control NLT cells displayed membrane ruffles and/or lamellipodia. After 10 min of Gas6 treatment, 63% ± 3% of NLT cells displayed these cytoskeletal modifications ($n = 9$, $P < 0.0001$). Consistent with the results obtained for NLT migration (Fig. 1D), Gas6-mediated cytoskeletal remodeling was significantly abolished by the Axl ECD and the anti-Ark318 IgG, while PI IgG had no effect (Fig. 2B) (percentages of cells displaying membrane ruffles and/or lamellipodia: Gas6, 65% ± 5%; Gas6 plus PI IgG, 54% ± 10%; Gas6 plus Ark318 IgG, 23% ± 2%; Gas6 plus Axl ECD, 22% ± 3%; $n = 6$; for the last two values, $P < 0.001$ versus the Gas6 value). Thus, Gas6-induced actin cytoskeletal remodeling and migration of NLT GnRH neuronal cells are Ark dependent.

Actin cytoskeletal dynamics are regulated by the Rho family of monomeric GTPases (17). Of the Rho family GTPases, Rho, Rac, and Cdc42, Rac is the principal regulator of membrane ruffling and lamellipodial formation (53). To examine whether Gas6 stimulated Ark signaling to Rac, active (GTP-bound) Rac was precipitated from Gas6-treated cells with the Rac binding domain of the effector protein PAK (PAK-PBD). Subsequently, precipitated Rac was detected by immunoblot analysis. Since the PAK-PBD interacts exclusively with active (GTP-bound) Rac, the Rac immunoblot represents the amount of active Rac in each sample (6). Gas6 treatment of NLT cells resulted in significant Rac activation that peaked within 5 min (12.3-fold), remained elevated at 10 min, and returned to near baseline by 30 min (Fig. 3A, top). Gas6 addition had no effect on the amount of total Rac (GDP plus GTP bound) detected in NLT lysates (Fig. 3A, bottom).

Next, Rac participation in Gas6/Ark-mediated cytoskeletal remodeling and migration was evaluated. NLT cells expressing adenoviral GFP (Ad GFP) developed prominent lamellipodia and membrane ruffles upon exposure to Gas6 in a manner similar to that of uninfected NLT cells in the same culture (Fig. 3B, left panels) (71% ± 5% of GFP-expressing cells underwent actin cytoskeletal reorganization following Gas6 treatment). In contrast, NLT cells expressing GFP and dominant negative Rac (Ad GFP/N17Rac) did not form lamellipodia in the presence of agonist, whereas uninfected neighboring neuronal cells responded to Gas6 with profound actin reorganization (Fig. 3B, right panels) (7% ± 2% of GFP/N17Rac-expressing cells responded to Gas6; $n = 9$, $P < 0.0001$). Similarly, NLT cells expressing Ad GFP migrated in response to Gas6 (1.82-fold increase), whereas cells expressing Ad GFP/N17Rac were unresponsive to agonist treatment (1.05-fold increase relative to control) (Fig. 3C) ($n = 4$, $P < 0.05$). In addition, the basal migration of GFP/N17Rac-expressing neuronal cells was only 29% ± 8% of that of GFP-expressing cells. Together, these data demonstrate that Rac activity is obligatory for both basal and Gas6/Ark-mediated cytoskeletal reorganization and chemotaxis of NLT GnRH neuronal cells.

The ERK pathway is not essential for Gas6/Ark-induced migration of GnRH neuronal cells. Previous studies from our laboratory implicated the ERK pathway in Gas6/Ark mediated GnRH neuronal survival and regulation of GnRH gene expression (2; M. P. Allen et al., 82nd Ann. Meet. Endocr. Soc. abstr. 519, 2000). Furthermore, ERK is required for migration of other cell types (69). Therefore, we investigated whether the ERK pathway played a role in Gas6/Ark-mediated GnRH neuronal migration. In NLT GnRH neuronal cells, Gas6 stimulated a rapid and transient activation of the ERK pathway that peaked at 5 min (4.1-fold) and returned to baseline by 30 min (Fig. 4A). Furthermore, Gas6-stimulated ERK activation was effectively abolished by the MEK1/2 inhibitor PD98059 (Fig. 4A). To determine if the ERK pathway was required for Gas6/Ark-induced ruffling and lamellipodial formation, NLT cells were incubated with PD98059 (30 μM, 4 h), stimulated with agonist for 10 min, and stained with rhodamine phalloidin (Fig. 4B). Although PD98059 clearly blocked ERK activation (Fig. 4A), it had no discernible effect on Gas6-mediated actin remodeling of NLT cells (Fig. 4B) (Gas6 plus dimethyl sulfoxide [DMSO], 71% ± 5% ruffling and/or lamellipodia, versus Gas6 plus PD98059, 61% ± 3%; $n = 9$, $P = 0.13$). Likewise, the MEK1/2 inhibitor only partially attenuated Gas6-stimulated NLT migration (vehicle, 2.7-fold increase; PD98059, 2.0-fold increase; $n = 5$, $P = 0.05$) (Fig. 4C) (similar results were obtained with the structurally distinct MEK inhibitor, UO126; data not shown). Thus, although the ERK pathway acts downstream of Gas6 and Ark to influence GnRH neuronal survival and gene expression, it is not essential in the migratory signaling pathway.

Gas6/Ark signaling induces migration of GnRH neuronal cells via a Rac → p38 MAPK → MAPKAP kinase 2 → HSP25 pathway. Recent studies have suggested a role for p38 MAPK in smooth muscle cell motility (20). Therefore, Gas6/Ark-induced p38 activation in NLT neuronal cells was examined by immunoblotting with a phospho-specific p38 antiserum (Fig. 5A). Agonist treatment resulted in marked p38 activation within 5 min (3.0-fold) that remained elevated for at least 1 h. In smooth muscle cells, growth factor-induced migration involves activation of a p38 MAPK → MAPKAP kinase 2 → heat shock protein 27 (HSP27) pathway, where HSP27 functions as an actin-capping protein and is thought to modulate actin polymerization and cell shape (29). Gas6/Ark-induced MAPKAP kinase 2 activity was evaluated in NLT cells by using an immunoprecipitation-kinase assay (Fig. 5B). MAPKAP kinase 2 was immunoprecipitated from Gas6-treated cells and incubated with recombinant human HSP27 in a kinase assay, and phosphorylated HSP27 was detected by using a phospho-specific HSP27 antiserum. As shown in Fig. 5B, Gas6 treatment resulted in a 12.9-fold increase in MAPKAP kinase 2 activity within 5 min that remained elevated for at least 1 h. To examine if endogenous NLT HSP25 (the murine isoform of HSP27) was activated (phosphorylated) following agonist treatment, an HSP25 immunoblot was performed (Fig. 5C).

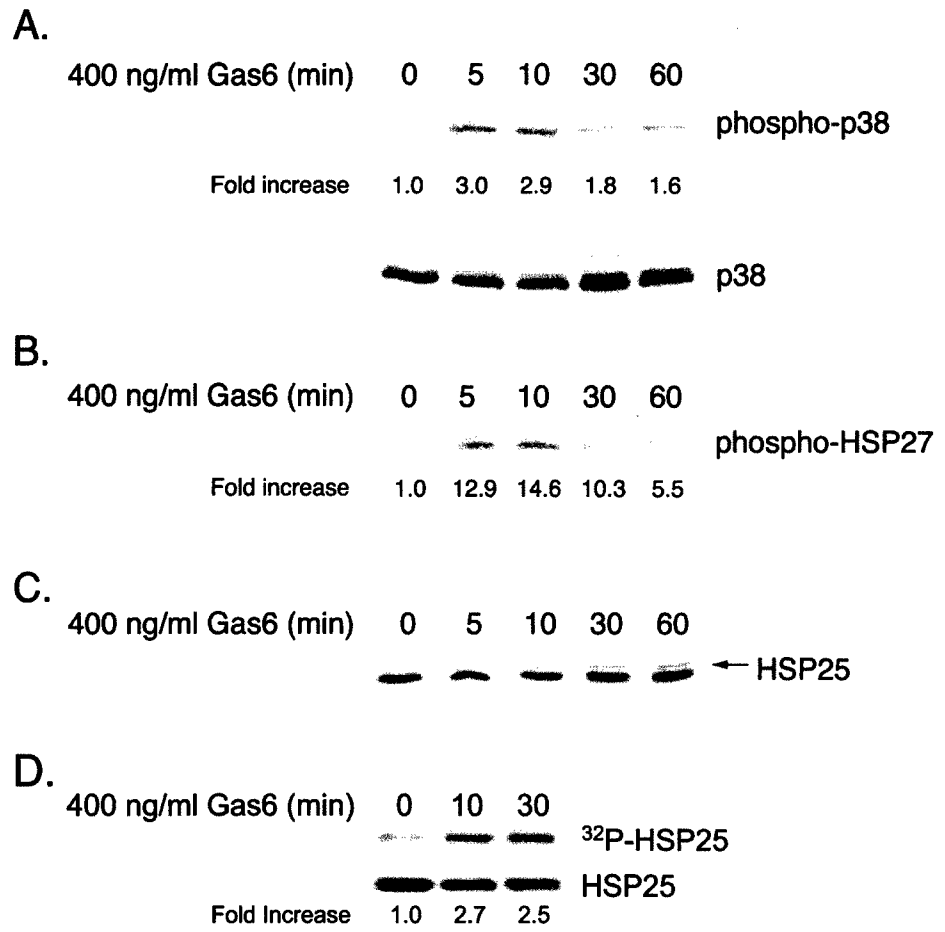

FIG. 5. Gas6/Ark signaling activates a p38 MAPK → MAPKAP kinase 2 → HSP25 signaling cascade in NLT GnRH neuronal cells. (A) NLT cells were treated for the indicated times with Gas6 (400 ng/ml) and immunoblotted for phospho-p38 and total p38. The data are representative of three independent experiments. The increase in phospho-p38 was calculated by dividing the phospho-p38 density by the total p38 density at each time point and setting the zero time point value to 1. (B) MAPKAP kinase 2 was immunoprecipitated from Gas6-treated neuronal cells and exposed to recombinant human HSP27 in a kinase assay, and phosphorylated HSP27 was detected by phospho-HSP27 immunoblotting. The data are representative of two independent experiments. The increase in phospho-HSP27 was calculated by setting the zero time point value at 1. (C) NLT cells were treated for the indicated times with Gas6 (400 ng/ml) and immunoblotted for HSP25. The arrow indicates a slower-migrating form of HSP25 consistent with phosphorylation. The data are representative of two independent experiments. (D) NLT cells were labeled with $^{32}P_i$ and stimulated with Gas6. HSP25 was immunoprecipitated from the cell lysates, transferred to PVDF, and analyzed by autoradiography (top) or HSP25 immunoblotting (bottom). The increase in ^{32}P-labeled HSP25 was calculated by dividing the ^{32}P-labeled-HSP25 density by the total HSP25 density at each time point and setting the zero time point value to 1. The data are representative of two experiments.

Exposure to Gas6 resulted in the increased formation of a slower-migrating form of HSP25 within 30 min that was sustained to 60 min, suggesting that Gas6 had indeed stimulated phosphorylation of HSP25. To confirm the phosphorylation of HSP25, NLT cells were pretreated with $^{32}P_i$ to radiolabel the cellular ATP, and HSP25 was immunoprecipitated from lysates that had been treated with Gas6 for 10 to 30 min. Gas6 treatment resulted in a 2.7-fold increase in the incorporation of $^{32}P_i$ into HSP25 within 10 min (Fig. 5D, top) while having no effect on the total amount of HSP25 present in the cells (Fig. 5D, bottom). Thus, Gas6/Ark signaling promotes the sequential activation of p38 MAPK, MAPKAP kinase 2, and HSP25 in NLT GnRH neuronal cells.

Rac and Cdc42 GTPases have been shown to function upstream of p38 MAPK (71). To resolve whether Gas6/Ark-stimulated p38 MAPK activation was downstream of Rac, NLT cells were infected with Ad GFP or with Ad GFP/N17Rac prior to Gas6 addition (Fig. 6A). Gas6 treatment of GFP-expressing NLT neuronal cells resulted in p38 activation (2.2-fold), while cells expressing GFP/N17Rac were unresponsive to the agonist (0.7-fold), demonstrating that p38 is downstream of Rac in this receptor system (Fig. 6A). In addition, expression of adenoviral constitutively active Rac (Ad GFP/V12Rac) in NLT cells resulted in ligand-independent p38 activation (2.7-fold) (Fig. 6B) and induced dramatic membrane ruffling (Fig. 6C, left panels). Furthermore, V12Rac-stimulated ruffling (GFP/V12Rac without SB203580, 82% ± 5%) was markedly inhibited upon exposure to the selective p38 inhibitor, SB203580 (34% ± 7%), demonstrating that p38 activation was required for V12Rac-induced cytoskeletal remodeling (Fig. 6C, right panels) ($n = 12$, $P < 0.0001$). Finally, NLT cells coinfected with adenoviral MKK6CA and Flag-tagged wild-type p38α were examined by immunoblot analysis (Fig. 7B) and in the actin assay (Fig. 6D). Expression of adenoviral

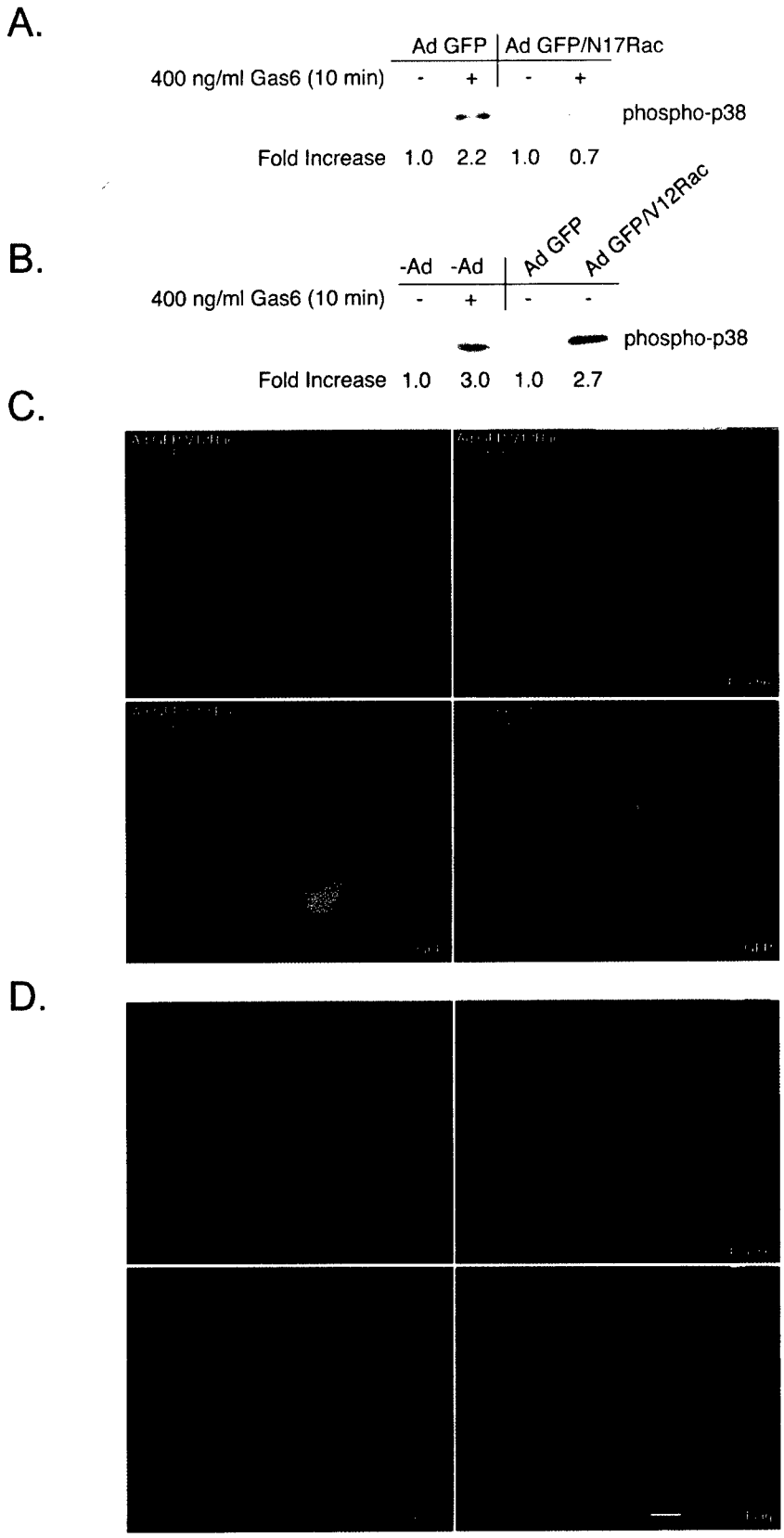

FIG. 6. p38 activation promotes actin reorganization downstream of Rac in NLT GnRH neuronal cells. (A) NLT cells expressing Ad GFP or GFP/N17Rac were treated for 10 min with Gas6 (400 ng/ml) and then immunoblotted for phospho-p38. The data are representative of two independent experiments. The increase in phospho-p38 was calculated by setting the density of the no-Gas6 samples to 1. (B) uninfected NLT cells or those expressing Ad GFP or GFP/V12Rac were treated for 10 min with Gas6 (400 ng/ml) or vehicle and then immunoblotted for phospho-p38.

MKK6CA and Flag-p38α in NLT neuronal cells resulted in robust p38 activation (Fig. 7B, phospho-p38 blot). Consistent with p38 activation promoting cytoskeletal reorganization, NLT cells positive for the Flag epitope (p38α) exhibited ligand-independent lamellipodial advance (Fig. 6D, right panels), whereas uninfected cells did not extend lamellipodia (Fig. 6D, left panels) (9% ± 2% for uninfected cells versus 76% ± 4% for MKK6CA/p38α-infected cells; $n = 18$, $P < 0.0001$). Collectively, these data demonstrate that p38 lies downstream of Rac and is the major Rac target engaged in NLT GnRH neuronal cells to elicit actin cytoskeletal remodeling.

Next we investigated the role of p38 in Gas6/Ark-stimulated lamellipodial extension and migration. Pretreatment of NLT cells with the p38 inhibitor SB203580 (30 μM, 4 h), resulted in a striking inhibition of Gas6/Ark-mediated cytoskeletal remodeling (Fig. 7A) (71% ± 5% membrane ruffles and/or lamellipodia for Gas6 plus DMSO versus 20% ± 3% for Gas6 plus SB303580; $n = 9$, $P < 0.0001$). SB203580 also markedly blocked Gas6-induced NLT migration, decreasing the Gas6 effect from 2.6-fold to 0.96-fold (Fig. 7B) ($n = 3$, $P < 0.05$).

To further verify that p38 MAPK was required for NLT migration via Gas6/Ark signaling, NLT cells infected with adenoviral Flag-tagged p38αDN were tested in the migration assay. As shown in Fig. 7B, the Flag-p38αDN was efficiently expressed in the NLT cells (Flag immunoblot). However, in the presence of adenovirally expressed MKK6CA, p38 activation was blocked in p38αDN-expressing neuronal cells, while those expressing wild-type p38α exhibited significant increases in active p38 (phospho-p38 blot). These data confirmed that p38αDN functioned in a dominant negative fashion. In addition, cells infected with empty adenovirus (Ad-CMV) responded to Gas6 similarly to uninfected cells (2.0- versus 2.3-fold increase relative to control). NLT cells infected with Ad-p38αDN, however, were unresponsive to Gas6 (1.14-fold stimulation) ($n = 4$, $P < 0.01$ for uninfected cells and $P < 0.05$ for cells infected with Ad-CMV). Together, the data illustrate that Gas6/Ark-mediated GnRH neuronal migration requires p38 MAPK.

DISCUSSION

The intrinsic signaling mechanisms that regulate GnRH neuron migration are unknown. In the present study, we used immortalized GnRH neuronal cell lines that retain properties found in vivo in either migratory or postmigratory GnRH neurons to investigate the mechanism underlying GnRH neuron migration. Because Ark is expressed in immortalized migratory GnRH neuronal cell lines (10) and along the GnRH neuron pathway during development (1), we examined a role for Ark in GnRH neuronal motility. Our results identified the Gas6/Ark interaction as a novel signaling complex that promotes NLT GnRH neuronal-cell migration. Characterization of the signaling pathway downstream of Gas6/Ark revealed that the small GTPase, Rac, signals to p38 MAPK to induce NLT GnRH neuronal motility. These data are the first to describe a receptor-initiated signal transduction cascade that directly regulates the migration of GnRH neuronal cells.

The Ark receptor ECD contains fibronectin type III repeats and immunoglobulin domains related to cell adhesion molecules. Not surprisingly, Ark has recently been implicated in cell adhesion and aggregation (4, 38). Moreover, Fridell et al. (13) recently provided evidence for Axl (the human homolog of Ark)-mediated chemotaxis of vascular smooth muscle cells. However, the signaling pathways downstream of Axl were not identified. While examining a role for Ark in GnRH neuron migration, we found that Gas6, the Ark ligand, potentiated the migration of Ark-expressing GN10 and NLT GnRH neuronal cell lines while having no discernible effect on GT1-7 cells. In addition, Gas6-induced motility was chemotactic and was blocked by an antibody to the Ark ECD and by sequestration of Gas6 with recombinant Axl ECD. Thus, Gas6 occupancy of the Ark receptor stimulates GnRH neuronal-cell migration.

To examine signaling pathways involved in motility downstream of Gas6/Ark, we first looked at changes in the actin cytoskeleton. In NLT cells, Gas6/Ark signaling stimulated dramatic lamellipodial extension and membrane ruffling. Members of the Rho family of small GTPases, Rho, Rac, and Cdc42, regulate morphological changes of the actin cytoskeleton and, as a result, elicit profound effects on cellular adhesion and motility (17). Rac is known to promote formation of lamellipodia and membrane ruffles (53). Thus, the actin remodeling observed upon Gas6 treatment suggested that Rac was activated downstream of the receptor-ligand interaction in GnRH neuronal cells. Indeed, direct measurement of active (GTP-bound) Rac revealed that Gas6 induced robust Rac activation in NLT cells. Moreover, dominant negative N17Rac significantly abolished both Gas6-induced actin cytoskeletal remodeling and migration of NLT cells. Together, these results demonstrated that the Ark receptor couples to the Rho family GTPase Rac to orchestrate actin cytoskeletal changes and chemotaxis of GnRH neuronal cells. These findings are consistent with a recently recognized role for Rac GTPase in the regulation of neuronal migration (73). Although several neuron-specific guanine nucleotide exchange factors, including Tiam-1 (9, 31), ASEF (25), and Trio (3, 34, 43), upstream of Rac have been described, downstream targets of Rac in neurons are largely unknown.

Both ERK and p38 MAPK pathways have previously been described to play a role in nonneuronal-cell migration (20, 69), and both pathways have been shown to be activated via Rac GTPase (7, 71). Therefore, we focused on the potential role of these two MAPK signaling pathways downstream of Rac in Gas6/Ark-stimulated GnRH neuronal-cell motility. Although the MEK1/2 inhibitor PD98059 clearly blocked Gas6/Ark-stimulated ERK activation, it had only modest effects on cytoskeletal changes and motility. The effect of PD98059 on

The data are representative of two independent experiments. (C) NLT cells were infected with adenoviruses expressing GFP/V12Rac (see Materials and Methods), treated for 4 h with vehicle (DMSO) or SB203580 (30 μM) and then stained with rhodamine phalloidin. The data are representative of two independent experiments. Actin is shown in red and GFP is in green. Bar = 20 μm. (D) NLT cells infected with adenoviral MKK6CA and Flag-p38α were visualized with rhodamine phalloidin and anti-Flag immunocytochemistry (left panels, uninfected cells; right panels, cells infected with MKK6CA and Flag-p38α). Bar = 20 μm.

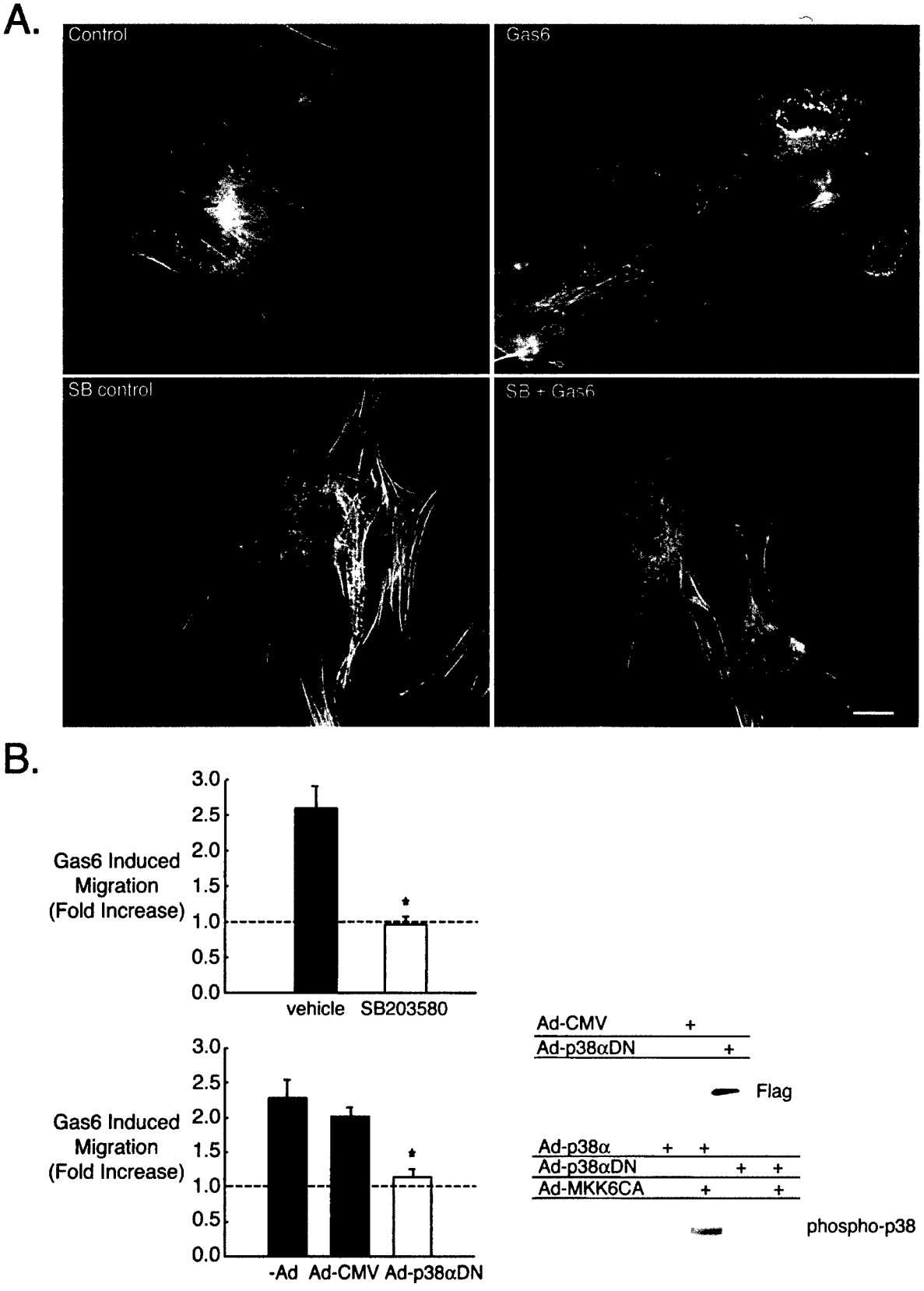

FIG. 7. Gas6/Ark-mediated GnRH neuronal cytoskeletal remodeling and migration requires p38 MAPK. (A) NLT cells were pretreated for 4 h with SB203580 (SB) (30 μM), stimulated with Gas6 (10 min), and then stained with rhodamine phalloidin. Bar = 20 μm. The data are representative of four independent experiments. (B) (Left) The effect of Gas6 on NLT migration was examined in the presence of vehicle (DMSO) or SB (30 μM) and in neurons infected with either Ad-CMV or Ad-p38αDN as described in Materials and Methods. *, $P < 0.05$ for SB versus vehicle ($n = 3$, t test); $P < 0.01$ for p38αDN versus −Ad and $P < 0.05$ for p38αDN versus Ad-CMV ($n = 4$, Tukey-Kramer multiple comparisons test). (Right) Anti-Flag immunoblotting demonstrated that adenoviral Flag-p38αDN was efficiently expressed in the NLT neurons. The phospho-p38 blot demonstrated that wild-type p38α (Ad-p38α) was activated in the presence of Ad-MKK6CA, but Ad-p38αDN was not.

Gas6-induced migration reached statistical significance ($P = 0.05$), however, suggesting that the ERK pathway may regulate a Rac-independent pathway involved in migration. For instance, recent studies have shown that Rho activity is regulated by the ERK-MAPK pathway (56). Since Rho is required for focal adhesion turnover at both the leading and trailing edges of the cell, disruption of Rho signaling results in decreased motility. Thus, in NLT cells, the ERK pathway blockade may inhibit motility via partial disruption of Rho signaling. Alternatively, PD98059 may affect NLT survival, consistent with our previous studies showing that Ark promotes GnRH neuronal survival via an ERK-dependent mechanism (2).

In contrast, pharmacological p38 MAPK inhibition dramatically attenuated Gas6/Ark-induced cytoskeletal reorganization and migration. Similarly, p38αDN completely blocked Gas6-induced GnRH neuronal chemotaxis. In addition, p38 MAPK was demonstrated to function as a downstream Rac target, since Gas6 activation of p38 was abolished in dominant negative-N17Rac-expressing cells. Moreover, constitutively active V12Rac stimulated p38 activation and induced dramatic membrane ruffling of NLT cells. The latter effect was significantly inhibited by blockade of p38 activation with SB203580, suggesting that p38 is the major Rac target engaged in GnRH neuronal cells to elicit cytoskeletal reorganization. Finally, overexpression of constitutively active p38 was sufficient to induce lamellipodial advance and membrane ruffling in NLT cells. Thus, p38 MAPK acts downstream of Rac GTPase to promote GnRH neuronal-cell motility.

The above findings were somewhat unexpected, since p38 activation in neurons was initially associated with increased apoptosis (27, 40, 68). Recently, p38 has also been shown to modulate PC12 pheochromocytoma cell neurite outgrowth during differentiation (18, 22, 41, 63). Coupled with our observation that p38 lies downstream of Rac in Gas6/Ark-stimulated GnRH neuron motility, these results are consistent with a much broader role for p38 MAPK in neurons, perhaps in the regulation of migration and neurite outgrowth during development and differentiation.

p38 MAPK has been shown to modulate nonneuronal-cell motility (20, 21, 26, 37, 44, 55). Recent studies suggest that p38 MAPK activates a MAPKAP kinase 2/HSP27 (HSP25 in mouse) signaling cascade that is important in smooth muscle cell actin cytoskeletal remodeling and motility (20, 30, 46, 55). HSP27 is an actin-capping protein whose activity is regulated via serine phosphorylation by upstream kinases such as MAPKAP kinase 2. Although the mechanism is not completely understood, HSP27 regulation of actin polymerization is involved in cortical actin cytoskeletal rearrangements such as membrane ruffling (29). Similar to growth factor stimulation of smooth muscle cells (20), we found that NLT GnRH neuronal cells treated with Gas6 exhibited increased MAPKAP kinase 2 activity and HSP25 phosphorylation. These data are consistent with a mechanism by which Gas6/Ark signaling stimulates GnRH neuronal migration via a Rac → p38 MAPK → MAPKAP kinase 2 → HSP25 pathway. The role of additional signaling pathways downstream of p38 that may also influence motility remains to be clarified.

In summary, we have utilized GnRH neuronal cell lines as a model system to identify and characterize factors potentially involved in GnRH neuron migration. Our studies point to several new candidate proteins, including Gas6, Ark, and p38 MAPK, as potential regulators of GnRH neuron migration in vivo. These factors will be targeted in future in vivo studies to determine if they are required for the proper migration of GnRH neurons during development.

ACKNOWLEDGMENTS

We thank Carrie Swartz and Peter Watson for their assistance in developing the migration assays. We are also grateful to Tracey Laessig for preparing adenoviruses and Ron Bouchard for his expertise in cellular imaging and figure production. Finally, we thank Roger Davis for the p38 MAPK and MKK6CA plasmids.

This work was supported by National Institutes of Health grants HD08667-02 to M.P.A. and HD31191-03 to M.E.W.

REFERENCES

1. **Allen, M. P., M. Xu, C. Zeng, S. A. Tobet, and M. E. Wierman.** 2000. Myocyte enhancer factors-2B and -2C are required for adhesion related kinase repression of neuronal gonadotropin releasing hormone gene expression. J. Biol. Chem. **275:**39662–39670.
2. **Allen, M. P., C. Zeng, K. Schneider, X. Xiong, M. K. Meintzer, P. Bellosta, C. Basilico, B. Varnum, K. A. Heidenreich, and M. E. Wierman.** 1999. Growth arrest-specific gene 6 (Gas6)/adhesion related kinase (Ark) signaling promotes gonadotropin-releasing hormone neuronal survival via extracellular signal-regulated kinase (ERK) and Akt. Mol. Endocrinol. **13:**191–201.
3. **Bateman, J., H. Shu, and D. Van Vactor.** 2000. The guanine nucleotide exchange factor trio mediates axonal development in the Drosophila embryo. Neuron **26:**93–106.
4. **Bellosta, P., M. Costa, D. A. Lin, and C. Basilico.** 1995. The receptor tyrosine kinase ARK mediates cell aggregation by homophilic binding. Mol. Cell. Biol. **15:**614–625.
5. **Bellosta, P., Q. Zhang, S. P. Goff, and C. Basilico.** 1997. Signaling through the ARK tyrosine kinase receptor protects from apoptosis in the absence of growth stimulation. Oncogene **15:**2387–2397.
6. **Benard, V., B. P. Bohl, and G. M. Bokoch.** 1999. Characterization of rac and cdc42 activation in chemoattractant-stimulated human neutrophils using a novel assay for active GTPases. J. Biol. Chem. **274:**13198–13204.
7. **Clerk, A., F. H. Pham, S. J. Fuller, E. Sahai, K. Aktories, R. Marais, C. Marshall, and P. H. Sugden.** 2001. Regulation of mitogen-activated protein kinases in cardiac myocytes through the small G protein Rac1. Mol. Cell. Biol. **21:**1173–1184.
8. **Crosier, K. E., and P. S. Crosier.** 1997. New insights into the control of cell growth; the role of the Axl family. Pathology **29:**131–135.
9. **Ehler, E., F. van Leeuwen, J. G. Collard, and P. C. Salinas.** 1997. Expression of Tiam-1 in the developing brain suggests a role for the Tiam-1-Rac signaling pathway in cell migration and neurite outgrowth. Mol. Cell. Neurosci. **9:**1–12.
10. **Fang, Z., X. Xiong, A. James, D. F. Gordon, and M. E. Wierman.** 1998. Identification of novel factors that regulate GnRH gene expression and neuronal migration. Endocrinology **139:**3654–3657.
11. **Franco, B., S. Guioli, A. Pragliola, B. Incerti, B. Bardoni, R. Tonlorenzi, R. Carrozzo, E. Maestrini, M. Pieretti, and P. Taillon-Miller.** 1991. A gene deleted in Kallmann's syndrome shares homology with neural cell adhesion and axonal path-finding molecules. Nature **353:**529–536.
12. **Fridell, Y. W., Y. Jin, L. A. Quilliam, A. Burchert, P. McCloskey, G. Spizz, B. Varnum, C. Der, and E. T. Liu.** 1996. Differential activation of the Ras/extracellular-signal-regulated protein kinase pathway is responsible for the biological consequences induced by the Axl receptor tyrosine kinase. Mol. Cell. Biol. **16:**135–145.
13. **Fridell, Y. W., J. Villa, Jr., E. C. Attar, and E. T. Liu.** 1998. GAS6 induces Axl-mediated chemotaxis of vascular smooth muscle cells. J. Biol. Chem. **273:**7123–7126.
14. **Gomez-Foix, A. M., W. S. Coats, S. Baque, T. Alam, R. D. Gerard, and C. B. Newgard.** 1992. Adenovirus-mediated transfer of the muscle glycogen phosphorylase gene into hepatocytes confers altered regulation of glycogen metabolism. J. Biol. Chem. **267:**25129–25134.
15. **Goruppi, S., E. Ruaro, and C. Schneider.** 1996. Gas6, the ligand of Axl tyrosine kinase receptor, has mitogenic and survival activities for serum starved NIH3T3 fibroblasts. Oncogene **12:**471–480.
16. **Goruppi, S., E. Ruaro, B. Varnum, and C. Schneider.** 1999. Gas6-mediated survival in NIH3T3 cells activates stress signalling cascade and is independent of Ras. Oncogene **18:**4224–4236.
17. **Hall, A.** 1998. Rho GTPases and the actin cytoskeleton. Science **279:**509–514.
18. **Hansen, T. O., J. F. Rehfeld, and F. C. Nielsen.** 2000. Cyclic AMP-induced neuronal differentiation via activation of p38 mitogen-activated protein kinase. J. Neurochem. **75:**1870–1877.
19. **He, T. C., S. Zhou, L. T. da Costa, J. Yu, K. W. Kinzler, and B. Vogelstein.**

1998. A simplified system for generating recombinant adenoviruses. Proc. Natl. Acad. Sci. USA **95**:2509–2514.
20. **Hedges, J. C., M. A. Dechert, I. A. Yamboliev, J. L. Martin, E. Hickey, L. A. Weber, and W. T. Gerthoffer.** 1999. A role for p38(MAPK)/HSP27 pathway in smooth muscle cell migration. J. Biol. Chem. **274**:24211–24219.
21. **Heuertz, R. M., S. M. Tricomi, U. R. Ezekiel, and R. O. Webster.** 1999. C-reactive protein inhibits chemotactic peptide-induced p38 mitogen-activated protein kinase activity and human neutrophil movement. J. Biol. Chem. **274**:17968–17974.
22. **Iwasaki, S., M. Iguchi, K. Watanabe, R. Hoshino, M. Tsujimoto, and M. Kohno.** 1999. Specific activation of the p38 mitogen-activated protein kinase signaling pathway and induction of neurite outgrowth in PC12 cells by bone morphogenetic protein-2. J. Biol. Chem. **274**:26503–26510.
23. **Janssen, J. W., A. S. Schulz, A. C. Steenvoorden, M. Schmidberger, S. Strehl, P. F. Ambros, and C. R. Bartram.** 1991. A novel putative tyrosine kinase receptor with oncogenic potential. Oncogene **6**:2113–2120.
24. **Kallmann, F. J., W. A. Schoenfeld, and S. E. Barrera.** 1944. The genetic aspects of primary eunuchoidism. Am. J. Ment. Defic. **48**:203–236.
25. **Kawasaki, Y., T. Senda, T. Ishidate, R. Koyama, T. Morishita, Y. Iwayama, O. Higuchi, and T. Akiyama.** 2000. Asef, a link between the tumor suppressor APC and G-protein signaling. Science **289**:1194–1197.
26. **Kimura, T., T. Watanabe, K. Sato, J. Kon, H. Tomura, K. Tamama, A. Kuwabara, T. Kanda, I. Kobayashi, H. Ohta, M. Ui, and F. Okajima.** 2000. Sphingosine 1-phosphate stimulates proliferation and migration of human endothelial cells possibly through the lipid receptors, Edg-1 and Edg-3. Biochem. J. **348**(Pt. 1):71–76.
27. **Kummer, J. L., P. K. Rao, and K. A. Heidenreich.** 1997. Apoptosis induced by withdrawal of trophic factors is mediated by p38 mitogen-activated protein kinase. J. Biol. Chem. **272**:20490–20494.
28. **Lai, C., and G. Lemke.** 1991. An extended family of protein-tyrosine kinase genes differentially expressed in the vertebrate nervous system. Neuron **6**:691–704.
29. **Landry, J., and J. Huot.** 1995. Modulation of actin dynamics during stress and physiological stimulation by a signaling pathway involving p38 MAP kinase and heat-shock protein 27. Biochem. Cell Biol. **73**:703–707.
30. **Landry, J., H. Lambert, M. Zhou, J. N. Lavoie, E. Hickey, L. A. Weber, and C. W. Anderson.** 1992. Human HSP27 is phosphorylated at serines 78 and 82 by heat shock and mitogen-activated kinases that recognize the same amino acid motif as S6 kinase II. J. Biol. Chem. **267**:794–803.
31. **Leeuwen, F. N., H. E. Kain, R. A. Kammen, F. Michiels, O. W. Kranenburg, and J. G. Collard.** 1997. The guanine nucleotide exchange factor Tiam1 affects neuronal morphology: opposing roles for the small GTPases Rac and Rho. J. Cell Biol. **139**:797–807.
32. **Legouis, R., J. P. Hardelin, J. Levilliers, J. M. Claverie, S. Compain, V. Wunderle, P. Millasseau, D. Le Paslier, D. Cohen, D. Caterina, et al.** 1991. The candidate gene for the X-linked Kallmann syndrome encodes a protein related to adhesion molecules. Cell **67**:423–435.
33. **Li, R., J. Chen, G. Hammonds, H. Phillips, M. Armanini, P. Wood, R. Bunge, P. J. Godowski, M. X. Sliwkowski, and J. P. Mather.** 1996. Identification of Gas6 as a growth factor for human Schwann cells. J. Neurosci. **16**:2012–2019.
34. **Liebl, E. C., D. J. Forsthoefel, L. S. Franco, S. H. Sample, J. E. Hess, J. A. Cowger, M. P. Chandler, A. M. Shupert, and M. A. Seeger.** 2000. Dosage-sensitive, reciprocal genetic interactions between the Abl tyrosine kinase and the putative GEF Trio reveal Trio's role in axon pathfinding. Neuron **26**: 107–118.
35. **Lu, Q., M. Gore, Q. Zhang, T. Camenisch, S. Boast, F. Casagranda, C. Lai, M. K. Skinner, R. Klein, G. K. Matsushima, H. S. Earp, S. P. Goff, and G. Lemke.** 1999. Tyro-3 family receptors are essential regulators of mammalian spermatogenesis. Nature **398**:723–728.
36. **Maggi, R., F. Pimpinelli, L. Molteni, M. Milani, L. Martini, and F. Piva.** 2000. Immortalized luteinizing hormone-releasing hormone neurons show a different migratory activity in vitro. Endocrinology **141**:2105–2112.
37. **Matsumoto, T., K. Yokote, K. Tamura, M. Takemoto, H. Ueno, Y. Saito, and S. Mori.** 1999. Platelet-derived growth factor activates p38 mitogen-activated protein kinase through a Ras-dependent pathway that is important for actin reorganization and cell migration. J. Biol. Chem. **274**:13954–13960.
38. **McCloskey, P., Y. W. Fridell, E. Attar, J. Villa, Y. Jin, B. Varnum, and E. T. Liu.** 1997. GAS6 mediates adhesion of cells expressing the receptor tyrosine kinase Axl. J. Biol. Chem. **272**:23285–23291.
39. **Mellon, P. L., J. J. Windle, P. C. Goldsmith, C. A. Padula, J. L. Roberts, and R. I. Weiner.** 1990. Immortalization of hypothalamic GnRH neurons by genetically targeted tumorigenesis. Neuron **5**:1–10.
40. **Michael, Z. W., M. K. Meintzer, P. Rao, J. Marotti, X. Wang, J. E. Esplen, E. D. Clarkson, C. R. Freed, and K. A. Heidenreich.** 2001. Inhibitors of p38 MAP kinase increase the survival of transplanted dopamine neurons. Brain Res. **891**:185–196.
41. **Morooka, T., and E. Nishida.** 1998. Requirement of p38 mitogen-activated protein kinase for neuronal differentiation in PC12 cells. J. Biol. Chem. **273**:24285–24288.
42. **Nagata, K., K. Ohashi, T. Nakano, H. Arita, C. Zong, H. Hanafusa, and K. Mizuno.** 1996. Identification of the product of growth arrest-specific gene 6 as a common ligand for Axl, Sky, and Mer receptor tyrosine kinases. J. Biol. Chem. **271**:30022–30027.
43. **Newsome, T. P., S. Schmidt, G. Dietzl, K. Keleman, B. Asling, A. Debant, and B. J. Dickson.** 2000. Trio combines with Dock to regulate Pak activity during photoreceptor axon pathfinding in Drosophila. Cell **101**:283–294.
44. **Nick, J. A., S. K. Young, K. K. Brown, N. J. Avdi, P. G. Arndt, B. T. Suratt, M. S. Janes, P. M. Henson, and G. S. Worthen.** 2000. Role of p38 mitogen-activated protein kinase in a murine model of pulmonary inflammation. J. Immunol. **164**:2151–2159.
45. **O'Bryan, J. P., R. A. Frye, P. C. Cogswell, A. Neubauer, B. Kitch, C. Prokop, R. Espinosa III, M. M. Le Beau, H. S. Earp, and E. T. Liu.** 1991. *axl*, a transforming gene isolated from primary human myeloid leukemia cells, encodes a novel receptor tyrosine kinase. Mol. Cell. Biol. **11**:5016–5031.
46. **Piotrowicz, R. S., J. L. Martin, W. H. Dillman, and E. G. Levin.** 1997. The 27-kDa heat shock protein facilitates basic fibroblast growth factor release from endothelial cells. J. Biol. Chem. **272**:7042–7047.
47. **Prieto, A. L., J. L. Weber, and C. Lai.** 2000. Expression of the receptor protein-tyrosine kinases Tyro-3, Axl, and mer in the developing rat central nervous system. J. Comp. Neurol. **425**:295–314.
48. **Prieto, A. L., J. L. Weber, S. Tracy, M. J. Heeb, and C. Lai.** 1999. Gas6, a ligand for the receptor protein-tyrosine kinase Tyro-3, is widely expressed in the central nervous system. Brain Res. **816**:646–661.
49. **Radovick, S., S. Wray, E. Lee, D. K. Nicols, Y. Nakayama, B. D. Weintraub, H. Westphal, G. B. Cutler, Jr., and F. E. Wondisford.** 1991. Migratory arrest of gonadotropin-releasing hormone neurons in transgenic mice. Proc. Natl. Acad. Sci. USA **88**:3402–3406.
50. **Raingeaud, J., S. Gupta, J. S. Rogers, M. Dickens, J. Han, R. J. Ulevitch, and R. J. Davis.** 1995. Pro-inflammatory cytokines and environmental stress cause p38 mitogen-activated protein kinase activation by dual phosphorylation on tyrosine and threonine. J. Biol. Chem. **270**:7420–7426.
51. **Raingeaud, J., A. J. Whitmarsh, T. Barrett, B. Derijard, and R. J. Davis.** 1996. MKK3- and MKK6-regulated gene expression is mediated by the p38 mitogen-activated protein kinase signal transduction pathway. Mol. Cell. Biol. **16**:1247–1255.
52. **Rescigno, J., A. Mansukhani, and C. Basilico.** 1991. A putative receptor tyrosine kinase with unique structural topology. Oncogene **6**:1909–1913.
53. **Ridley, A. J., H. F. Paterson, C. L. Johnston, D. Diekmann, and A. Hall.** 1992. The small GTP-binding protein rac regulates growth factor-induced membrane ruffling. Cell **70**:401–410.
54. **Ronnekleiv, O. K., and J. A. Resko.** 1990. Ontogeny of gonadotropin-releasing hormone-containing neurons in early fetal development of rhesus macaques. Endocrinology **126**:498–511.
55. **Rousseau, S., F. Houle, J. Landry, and J. Huot.** 1997. p38 MAP kinase activation by vascular endothelial growth factor mediates actin reorganization and cell migration in human endothelial cells. Oncogene **15**:2169–2177.
56. **Sahai, E., M. F. Olson, and C. J. Marshall.** 2001. Cross-talk between Ras and Rho signalling pathways in transformation favours proliferation and increased motility. EMBO J. **20**:755–766.
57. **Schaack, J., S. Langer, and X. Guo.** 1995. Efficient selection of recombinant adenoviruses by vectors that express beta-galactosidase. J. Virol. **69**:3920–3923.
58. **Schwanzel-Fukuda, M., D. Bick, and D. W. Pfaff.** 1989. Luteinizing hormone-releasing hormone (LHRH)-expressing cells do not migrate normally in an inherited hypogonadal (Kallmann) syndrome. Brain Res. Mol. Brain Res. **6**:311–326.
59. **Schwanzel-Fukuda, M., and D. W. Pfaff.** 1989. Origin of luteinizing hormone-releasing hormone neurons. Nature **338**:161–164.
60. **Seminara, S. B., F. J. Hayes, and W. F. Crowley, Jr.** 1998. Gonadotropin-releasing hormone deficiency in the human (idiopathic hypogonadotropic hypogonadism and Kallmann's syndrome): pathophysiological and genetic considerations. Endocr. Rev. **19**:521–539.
61. **Silverman, A. J., J. L. Roberts, K. W. Dong, G. M. Miller, and M. J. Gibson.** 1992. Intrahypothalamic injection of a cell line secreting gonadotropin-releasing hormone results in cellular differentiation and reversal of hypogonadism in mutant mice. Proc. Natl. Acad. Sci. USA **89**:10668–10672.
62. **Soussi-Yanicostas, N., J. P. Hardelin, M. M. Arroyo-Jimenez, O. Ardouin, R. Legouis, J. Levilliers, F. Traincard, J. M. Betton, L. Cabanie, and C. Petit.** 1996. Initial characterization of anosmin-1, a putative extracellular matrix protein synthesized by definite neuronal-cell populations in the central nervous system. J. Cell Sci. **109**(Pt. 7):1749–1757.
63. **Takeda, K., T. Hatai, T. S. Hamazaki, H. Nishitoh, M. Saitoh, and H. Ichijo.** 2000. Apoptosis signal-regulating kinase 1 (ASK1) induces neuronal differentiation and survival of PC12 cells. J. Biol. Chem. **275**:9805–9813.
64. **Varnum, B. C., C. Young, G. Elliott, A. Garcia, T. D. Bartley, Y. W. Fridell, R. W. Hunt, G. Trail, C. Clogston, and R. J. Toso.** 1995. Axl receptor tyrosine kinase stimulated by the vitamin K-dependent protein encoded by growth-arrest-specific gene 6. Nature **373**:623–626.
65. **Wetsel, W. C., M. M. Valenca, I. Merchenthaler, Z. Liposits, F. J. Lopez, R. I. Weiner, P. L. Mellon, and A. Negro-Vilar.** 1992. Intrinsic pulsatile secretory activity of immortalized luteinizing hormone-releasing hormone-secreting neurons. Proc. Natl. Acad. Sci. USA **89**:4149–4153.
66. **Wray, S., P. Grant, and H. Gainer.** 1989. Evidence that cells expressing

luteinizing hormone-releasing hormone mRNA in the mouse are derived from progenitor cells in the olfactory placode. Proc. Natl. Acad. Sci. USA **86:**8132–8136.

67. **Wray, S., S. Key, R. Qualls, and S. M. Fueshko.** 1994. A subset of peripherin positive olfactory axons delineates the luteinizing hormone releasing hormone neuronal migratory pathway in developing mouse. Dev. Biol. **166:**349–354.
68. **Xia, Z., M. Dickens, J. Raingeaud, R. J. Davis, and M. E. Greenberg.** 1995. Opposing effects of ERK and JNK-p38 MAP kinases on apoptosis. Science **270:**1326–1331.
69. **Yamboliev, I. A., K. M. Wiesmann, C. A. Singer, J. C. Hedges, and W. T. Gerthoffer.** 2000. Phosphatidylinositol 3-kinases regulate ERK and p38 MAP kinases in canine colonic smooth muscle. Am. J. Physiol. Cell Physiol. **279:** C352–C360.
70. **Yoshida, K., S. A. Tobet, J. E. Crandall, T. P. Jimenez, and G. A. Schwarting.** 1995. The migration of luteinizing hormone-releasing hormone neurons in the developing rat is associated with a transient, caudal projection of the vomeronasal nerve. J. Neurosci. **15:**7769–7777.
71. **Zhang, S., J. Han, M. A. Sells, J. Chernoff, U. G. Knaus, R. J. Ulevitch, and G. M. Bokoch.** 1995. Rho family GTPases regulate p38 mitogen-activated protein kinase through the downstream mediator Pak1. J. Biol. Chem. **270:** 23934–23936.
72. **Zhen, S., I. C. Dunn, S. Wray, Y. Liu, P. E. Chappell, J. E. Levine, and S. Radovick.** 1997. An alternative gonadotropin-releasing hormone (GnRH) RNA splicing product found in cultured GnRH neurons and mouse hypothalamus. J. Biol. Chem. **272:**12620–12625.
73. **Zipkin, I. D., R. M. Kindt, and C. J. Kenyon.** 1997. Role of a new Rho family member in cell migration and axon guidance in C. elegans. Cell **90:**883–894.

Cellular/Molecular Neuroscience
Dr. Gary L. Westbrook, Senior Editor

Insulin-like Growth Factor-I Blocks Bim Induction and Intrinsic Death Signaling in Cerebellar Granule Neurons

Daniel A. Linseman, Reid A. Phelps, Ron J. Bouchard, Shoshona S. Le, Tracey A. Laessig, Maria L. McClure, and Kim A. Heidenreich

Department of Pharmacology, University of Colorado Health Sciences Center and the Denver Veterans Affairs Medical Center, Denver, Colorado 80262

Abbreviated Title: IGF-I Rescues CGNs by Blocking Bim Expression

Number of Text Pages: 39 **Figures:** 8 **Tables:** 0

Number of Words in – Abstract: 200 **Introduction:** 499 **Discussion:** 1587

To whom correspondence should be sent: Kim A. Heidenreich, Ph.D.
University of Colorado Health Sciences Center
Department of Pharmacology (C236)
4200 East Ninth Avenue
Denver, CO 80262
Tel.: (303)-399-8020 (ext. 3891)
Fax: (303)-393-5271
E-mail: Kim.Heidenreich@UCHSC.edu

Acknowledgments: This work was supported by a Department of Veterans Affairs Merit Award (K.A.H.), a Department of Defense Grant DAMD17-99-1-9481 (K.A.H.), an NIH Grant NS38619-01A1 (K.A.H.), and a Department of Veterans Affairs Research Enhancement Award Program (K.A.H. and D.A.L.). The authors thank Mary Kay Meintzer for her help with preparation of the manuscript.

Key Words: Insulin-like growth factor; cerebellar granule neuron; apoptosis; mitochondria; Bim; forkhead transcription factor

Cerebellar granule neurons depend on insulin-like growth factor-I (IGF-I) for their survival. However, the mechanism underlying the neuroprotective effects of IGF-I is presently unclear. Here, we show that IGF-I protects granule neurons by suppressing key elements of the intrinsic (mitochondrial) death pathway. IGF-I blocked activation of the executioner caspase-3 and the intrinsic initiator caspase-9 in primary cerebellar granule neurons deprived of serum and depolarizing potassium. IGF-I inhibited cytochrome C release from mitochondria and prevented its redistribution to neuronal processes. The effects of IGF-I on cytochrome C release were not mediated by blockade of the mitochondrial permeability transition pore since IGF-I failed to inhibit mitochondrial swelling or depolarization. In contrast, IGF-I blocked induction of the BH3-only Bcl-2 family member, Bim, a mediator of Bax-dependent cytochrome C release. The suppression of Bim expression by IGF-I did not involve inhibition of the c-Jun transcription factor. Instead, IGF-I prevented activation of the forkhead family member, FKHRL1, another transcriptional regulator of Bim. Finally, adenoviral-mediated expression of dominant-negative AKT activated FKHRL1 and induced expression of Bim. These data suggest that IGF-I signaling via AKT promotes survival of cerebellar granule neurons by blocking the FKHRL1-dependent transcription of Bim, a principal effector of the intrinsic death signaling cascade.

INTRODUCTION

Insulin-like growth factor-I (IGF-I) has significant neurotrophic and neuroprotective effects. IGF-I expression is differentially regulated in various brain regions and is temporally associated with critical stages of central nervous system development (Rotwein et al., 1988; Bach et al., 1991). Deficits in IGF-I are observed in Alzheimer's disease (Mustafa et al., 1999) and degenerative cerebellar ataxias (Torres-Aleman et al., 1996), and recombinant IGF-I slows disease progression in sporadic amyotrophic lateral sclerosis (Lai et al., 1997). IGF-I decreases neuronal apoptosis and enhances functional recovery in animal models of neurodegeneration including toxin exposure (Fernandez et al., 1998), transient ischemia (Liu et al., 2001), and neurotransplantation (Clarkson et al., 2001). Similarly, IGF-I rescues primary neurons from apoptosis induced by trophic factor withdrawal (Russell et al., 1998), excitotoxicity (Tagami et al., 1997), and oxidative stress (Heck et al., 1999). Thus, IGF-I is essential for the survival of central nervous system neurons *in vivo* and *in vitro*.

Cerebellar granule neurons (CGNs) are critically dependent on IGF-I for their survival (Lin and Bulleit, 1997). In hereditary models of cerebellar Purkinje cell degeneration (pcd, lurcher), the primary death of Purkinje neurons induces the subsequent apoptosis of CGNs due to loss of Purkinje-derived IGF-I (Bartlett et al., 1991; Zhang et al., 1997; Selimi et al., 2000a). Transgenic mice overexpressing IGF-I exhibit a remarkable doubling of CGN number (Ye et al., 1996), and show decreased expression of caspase-3 in cerebellum (Chrysis et al., 2001). These observations illustrate that IGF-I protects CGNs from apoptosis *in vivo*.

Similarly, IGF-I rescues primary CGNs from apoptosis induced by removal of depolarizing potassium and serum (trophic factor withdrawal), an established *in vitro* model of neuronal apoptosis (D'Mello et al., 1993; Galli et al., 1995; Miller et al., 1997a). CGN apoptosis

involves activation of the intrinsic (mitochondrial) death pathway (Green, 1998). For example, trophic factor-deprived CGNs demonstrate Bax-dependent cytochrome C release from mitochondria (Desagher et al., 1999), and CGNs isolated from Bax knock-out mice are less sensitive to trophic factor withdrawal (Miller et al., 1997b). Moreover, the BH3-only, pro-apoptotic Bcl-2 family member, Bim (Bcl-2 interacting mediator of cell death), is induced in CGNs undergoing apoptosis (Harris and Johnson, 2001; Putcha et al., 2001). BH3-only proteins facilitate intrinsic death signaling in a Bax-dependent manner (Desagher et al., 1999; Zong et al., 2001). Although it is recognized that IGF-I rescues CGNs via phosphatidylinositol 3-kinase (PI3K) and AKT (Dudek et al., 1997; Miller et al., 1997a), the effects of IGF-I on components of the intrinsic death pathway have not been examined.

Here, we found that IGF-I suppresses induction of Bim, cytochrome C release from mitochondria, and activation of the intrinsic initiator caspase-9 and the executioner caspase-3 in trophic factor-deprived CGNs. Although JNK/c-Jun signaling has been implicated in the induction of Bim during neuronal apoptosis (Harris and Johnson, 2001; Whitfield et al., 2001), our data suggest that IGF-I suppresses Bim expression via a distinct mechanism involving inhibition of the forkhead transcription factor FKHRL1. These results indicate that the intrinsic death pathway is a principal target of IGF-I in neurons.

MATERIALS AND METHODS

Materials. Recombinant human IGF-I was provided by Margarita Quiroga (Chiron Corporation, Emeryville, CA). Polyclonal antibodies to Bim, Bcl-X_L, caspase-3, caspase-9, cytochrome C, and c-Jun were from Santa Cruz Biotechnology (Santa Cruz, CA). Polyclonal antibodies to phospho-c-Jun (Ser63), phospho-AKT (Ser473), and AKT were from Cell Signaling Technologies (Beverly, MA). Polyclonal antibodies to phospho-FKHRL1 (Ser253) and FKHRL1 were from Upstate Biotechnology (Lake Placid, NY). Cy3-conjugated secondary antibodies for immunocytochemistry were purchased from Jackson Immunoresearch Laboratories (West Grove, PA). Horseradish peroxidase-linked secondary antibodies and reagents for enhanced chemiluminescence detection were obtained from Amersham Pharmacia Biotechnologies (Piscataway, NJ). JC1, TMRE, and Mitotracker Green were from Molecular Probes (Eugene, OR). Wortmannin, Hoechst dye no. 33258 and DAPI (4,6-diamidino-2-phenylindole) were from Sigma (St. Louis, MO). Adenoviral CrmA was obtained from Dr. James DeGregori (UCHSC, Denver, CO). Adenoviral CMV (negative control adenovirus) was from Dr. Jerry Schaack (UCHSC, Denver, CO). Adenoviral, kinase-dead, K179M mutant (dominant-negative) AKT was obtained from Dr. Prem Sharma and Dr. Jerry Olefsky (University of California, San Diego, CA).

Cell culture. Rat CGNs were isolated from 7-day-old Sprague-Dawley rat pups (15-19g) as described previously (Li et al., 2000). Briefly, neurons were plated on 35-mm diameter plastic dishes coated with poly-L-lysine at a density of 2.0×10^6 cells/ml in basal modified Eagle's medium containing 10% fetal bovine serum, 25 mM KCl, 2 mM L-glutamine, and penicillin (100 units/ml)/streptomycin (100 μg/ml) (Life Technologies, Grand Island, NY). Cytosine arabinoside (10 μM) was added to the culture medium 24 hr after plating to limit the

growth of non-neuronal cells. Using this protocol, the cultures were approximately 95-99% pure for granule neurons. In general, experiments were performed after 7 days in culture.

Quantification of apoptosis. Apoptosis was induced by removing serum and decreasing the extracellular potassium concentration from 25 mM to 5 mM. After 24 hr, CGNs were fixed with 4% paraformaldehyde and nuclei were stained with either Hoechst dye or DAPI. Cells were considered apoptotic if their nuclei were either condensed or fragmented. In general, approximately 500 cells from at least two fields of a 35-mm well were counted. Data are presented as the percentage of cells in a given treatment group which were scored as apoptotic. Experiments were performed at least in triplicate.

Preparation of CGN cell extracts. Following incubation for the indicated times and with the reagents specified in the text, the culture medium was aspirated, cells were washed once with 2 ml of ice-cold phosphate-buffered saline (PBS, pH 7.4), placed on ice and scraped into lysis buffer (200 µl/35-mm well) containing 20 mM HEPES (pH 7.4), 1% Triton X-100, 50 mM NaCl, 1 mM EGTA, 5 mM β-glycerophosphate, 30 mM sodium pyrophosphate, 100 µM sodium orthovanadate, 1 mM phenylmethylsulfonyl fluoride, 10 µg/ml leupeptin, and 10 µg/ml aprotinin. Cell debris was removed by centrifugation at 6,000 x g for 3 min and the protein concentration of the supernatant was determined using a commercially available protein assay kit (Pierce Chemical Co., Rockford, IL). Aliquots (~150 µg) of supernatant protein were diluted to a final concentration of 1X sodium dodecyl sulfate-polyacrylamide gel electrophoresis (SDS-PAGE) sample buffer, boiled for 5 min, and electrophoresed through 10-15% polyacrylamide gels. Proteins were transferred to polyvinylidene membranes (Millipore Corp., Bedford, MA) and processed for immunoblot analysis.

Immunoblot analysis. Nonspecific binding sites were blocked in PBS (pH 7.4) containing 0.1% Tween 20 (PBS-T) and 1% BSA for 1 hr at room temperature. Primary antibodies were diluted in blocking solution and incubated with the membranes for 1 hr. Excess primary antibody was removed by washing the membranes three times in PBS-T. The blots were then incubated with the appropriate horseradish peroxidase-conjugated secondary antibody diluted in PBS-T for 1 hr and were subsequently washed three times in PBS-T. Immunoreactive proteins were detected by enhanced chemiluminescence. In some experiments, membranes were reprobed after stripping in 0.1 M Tris-HCl (pH 8.0), 2% SDS, and 100 mM β-mercaptoethanol for 30 min at 52°C. The blots were rinsed twice in PBS-T and processed as above with a different primary antibody. Autoluminograms shown are representative of at least three independent experiments.

Immunocytochemistry. CGNs were cultured on polyethyleneimine-coated glass cover slips at a density of approximately $2.5x10^5$ cells per coverslip. Following incubation as described in the text, cells were fixed in 4% paraformaldehyde and were then permeabilized and blocked in PBS (pH 7.4) containing 0.2% Triton X-100 and 5% BSA. Cells were then incubated for approximately 16 hr at 4°C with primary antibody diluted in PBS containing 0.2% Triton X-100 and 2% BSA. The primary antibody was aspirated and the cells were washed five times with PBS. The cells were then incubated with a Cy3-conjugated secondary antibody and DAPI for 1 hr at room temperature. CGNs were then washed five more times with PBS and coverslips were adhered to glass slides in mounting medium (0.1% *p*-phenylenediamine in 75% glycerol in PBS). Fluorescent images were captured using either 63X or 100X oil immersion objectives on a Zeiss Axioplan 2 microscope equipped with a Cooke Sensicam deep-cooled CCD camera and a

Slidebook software analysis program for digital deconvolution (Intelligent Imaging Innovations Inc., Denver, CO).

Measurement of mitochondrial swelling. CGNs were incubated as described in the text and JC1 (final concentration of 2 μg/ml) was added to the cultures 30 min prior to fixation to stain mitochondria. JC1 fluorescence was captured in paraformaldehyde-fixed cells using a Cy3 filter under 100X oil. The diameters of approximately 150 mitochondria per treatment condition were then measured from digitally deconvolved images obtained from a total of 15 to 20 CGNs (randomly pooled from four independent experiments).

Assessment of mitochondrial membrane potential. CGNs grown on glass coverslips were incubated as described in the text and TMRE (500 nM) was added directly to the cells 30 min prior to the end of the incubation period. Following incubation, coverslips were inverted onto slides into a small volume of phenol red-free medium containing TMRE (500 nM). Living cells were then imaged using a Cy3 filter to detect TMRE fluorescence under 100X oil. All images were acquired at equal exposure times for TMRE fluorescence to assess the relative mitochondrial membrane potentials.

Adenoviral Infection. Recombinant adenoviruses were purified by cesium chloride gradient ultracentrifugation. The viral titer (multiplicity of infection) was determined by measuring the absorbance at 260 nm (where 1.0 absorbance units=$1x10^{12}$ particles/ml) and infectious particles were verified by plaque assay. Adenoviral-CMV, -CrmA, or –dominant-negative (DN)-AKT were added to CGN cultures on day 5 at a multiplicity of infection of 50. Forty-eight hours post-infection, either CGN apoptosis was induced by removal of serum and depolarizing potassium for 24 hr (for Ad-CMV and Ad-CrmA) or cell lysates were directly prepared for western blotting for phospho-FKHRL1 and Bim (for Ad-CMV and Ad-DN-AKT).

Data analysis. Results shown represent the means±S.E.M. for the number (n) of independent experiments performed. Statistical differences between the means of unpaired sets of data were evaluated using one-way analysis of variance followed by a *post hoc* Dunnett's test. A p value of <0.01 was considered statistically significant.

RESULTS

IGF-I suppresses CGN apoptosis and activation of caspase-3 and caspase-9

Primary CGNs are dependent on depolarization-mediated calcium influx and serum-derived growth factors for their survival *in vitro* (D'Mello et al., 1993; Galli et al., 1995). Removal of serum and depolarizing potassium induced marked apoptosis of CGNs, characterized morphologically by chromatin condensation and fragmentation (Fig. 1*A*). Quantification of CGN apoptosis was performed by counting the number of cells with condensed and/or fragmented nuclei from several representative fields for each incubation condition. Basal CGN apoptosis was approximately 10% and increased to approximately 60% following 24 hr of trophic factor withdrawal (Fig. 1*B*). We utilized this cell system to investigate the mechanism of IGF-I neuroprotection. As described previously (D'Mello et al., 1993; Galli et al., 1995; Miller et al., 1997a), addition of IGF-I to cerebellar cultures immediately following trophic factor withdrawal resulted in an approximate 80% reduction in CGN apoptosis (Fig. 1*A*, *B*). The ability of IGF-I to rescue CGNs from apoptosis required activation of PI3K as demonstrated by the loss of protection observed in the presence of wortmannin (Fig. 1*A*, *B*). Activation of the executioner caspase-3 has been implicated in the apoptotic death of CGNs (Eldadah et al., 2000). Consistent with this, we observed cleavage of caspase-3 from the pro-form to an active fragment within 6 hr of serum and potassium deprivation (Fig. 1*C*). Like the results obtained for nuclear condensation and fragmentation, IGF-I inhibited caspase-3 activation in a PI3K-dependent manner (Fig. 1*C*). This latter result suggested that IGF-I blocks pro-apoptotic signaling events early in the apoptotic cascade since caspase-3 cleavage is commonly thought to signify commitment to apoptosis.

To identify potential targets of IGF-I action upstream of the executioner caspase-3 in the apoptotic cascade, we focused on components of the intrinsic (mitochondrial) death pathway

(Green, 1998). Recent data indicate that the intrinsic death pathway plays a significant role in CGN apoptosis evoked by trophic factor withdrawal (Miller et al., 1997b; Desagher et al., 1999). Immediately upstream of caspase-3 cleavage, activation of the initiator caspase-9 is the most distal event in the intrinsic pathway (Kuida et al., 1998). Recently, caspase-9 activation was shown to be required for caspase-3 cleavage in CGNs deprived of serum and depolarizing potassium (Gerhardt et al., 2001). Consistent with involvement of caspase-9 in CGN apoptosis, we found that infection of CGNs with adenoviral CrmA, an inhibitor of Group III caspases (including caspase-9) but not Group II caspases (such as caspase-3) (Garcia-Calvo et al., 1998), significantly decreased apoptosis from 72±8% (n=3) to 29±3% (n=3, $p<0.01$). In contrast, a negative control adenovirus (Ad-CMV) had no effect on CGN apoptosis (70±8%, n=3). Following acute serum and potassium deprivation, we observed marked cleavage of caspase-9 consistent with its activation (Fig. 1*D*). As was observed for caspase-3 cleavage, activation of caspase-9 was significantly inhibited by IGF-I in a PI3K-dependent manner (Fig. 1*D*), demonstrating that IGF-I suppresses a key component of the intrinsic death pathway in CGNs.

IGF-I inhibits release of cytochrome C from mitochondria and its redistribution to neuronal processes

Caspase-9 is activated following its association with Apaf-1 and cytochrome C, which assemble into a large oligomeric complex known as the apoptosome (Zou et al., 1999). Formation of the apoptosome occurs after release of the mitochondrial protein, cytochrome C, into the cytoplasm. In CGNs maintained in the presence of serum and depolarizing potassium, cytochrome C was localized predominantly in mitochondria (Fig. 2*A*), with only diffuse staining observed in neuronal processes (Fig. 2*C*, *E*). Removal of serum and depolarizing potassium for 4 hr resulted

in a rapid redistribution of cytochrome C from mitochondria to a diffuse staining throughout the cytoplasm. This redistribution was accompanied by the formation of many pronounced punctate areas of cytochrome C staining (Fig. 2*B*). The latter were observed primarily, although not exclusively, in distinct focal complexes localized to neuronal processes (Fig. 2*D*, *F*). In contrast to cytochrome C staining, no detectable redistribution of the mitochondrial marker, Mitotracker Green, was observed in neuronal processes under apoptotic conditions, indicating that the punctate areas of cytochrome C staining were not associated with intact mitochondria (data not shown). Inclusion of IGF-I during trophic factor withdrawal prevented the release and redistribution of cytochrome C from mitochondria (Fig. 2*G*). However, addition of wortmannin in combination with IGF-I restored the release of cytochrome C from mitochondria and its redistribution to focal complexes in neuronal processes (Fig. 2*H*), indicating that the effects of IGF-I on cytochrome C release were PI3K-dependent. Thus, IGF-I inhibits the release of cytochrome C from mitochondria, and in this manner, blocks the subsequent activation of the intrinsic initiator caspase-9.

Mitochondrial swelling and mitochondrial membrane depolarization are not prevented by IGF-I

There are two potential mechanisms underlying cytochrome C release from mitochondria that have received considerable attention. The first involves opening of the permeability transition pore (PTP). The PTP is a heteromeric protein complex that includes the voltage-dependent anion channel, the adenine nucleotide translocator, and cyclophilin D, as well as several other proteins (reviewed by Martinou and Green, 2001). The PTP is localized at contact sites between the inner and outer mitochondrial membranes. Some apoptotic stimuli are capable of opening

the PTP, resulting in disruption of the mitochondrial membrane potential (depolarization), a decline in ATP production, and entry of solutes and water into the mitochondrial matrix. Ultimately, mitochondrial swelling and rupture of the outer mitochondrial membrane occur, allowing the leakage of proteins (eg., cytochrome C) from the intermembrane space into the cytoplasm. We utilized the mitochondrial dye JC1 to visualize mitochondria in CGNs undergoing apoptosis. Although the absolute amount of JC1 accumulated in mitochondria varies with membrane potential, JC1 is extremely photostable and labels all mitochondria to some extent (White and Reynolds, 1996). Following incubation with JC1, CGNs were fixed and the diameters of labeled mitochondria were measured following digital deconvolution imaging. As shown in Figure 3, serum and potassium deprivation for 4 hr resulted in dramatic swelling of mitochondria in CGNs (Fig. 3*A*, *upper panels*). This effect was reversible if serum and depolarizing potassium were restored within the first 2 hr following trophic factor withdrawal (Fig. 3*A*, *lower right panel*). Inclusion of IGF-I during the apoptotic stimulus did not prevent the swelling of CGN mitochondria (Fig. 3*A*, *lower left panel*). The distribution of mitochondrial diameters under control, apoptotic, and apoptotic+IGF-I conditions is shown in Figure 3*B*, and the mean diameters are shown in Figure 3*C*. Serum and potassium deprivation resulted in a significant 50% increase in the mean mitochondrial diameter in CGNs (0.69±0.03 microns in control vs. 1.05±0.11 microns in apoptotic, $p<0.01$), an effect that was unaltered by IGF-I (0.96±0.12 microns) (Fig. 3*C*). Interestingly, inclusion of IGF-I in trophic factor-deprived CGNs failed to reverse the mitochondrial swelling even after 48 hr of incubation, although apoptosis was still blocked at this time point. However, re-addition of depolarizing potassium for the latter 24 hr of the incubation period did reverse the mitochondrial swelling, indicating that it is a depolarization-sensitive event that is unaffected by IGF-I (data not shown).

Next, we analyzed the mitochondrial membrane potential by incubating living CGNs with the membrane potential-sensitive dye tetramethylrhodamine ethyl ester (TMRE). TMRE is actively accumulated in mitochondria possessing an intact membrane potential, but is excluded or lost from mitochondria that are depolarized (Krohn et al., 1999). CGNs maintained in the presence of serum and depolarizing potassium displayed mitochondria that were brightly stained with TMRE, indicative of an intact membrane potential (Fig. 4, *upper left panel*). Since these experiments were conducted in living CGNs, we showed that the mitochondrial membrane potential of control CGNs was maintained throughout the duration required to capture all of the images described below (Fig. 4, *lower right panel*). Serum and potassium deprivation for 4 hr resulted in a marked loss of mitochondrial TMRE staining, consistent with mitochondrial membrane depolarization (Fig. 4, *upper right panel*). As was observed for mitochondrial swelling, addition of IGF-I to trophic factor-deprived CGNs did not prevent the loss of mitochondrial membrane potential (Fig. 4, *lower left panel*). The above results demonstrate that IGF-I does not block cytochrome C release from CGN mitochondria by inhibition of mitochondrial swelling or depolarization, suggesting that opening of the PTP does not play a significant role in cytochrome C release during apoptosis of CGNs.

IGF-I blocks induction of the BH3-only Bcl-2 family member Bim

The second potential mechanism by which cytochrome C release is regulated involves the formation of a Bax- or Bak-containing "pore" in the outer mitochondrial membrane that permits passage of proteins (Korsmeyer et al., 2000). Bax and Bak are pro-apoptotic members of the Bcl-2 family that appear to serve a redundant function in making the mitochondrial membrane permeable to cytochrome C (Wei et al., 2001). The BH3-only Bcl-2 family members, including

Bad, Bid, Dp5/Hrk, and Bim, have been shown to promote the pro-apoptotic effects of Bax and Bak, while concomitantly suppressing the pro-survival function of Bcl-2 (Desagher et al., 1999; Zong et al., 2001). Recently, Bim was shown to be up-regulated following either nerve growth factor (NGF) withdrawal from primary sympathetic neurons or serum and potassium withdrawal from CGNs (Putcha et al., 2001; Whitfield et al., 2001). Moreover, overexpression of Bim or related BH3-only family members promotes apoptosis of CGNs in a Bax-dependent manner (Harris and Johnson, 2001). Immunoblotting for Bim following acute trophic factor withdrawal in CGNs demonstrated a marked increase in the expression of Bim short (Bim_S, ~15 kDa) (Fig. 5*A*), the most pro-apoptotic splice variant of this protein family (O'Connor et al., 1998). Quantification of the change in protein expression by densitometry revealed that serum and potassium deprivation for 6 hr induced a significant 3.4±0.4 fold increase ($n=3$, $p<0.01$) in Bim_S (Fig. 5*B*). Inclusion of IGF-I completely blunted the induction of Bim_S (1.5±0.5 fold increase, n=3) in a PI3K-dependent manner (Fig. 5*A*, *B*). In contrast, the expression of the pro-survival Bcl-2 family member $BclX_L$ was unaffected by either trophic factor withdrawal or IGF-I (Fig. 5*A*). These data indicate that suppression of Bim is one mechanism by which IGF-I inhibits cytochrome C release in CGNs deprived of serum and depolarizing potassium.

IGF-I does not suppress Bim expression by inhibiting c-Jun

Activation of the transcription factor c-Jun is required for apoptosis of primary sympathetic neurons subjected to NGF withdrawal (Eilers et al., 1998) and CGNs undergoing serum and potassium deprivation (Watson et al., 1998). The ability of a dominant-negative mutant of c-Jun to rescue sympathetic neurons from apoptosis has recently been attributed, in part, to its ability to block induction of Bim (Whitfield et al., 2001). The transcriptional activity of c-Jun is

stimulated following its phosphorylation on multiple serine residues (including Ser63 and Ser73) by upstream kinases of the JNK family (Minden et al., 1994). Chemical inhibitors of JNK have been shown to inhibit apoptosis of CGNs (Harada and Sugimoto, 1999; Coffey et al., 2002) and to attenuate Bim mRNA expression in CGNs subjected to trophic factor withdrawal (Harris and Johnson, 2001). In the present study, we observed that incubation of trophic factor-deprived CGNs with the pyridinyl imidazole JNK/p38 inhibitor, SB203580 (Harada and Sugimoto, 1999; Coffey et al., 2002), blunted the phosphorylation of c-Jun on Ser63 (Fig. 6*A*) and prevented the increased expression of c-Jun detected by immunoblotting (Fig. 6*B*). Moreover, SB203580 significantly attenuated the induction of Bim_S, consistent with a role for c-Jun in the regulation of Bim expression in CGNs (Fig. 6*C*, *D*). To determine if IGF-I blocks Bim induction via an inhibition of c-Jun, we analyzed the effects of IGF-I on c-Jun phosphorylation and expression. Addition of IGF-I to CGNs deprived of serum and depolarizing potassium failed to attenuate either the phosphorylation of c-Jun on Ser63 (Fig. 6*E*) or the increased expression of c-Jun observed by western blot (Fig. 6*F*). Thus, IGF-I suppresses the induction of Bim in apoptotic CGNs via a mechanism that is independent of the transcription factor c-Jun.

IGF-I prevents dephosphorylation and nuclear translocation of the forkhead transcription factor FKHRL1

Recently, a member of the forkhead family of transcription factors, FKHRL1, was shown to regulate the induction of Bim in lymphocytes undergoing apoptosis in response to cytokine withdrawal (Dijkers et al., 2000). Furthermore, overexpression of a constitutively-active mutant of FKHRL1 was sufficient to increase Bim expression in B cells (Dijkers et al., 2000). The actions of forkhead family members are regulated by phosphorylation on serine and threonine

residues. The pro-survival kinase AKT is the main effector of IGF-I that is activated downstream of PI3K, and FKHRL1 has been identified as a principal substrate of AKT in neuronal cells (Brunet et al., 1999; Zheng et al., 2000). Therefore, we first assessed the phosphorylation status of AKT and FKHRL1 in CGNs by immunoblotting with phospho-site-specific antibodies. CGNs cultured in the presence of serum and depolarizing potassium showed marked phosphorylation of AKT on Ser473, indicative of high AKT activity (Fig. 7*A*, *first lane*). In parallel, control CGNs also exhibited high phosphorylation of FKHRL1 on Ser253, one of the sites targeted by AKT (Fig. 7*B*, *first lane*). Removal of serum and depolarizing potassium resulted in a pronounced dephosphorylation (inactivation) of AKT (Fig. 7*A*, *second lane*) and a corresponding loss of FKHRL1 phosphorylation (Fig. 7*B*, *second lane*). Addition of IGF-I to CGNs deprived of serum and depolarizing potassium maintained the phosphorylation of both AKT (Fig. 7*A*) and FKHRL1 (Fig. 7*B*), effects that were blocked by the PI3K inhibitor wortmannin.

Phosphorylation of FKHRL1 on Thr32 and Ser253 by AKT results in translocation of FKHRL1 from the nucleus to the cytoplasm where it is subsequently sequestered by 14-3-3 proteins (Brunet et al., 1999). Thus, IGF-I signaling via AKT has the potential to negatively regulate the transcriptional activity of FKHRL1 by excluding it from the nucleus. We next examined the cellular localization of FKHRL1 in CGNs. FKHRL1 was localized predominantly to the cytoplasm in CGNs maintained in the presence of trophic factors (Fig. 7*C*, *upper left panel*). Following acute trophic factor withdrawal, FKHRL1 underwent a dramatic translocation to the nucleus (Fig. 7*C*, *upper right panel*). The nuclear translocation of FKHRL1 was completely prevented by IGF-I (Fig. 7*C*, *lower left panel*) in a PI3K-dependent manner (Fig. 7*C*, *lower right panel*). Collectively, these results demonstrate that under conditions where IGF-I

blocks Bim induction (see Fig. 5), it concurrently sustains high AKT activity, robust FKHRL1 phosphorylation, and exclusion of FKHRL1 from the nucleus. These findings are consistent with a role for FKHRL1 in the regulation of Bim expression in CGNs. Moreover, these data suggest a novel mechanism by which IGF-I suppresses Bim induction in trophic factor-deprived CGNs by blocking the actions of FKHRL1.

Adenoviral-mediated expression of dominant-negative AKT results in dephosphorylation of FKHRL1 and induction of Bim

To more directly assess the role of AKT in the regulation of FKHRL1 activity and Bim expression, we infected CGNs with an adenovirus expressing a kinase-dead, dominant-negative mutant of AKT (Ad-DN-AKT). As described above, CGNs cultured in the presence of serum and depolarizing potassium showed marked phosphorylation of AKT on Ser473, indicative of high endogenous AKT activity (see Fig. 7*A*, *first lane*). Under these conditions, adenoviral-mediated expression of DN-AKT resulted in a marked dephosphorylation of FKHRL1 on the AKT target site Ser253 (Fig. 8*A*), when compared to CGNs infected with a negative control adenovirus (Ad-CMV). Moreover, the dephosphorylation of FKHRL1 induced by DN-AKT was associated with a coordinated increase in the expression of Bim_S (Fig. 8*B*). These data further support a mechanism by which IGF-I/AKT signaling blocks Bim induction at the level of the FKHRL1 transcription factor.

DISCUSSION

IGF-I promotes the survival of CGNs both *in vitro* and *in vivo* (Ye et al., 1996; Lin and Bulleit, 1997). In the current study, we have investigated the neuroprotective mechanism of IGF-I in CGNs by systematically analyzing its effects on components of the intrinsic death signaling cascade. First, we found that IGF-I suppressed activation of the executioner caspase-3 in CGNs subjected to trophic factor withdrawal. This effect was blocked by the PI3K inhibitor wortmannin, consistent with a role for PI3K/AKT signaling in the IGF-I-mediated survival of CGNs. Previously, ribozyme-mediated downregulation of caspase-3 was shown to inhibit CGN apoptosis (Eldadah et al., 2000), supporting involvement of this executioner caspase in the mechanism of cell death. Comparable to our results, IGF-I has been shown to attenuate caspase-3 activation in other models of neuronal apoptosis via a PI3K/AKT-dependent mechanism (Van Golen and Feldman, 2000; Barber et al., 2001). We also found that IGF-I blocked activation of the intrinsic initiator caspase-9 in a PI3K-dependent manner. Recently, selective peptide inhibitors of caspase-9 were shown to prevent caspase-3 activation in CGNs, demonstrating that caspase-9 activation occurs upstream of the executioner during CGN apoptosis (Gerhardt et al., 2001). Moreover, we found that adenoviral CrmA, an inhibitor of caspase-9, protected CGNs from apoptosis. Similar to our data, IGF-I has been shown to prevent caspase-9 activation in rat retinal ganglion cells following optic nerve transection (Kermer et al., 2000). Collectively, these data suggest a common mechanism by which IGF-I blocks activation of the executioner caspase-3 in neurons via inhibition of the upstream, intrinsic initiator caspase-9.

Since caspase-9 is activated following its recruitment into the apoptosome, we analyzed the effects of IGF-I on cytochrome C release from mitochondria. Acute trophic factor withdrawal from CGNs induced a rapid redistribution of cytochrome C from mitochondria to

focal complexes localized in neuronal processes. The precise nature of these complexes is currently under investigation, but it is possible that these cytochrome C-rich structures represent large aggregates of apoptosomes. This would allow for a localized activation of caspases in neuronal processes where many structural targets of these proteases exist (eg., cytoskeletal proteins). We are currently attempting to co-localize Apaf-1 and caspase-9 by immunocytochemical methods to these cytochrome C-containing complexes. Regardless of their exact content, IGF-I essentially abolished formation of these complexes and maintained cytochrome C in mitochondria. The effects of IGF-I on cytochrome C redistribution were prevented by wortmannin, consistent with a previously recognized role for PI3K/AKT in the inhibition of cytochrome C release (Kennedy et al., 1999). The above results suggest that IGF-I inhibits activation of caspase-9 by preventing the release of cytochrome C and the subsequent formation of apoptosomes.

We next examined the role of the mitochondrial PTP in mediating the release of cytochrome C during CGN apoptosis. In trophic factor-deprived CGNs, marked mitochondrial swelling and depolarization were observed, indicative of PTP opening. Although IGF-I has been shown to prevent mitochondrial depolarization in neuroblastoma cells exposed to hyperosmotic conditions (Van Golen and Feldman, 2000), we did not observe any effect of IGF-I on either mitochondrial swelling or depolarization in CGNs. Although IGF-I clearly blocked apoptosis in trophic factor-deprived CGNs, the observation that it failed to prevent mitochondrial swelling indicates that the neurons still have damaged mitochondria in the presence of IGF-I. This finding suggests that a slower non-apoptotic death process was unmasked in CGNs by blocking the more rapid apoptotic death with IGF-I. The characterization of a non-apoptotic death pathway in CGNs will require further investigation. Nonetheless, since IGF-I blocked

cytochrome C release under conditions where it failed to affect mitochondrial swelling or depolarization, we conclude that opening of the PTP is insufficient to promote cytochrome C release in trophic factor-deprived CGNs. These results are in agreement with those previously reported for hippocampal neurons exposed to staurosporine in which cytochrome C release and caspase-3 activation preceded mitochondrial depolarization (Krohn et al., 1999). Collectively, these results indicate that opening of the PTP may not be a principal mechanism for cytochrome C release in neurons.

The pro-apoptotic Bcl-2 family member, Bax, has been implicated in cytochrome C release and apoptosis of CGNs *in vitro* and *in vivo* (Miller et al., 1997b; Desagher et al., 1999; Selimi et al., 2000b). The pro-apoptotic function of Bax is attenuated by anti-apoptotic members of the Bcl-2 family (Bcl-2, Bcl-X_L) which heterodimerize with Bax and sequester it away from mitochondria (Otter et al., 1998). Conversely, BH3-only Bcl-2 family members promote the pro-apoptotic effects of Bax by binding to Bcl-2, thus freeing Bax to incorporate into the mitochondrial membrane (Zong et al., 2001). In addition, BH3-only proteins have also been shown to interact with Bax and induce a conformational change that facilitates its incorporation into mitochondria (Desagher et al., 1999). These findings illustrate that BH3-only proteins serve several key functions in the Bax-dependent release of cytochrome C and initiation of the intrinsic death pathway.

The BH3-only protein Bim was recently shown to be induced in both sympathetic neurons subjected to NGF withdrawal and in trophic factor-deprived CGNs (Putcha et al., 2001; Whitfield et al., 2001). Sympathetic neuron apoptosis was attenuated by injection of Bim antisense oligonucleotides (Whitfield et al., 2001), and neurons from Bim knock-out mice were less sensitive to apoptosis than neurons from wild-type mice (Putcha et al., 2001). In addition,

overexpression of Bim induced apoptosis in sympathetic neurons (Whitfield et al., 2001) and in CGNs in a Bax-dependent manner (Harris and Johnson, 2001). Multiple isoforms of Bim have been identified that apparently arise by alternative splicing (O'Connor et al., 1998). In the works cited above (Putcha et al., 2001; Whitfield et al., 2001), Bim_{EL} was induced during neuronal apoptosis, whereas we observed induction of Bim_S in CGNs subjected to trophic factor withdrawal. These isoform-specific differences may be a result of the specific antibodies utilized to detect Bim. The polyclonal antibody used in the current study detected primarily a single ~15 kDa protein in CGN lysates, and in HEK293 cell lysates (data not shown), consistent with the apparent molecular weight of Bim_S. We observed an approximately three-fold induction of Bim_S protein following acute trophic factor withdrawal that was completely prevented by inclusion of IGF-I, in a PI3K-dependent manner. These results suggest that IGF-I suppresses the intrinsic death pathway upstream of Bim synthesis. Consistent with this conclusion, Harris and Johnson (2001) recently showed that IGF-I was unable to rescue CGNs from apoptosis induced by overexpression of the BH3-only protein Dp5/Hrk. Thus, our data are the first to identify the up-regulation of Bim as a major target of IGF-I action in neurons undergoing apoptosis.

Bim expression is regulated by multiple transcription factors. In NGF-deprived sympathetic neurons, dominant-negative c-Jun partially attenuated the induction of Bim mRNA and Bim_{EL} protein, inhibited cytochrome C release, and rescued sympathetic neurons from apoptosis (Whitfield et al., 2001). c-Jun has also been implicated in the apoptosis of CGNs (Watson et al., 1998), and an inhibitor of the JNK signaling pathway (CEP-1347) was recently shown to partially blunt the induction of Bim mRNA in CGNs subjected to trophic factor withdrawal (Harris and Johnson, 2001). In agreement with JNK/c-Jun involvement in the induction of Bim_S in CGNs undergoing apoptosis, the p38/JNK inhibitor, SB203580,

significantly attenuated both the activation of c-Jun and the increase in Bim_s expression. However, IGF-I failed to inhibit c-Jun activation under conditions where it significantly blocked induction of Bim_s. These results indicate that c-Jun plays a role in the regulation of Bim expression during CGN apoptosis, but IGF-I suppresses the induction of Bim via a mechanism that does not involve modulation of JNK/c-Jun signaling. This conclusion is in agreement with the work of Whitfield et al. (2001) who proposed that JNK/c-Jun signaling cooperates with a distinct JNK/c-Jun-independent pathway to stimulate the expression of Bim in sympathetic neurons deprived of NGF.

In this context, the forkhead transcription factor, FKHRL1, has recently been shown to regulate Bim expression in hematopoietic cells (Dijkers et al., 2000). Cytokine withdrawal from a pro-B cell line induced activation (dephosphorylation) of FKHRL1, induction of Bim, and apoptosis (Dijkers et al., 2000). Moreover, expression of a constitutively-active mutant of FKHRL1, in which three putative AKT phosphorylation sites are mutated to alanine, induced Bim expression, cytochrome C release, and apoptosis in hematopoietic cells (Dijkers et al., 2002). Given that FKHRL1 has been shown to be a substrate for AKT in neurons (Zheng et al., 2000), the AKT-mediated inactivation of FKHRL1 may be one mechanism by which IGF-I inhibits apoptosis. Indeed, overexpression of a constitutively-active, FKHRL1 triple phosphorylation-site mutant is sufficient to induce apoptosis of CGNs (Brunet et al., 1999). In the present study, we showed that trophic factor withdrawal from CGNs led to an inactivation of AKT, a corresponding activation of FKHRL1, and translocation of FKHRL1 to the nucleus. All of these effects, along with the induction of Bim, were prevented by IGF-I in a PI3K-dependent manner. In addition, adenoviral expression of a dominant-negative mutant of AKT was sufficient to activate FKHRL1 and induce Bim expression in CGNs maintained in the presence

of serum and depolarizing potassium. Taken together, our data suggest that IGF-I attenuates the induction of Bim in trophic factor-deprived CGNs via a PI3K/AKT-mediated inactivation of the FKHRL1 transcription factor.

In summary, our results demonstrate that suppression of the intrinsic death signaling cascade is a principal mechanism underlying the neuroprotective effects of IGF-I. IGF-I blocks Bim induction, cytochrome C release, and activation of the intrinsic initiator caspase-9 and the executioner caspase-3 in CGNs deprived of trophic support. Moreover, IGF-I inhibits the actions of FKHRL1, a transcriptional regulator of Bim, suggesting a novel c-Jun-independent mechanism for the modulation of Bim in neurons.

REFERENCES

Bach MA, Shen-Orr Z, Lowe WLJr, Roberts CTJr, LeRoith D (1991) Insulin-like growth factor I mRNA levels are developmentally regulated in specific regions of the rat brain. Brain Res Mol Brain Res 10: 43-48.

Barber AJ, Nakamura M, Wolpert EB, Reiter CE, Seigel GM, Antonetti DA, Gardner TW (2001) Insulin rescues retinal neurons from apoptosis by a phosphatidylinositol 3-kinase/Akt-mediated mechanism that reduces the activation of caspase-3. J Biol Chem 276: 32814-32821.

Bartlett WP, Li XS, Williams M, Benkovic S (1991) Localization of insulin-like growth factor-I mRNA in murine central nervous system during postnatal development. Dev Biol 147: 239-250.

Brunet A, Bonni A, Zigmond MJ, Lin MZ, Juo P, Hu LS, Anderson MJ, Arden KC, Blenis J, Greenberg ME (1999) Akt promotes cell survival by phosphorylating and inhibiting a Forkhead transcription factor. Cell 96: 857-868.

Chrysis D, Calikoglu AS, Ye P, D'Ercole AJ (2001) Insulin-like growth factor-I overexpression attenuates cerebellar apoptosis by altering the expression of Bcl family proteins in a developmentally specific manner. J Neurosci 21: 1481-1489.

Clarkson ED, Zawada WM, Bell KP, Esplen JE, Choi PK, Heidenreich KA, Freed CR (2001) IGF-I and bFGF improve dopamine neuron survival and behavioral outcome in parkinsonian rats receiving cultured human fetal tissue strands. Exp Neurol 168: 183-191.

Coffey ET, Smiciene G, Hongisto V, Cao J, Brecht S, Herdegen T, Courtney MJ (2002) c-Jun N-terminal protein kinase (JNK) 2/3 is specifically activated by stress, mediating c-Jun

activation, in the presence of constitutive JNK1 activity in cerebellar neurons. J Neurosci 22: 4335-4345.

Desagher S, Osen-Sand A, Nichols A, Eskes R, Montessuit S, Lauper S, Maundrell K, Antonsson B, Martinou JC (1999) Bid-induced conformational change of Bax is responsible for mitochondrial cytochrome c release during apoptosis. J Cell Biol 144: 891-901.

Dijkers PF, Medema RH, Lammers JW, Koenderman L, Coffer PJ (2000) Expression of the pro-apoptotic Bcl-2 family member Bim is regulated by the forkhead transcription factor FKHR-L1. Curr Biol 10: 1201-1204.

Dijkers PF, Birkenkamp KU, Lam EW, Thomas NS, Lammers JW, Koenderman L, Coffer PJ (2002) FKHR-L1 can act as a critical effector of cell death induced by cytokine withdrawal: protein kinase B-enhanced cell survival through maintenance of mitochondrial integrity. J Cell Biol 156: 531-542.

D'Mello SR, Galli C, Ciotti T, Calissano P (1993) Induction of apoptosis in cerebellar granule neurons by low potassium: inhibition of death by insulin-like growth factor I and cAMP. Proc Natl Acad Sci USA 90: 10989-10993.

Dudek H, Datta SR, Franke TF, Birnbaum MJ, Yao R, Cooper GM, Segal RA, Kaplan DR, Greenberg ME (1997) Regulation of neuronal survival by the serine-threonine protein kinase Akt. Science 275: 661-665.

Eilers A, Whitfield J, Babij C, Rubin LL, Ham J (1998) Role of the Jun kinase pathway in the regulation of c-Jun expression and apoptosis in sympathetic neurons. J Neurosci 18: 1713-1724.

Eldadah BA, Ren RF, Faden AI (2000) Ribozyme-mediated inhibition of caspase-3 protects cerebellar granule cells from apoptosis induced by serum-potassium deprivation. J Neurosci 20: 179-186.

Fernandez AM, de la Vega AG, Torres-Aleman I (1998) Insulin-like growth factor I restores motor coordination in a rat model of cerebellar ataxia. Proc Natl Acad Sci USA 95: 1253-1258.

Galli C, Meucci O, Scorziello A, Werge TM, Calissano P, Schettini G (1995) Apoptosis in cerebellar granule cells is blocked by high KCl, forskolin, and IGF-1 through distinct mechanisms of action: the involvement of intracellular calcium and RNA synthesis. J Neurosci 15: 1172-1179.

Garcia-Calvo M, Peterson EP, Leiting B, Ruel R, Nicholson DW, Thornberry NA (1998) Inhibition of human caspases by peptide-based and macromolecular inhibitors. J Biol Chem 273: 32608-32613.

Gerhardt E, Kugler S, Leist M, Beier C, Berliocchi L, Volbracht C, Weller M, Bahr M, Nicotera P, Schulz JB (2001) Cascade of caspase activation in potassium-deprived cerebellar granule neurons: targets for treatment with peptide and protein inhibitors of apoptosis. Mol Cell Neurosci 17: 717-731.

Green DR (1998) Apoptotic pathways: the roads to ruin. Cell 94: 695-698.

Harada J, Sugimoto M (1999) An inhibitor of p38 and JNK MAP kinases prevents activation of caspase and apoptosis of cultured cerebellar granule neurons. Jpn J Pharmacol 79: 369-378.

Harris CA, Johnson EMJr (2001) BH3-only Bcl-2 family members are coordinately regulated by the JNK pathway and require Bax to induce apoptosis in neurons. J Biol Chem 276: 37754-37760.

Heck S, Lezoualc'h F, Engert S, Behl C (1999) Insulin-like growth factor-1-mediated neuroprotection against oxidative stress is associated with activation of nuclear factor kappaB. J Biol Chem 274: 9828-9835.

Kennedy SG, Kandel ES, Cross TK, Hay N (1999) Akt/Protein kinase B inhibits cell death by preventing the release of cytochrome c from mitochondria. Mol Cell Biol 19: 5800-5810.

Kermer P, Ankerhold R, Klocker N, Krajewski S, Reed JC, Bahr M (2000) Caspase-9: involvement in secondary death of axotomized rat retinal ganglion cells in vivo. Brain Res Mol Brain Res 85: 144-150.

Korsmeyer SJ, Wei MC, Saito M, Weiler S, Oh KJ, Schlesinger PH (2000) Pro-apoptotic cascade activates BID, which oligomerizes BAK or BAX into pores that result in the release of cytochrome c. Cell Death Differ 7: 1166-1173.

Krohn AJ, Wahlbrink T, Prehn JH (1999) Mitochondrial depolarization is not required for neuronal apoptosis. J Neurosci 19: 7394-7404.

Kuida K, Haydar TF, Kuan CY, Gu Y, Taya C, Karasuyama H, Su MS, Rakic P, Flavell RA (1998) Reduced apoptosis and cytochrome c-mediated caspase activation in mice lacking caspase 9. Cell 94: 325-337.

Lai EC, Felice KJ, Festoff BW, Gawel MJ, Gelinas DF, Kratz R, Murphy MF, Natter HM, Norris FH, Rudnicki SA (1997) Effect of recombinant human insulin-like growth factor-I on progression of ALS. A placebo-controlled study. The North America ALS/IGF-I Study Group. Neurology 49: 1621-1630.

Li M, Wang X, Meintzer MK, Laessig T, Birnbaum MJ, Heidenreich KA (2000) Cyclic AMP promotes neuronal survival by phosphorylation of glycogen synthase kinase 3beta. Mol Cell Biol 20: 9356-9363.

Lin X, Bulleit RF (1997) Insulin-like growth factor I (IGF-I) is a critical trophic factor for developing cerebellar granule cells. Brain Res Dev Brain Res 99: 234-242.

Liu XF, Fawcett JR, Thorne RG, Frey WH2nd (2001) Non-invasive intranasal insulin-like growth factor-I reduces infarct volume and improves neurologic function in rats following middle cerebral artery occlusion. Neurosci Lett 308: 91-94.

Martinou JC, Green DR (2001) Breaking the mitochondrial barrier. Nat Rev Mol Cell Biol 2: 63-67.

Miller TM, Tansey MG, Johnson EMJr, Creedon DJ (1997a) Inhibition of phosphatidylinositol 3-kinase activity blocks depolarization- and insulin-like growth factor I-mediated survival of cerebellar granule cells. J Biol Chem 272: 9847-9853.

Miller TM, Moulder KL, Knudson CM, Creedon DJ, Deshmukh M, Korsmeyer SJ, Johnson E M Jr (1997b) Bax deletion further orders the cell death pathway in cerebellar granule cells and suggests a caspase-independent pathway to cell death. J Cell Biol 139: 205-217.

Minden A, Lin A, Smeal T, Derijard B, Cobb M, Davis R, Karin M (1994) c-Jun N-terminal phosphorylation correlates with activation of the JNK subgroup but not the ERK subgroup of mitogen-activated protein kinases. Mol Cell Biol 14: 6683-6688.

Mustafa A, Lannfelt L, Lilius L, Islam A, Winblad B, Adem A (1999) Decreased plasma insulin-like growth factor-I level in familial Alzheimer's disease patients carrying the Swedish APP 670/671 mutation. Dement Geriatr Cogn Disord 10: 446-451.

O'Connor L, Strasser A, O'Reilly LA, Hausmann G, Adams JM, Cory S, Huang DC (1998) Bim: a novel member of the Bcl-2 family that promotes apoptosis. EMBO J 17: 384-395.

Otter I, Conus S, Ravn U, Rager M, Olivier R, Monney L, Fabbro D, Borner C (1998) The binding properties and biological activities of Bcl-2 and Bax in cells exposed to apoptotic stimuli. J Biol Chem 273: 6110-6120.

Putcha GV, Moulder KL, Golden JP, Bouillet P, Adams JA, Strasser A, Johnson EMJr (2001) Induction of BIM, a proapoptotic BH3-only BCL-2 family member, is critical for neuronal apoptosis. Neuron 29: 615-628.

Rotwein P, Burgess SK, Milbrandt JD, Krause JE (1988) Differential expression of insulin-like growth factor genes in rat central nervous system. Proc Natl Acad Sci USA 85: 265-269.

Russell JW, Windebank AJ, Schenone A, Feldman EL (1998) Insulin-like growth factor-I prevents apoptosis in neurons after nerve growth factor withdrawal. J Neurobiol 36: 455-467.

Selimi F, Doughty M, Delhaye-Bouchaud N, Mariani J (2000a) Target-related and intrinsic neuronal death in Lurcher mutant mice are both mediated by caspase-3 activation. J Neurosci 20: 992-1000.

Selimi F, Vogel MW, Mariani J (2000b) Bax inactivation in lurcher mutants rescues cerebellar granule cells but not purkinje cells or inferior olivary neurons. J Neurosci 20: 5339-5345.

Tagami M, Yamagata K, Nara Y, Fujino H, Kubota A, Numano F, Yamori Y (1997) Insulin-like growth factors prevent apoptosis in cortical neurons isolated from stroke-prone spontaneously hypertensive rats. Lab Invest 76: 603-612.

Torres-Aleman I, Barrios V, Lledo A, Berciano J (1996) The insulin-like growth factor I system in cerebellar degeneration. Ann Neurol 39: 335-342.

Van Golen CM, Feldman EL (2000) Insulin-like growth factor I is the key growth factor in serum that protects neuroblastoma cells from hyperosmotic-induced apoptosis. J Cell Physiol 182: 24-32.

Watson A, Eilers A, Lallemand D, Kyriakis J, Rubin LL, Ham J (1998) Phosphorylation of c-Jun is necessary for apoptosis induced by survival signal withdrawal in cerebellar granule neurons. J Neurosci 18: 751-762.

Wei MC, Zong WX, Cheng EH, Lindsten T, Panoutsakopoulou V, Ross AJ, Roth KA, MacGregor GR, Thompson CB, Korsmeyer SJ (2001) Proapoptotic BAX and BAK: a requisite gateway to mitochondrial dysfunction and death. Science 292: 727-730.

White RJ, Reynolds IJ (1996) Mitochondrial depolarization in glutamate-stimulated neurons: an early signal specific to excitotoxin exposure. J Neurosci 16: 5688-5697.

Whitfield J, Neame SJ, Paquet L, Bernard O, Ham J (2001) Dominant-negative c-Jun promotes neuronal survival by reducing BIM expression and inhibiting mitochondrial cytochrome c release. Neuron 29: 629-643.

Ye P, Xing Y, Dai Z, D'Ercole AJ (1996) In vivo actions of insulin-like growth factor-I (IGF-I) on cerebellum development in transgenic mice: evidence that IGF-I increases proliferation of granule cell progenitors. Brain Res Dev Brain Res 95: 44-54.

Zhang W, Ghetti B, Lee WH (1997) Decreased IGF-I gene expression during the apoptosis of Purkinje cells in pcd mice. Brain Res Dev Brain Res 98: 164-176.

Zheng WH, Kar S, Quirion R (2000) Insulin-like growth factor-1-induced phosphorylation of the forkhead family transcription factor FKHRL1 is mediated by Akt kinase in PC12 cells. J Biol Chem 275: 39152-39158.

Zong WX, Lindsten T, Ross AJ, MacGregor GR, Thompson CB (2001) BH3-only proteins that bind pro-survival Bcl-2 family members fail to induce apoptosis in the absence of Bax and Bak. Genes Dev 15: 1481-1486.

Zou H, Li Y, Liu X, Wang X (1999) An APAF-1.cytochrome c multimeric complex is a functional apoptosome that activates procaspase-9. J Biol Chem 274: 11549-11556.

FIGURE LEGENDS

Figure 1. IGF-I inhibits apoptosis and activation of the executioner caspase-3 and the intrinsic initiator caspase-9 in CGNs subjected to trophic factor withdrawal. *A*, CGNs were incubated for 24 hr in either control (25K+Ser) or apoptotic (5K-Ser) medium containing either PBS vehicle (VEH) or IGF-I (200 ng/ml) in the absence or presence of wortmannin (WORT, 100 nM). Following incubation, CGNs were fixed and nuclei were stained with DAPI. Scale bar=10 microns. *B*, The percentages of apoptotic CGNs observed under the conditions described in *A* were quantified by counting approximately 500 CGNs per field in two fields per condition. Values represent the means±S.E.M. for three independent experiments, each performed in triplicate. *Significantly different from the 25K+Ser control ($p<0.01$). *C*, CGNs were incubated as described in *A*, but for only 6 hr. Detergent-soluble cell lysates were subjected to SDS-PAGE on 15% polyacrylamide gels and proteins were transferred to PVDF membranes. Activation of caspase-3 was assessed by immunoblotting (IB) with a polyclonal antibody that recognizes both the pro-form (~32 kDa) and the cleaved form (~19 kDa active fragment) of the enzyme. The blot shown is representative of results obtained in three separate experiments. *D*, CGNs were incubated exactly as described in *C* and cell lysates were electrophoresed as described in *C*. Activation of caspase-9 was assessed by western blotting with a polyclonal antibody that specifically recognizes the cleaved form (active fragment) of the caspase. The blot shown is representative of three independent experiments.

Figure 2. IGF-I blocks cytochrome C release from mitochondria and prevents its redistribution to focal complexes localized in neuronal processes. CGNs were incubated for 4 hr in control

(25K+Ser) or apoptotic (5K-Ser) medium containing either PBS vehicle or IGF-I (200 ng/ml) in the absence or presence of wortmannin (WORT, 100 nM). Following incubation, CGNs were fixed in 4% paraformaldehyde, permeabilized with 0.2% Triton-X-100, and blocked with 5% BSA. Cytochrome C was localized by incubating the cells with a polyclonal antibody to cytochrome C and a Cy3-conjugated secondary antibody. Digitally deconvolved images were then captured using a 63X oil objective. The images shown are representative of results obtained in three separate experiments. Scale bar=10 microns. *A*, CGNs incubated in control medium demonstrated intense cytochrome C staining in the perinuclear region consistent with localization to mitochondria. Very diffuse staining was observed in neuronal processes. *B*, CGNs incubated in apoptotic medium for 4 hr showed a marked redistribution of cytochrome C. Note the overall diffuse staining throughout the cytoplasm accompanied by the formation of distinct, brightly fluorescent focal complexes on the cell bodies and processes. *C*, The area demarcated by the box in *A* is enlarged to show the diffuse cytochrome C staining in a control neuronal process. *D*, The area demarcated by the box in *B* is enlarged to show the intense cytochrome C staining localized to discrete focal complexes (indicated by the arrowheads) in neuronal processes of CGNs deprived of serum and depolarizing potassium. *E*, A region containing multiple processes (proc) from control CGNs is shown. Note the overall diffuse cytochrome C staining. *F*, A region containing multiple processes from CGNs incubated in apoptotic medium for 4 hr is shown. Note the presence of many distinct focal areas of intense cytochrome C staining (indicated by the arrowheads). *G*, CGNs incubated in apoptotic medium containing exogenous IGF-I displayed cytochrome C localization to mitochondria similar to control CGNs (see panel *A* for comparison). *H*, CGNs incubated in apoptotic medium containing both IGF-I and wortmannin showed cytochrome C staining similar to CGNs incubated in

apoptotic medium alone (see panel *B* for comparison). Focal complexes of cytochrome C staining are indicated by the arrowheads.

Figure 3. Mitochondrial swelling induced by trophic factor withdrawal is not inhibited by IGF-I. CGNs were incubated for 4 hr in either control (25K+Ser) or apoptotic (5K-Ser) medium containing either PBS vehicle (VEH) or IGF-I (200 ng/ml). To test for reversibility of mitochondrial swelling, CGNs were first incubated for 2 hr in apoptotic medium and were then returned to control medium for an additional 2 hr prior to staining (REV). In preliminary time course experiments, a 2 hr incubation in apoptotic medium was found sufficient to induce marked mitochondrial swelling (data not shown). Thirty minutes prior to fixation, JC1 (final concentration of 2 μg/ml) and Hoechst dye were added to the cultures to stain mitochondria and nuclei, respectively. JC1 fluorescence was captured using a Cy3 filter under 100X oil. *A*. Representative images of CGNs incubated as described above and stained with Hoechst and JC1. Mitochondria are indicated by the arrowheads. Note the dramatic swelling of mitochondria in CGNs incubated in apoptotic medium in either the absence or presence of IGF-I. Mitochondrial swelling was completely reversible if control medium was replaced within 2 hr (REV). The images shown are representative of CGNs from four separate experiments. Scale bar=10 microns. *B*, Distribution of mitochondrial diameters from CGNs observed under the conditions described in *A*. The diameters of approximately 150 mitochondria per treatment condition were measured from digitally deconvolved images obtained from a total of 15 to 20 CGNs (randomly pooled from four independent experiments). The mitochondrial diameters were categorized into the indicated size groups and graphed as a percentage of the total mitochondria with a given diameter. *C*, Quantification of the mean mitochondrial diameters for CGNs observed under the

conditions described in *A*. Values represent the means±S.E.M. mitochondrial diameters obtained from the mitochondria measured in *B*. *Significantly different from the 25K+Ser control ($p<0.01$).

Figure 4. Mitochondrial membrane depolarization elicited by trophic factor withdrawal is not prevented by IGF-I. CGNs grown on glass coverslips were incubated for 4 hr in either control (25K+Ser) or apoptotic (5K-Ser) medium alone or containing IGF-I (200 ng/ml). Thirty minutes prior to the end of the incubation period, tetramethylrhodamine ethyl ester (TMRE, 500 nM) and Hoechst were added directly to the cells. Following incubation, coverslips were inverted onto slides into a small volume of phenol red-free medium lacking serum or depolarizing potassium but containing TMRE (500 nM). Living cells were then imaged under 100X oil. Nuclear staining with Hoechst is shown in blue and TMRE is shown in red. Scale bar =10 microns. CGNs maintained in control medium during the 4 hr incubation period displayed many mitochondria that were intensely stained with TMRE, indicative of an intact membrane potential (*upper left panel*). In contrast, CGNs incubated in apoptotic medium in either the absence (*upper right panel*) or presence (*lower left panel*) of IGF-I expressed very little detectable mitochondrial TMRE staining, characteristic of a loss of mitochondrial membrane potential or depolarization. Approximately 5 to 10 min were required to capture the images described above. Therefore, at the end of the capture duration a final image was acquired of another control CGN to show that the mitochondrial membrane potential was not compromised during the time required to capture images (25K+Ser POST). The images shown were all acquired at equal exposure times for TMRE fluorescence and are representative of results obtained from three independent experiments, each performed in duplicate.

Figure 5. IGF-I inhibits induction of the BH3-only Bcl-2 family member Bim in a PI3K-dependent manner. *A*, CGNs were incubated for 6 hr in either control (25K+Ser) or apoptotic (5K-Ser) medium containing either PBS vehicle (VEH) or IGF-I (200 ng/ml) ± wortmannin (WORT, 100 nM). Following incubation, cell lysates were subjected to SDS-PAGE on 15% polyacrylamide gels and proteins were transferred to PVDF membranes. Bim expression was assessed by immunoblotting with a polyclonal antibody to Bim that specifically recognized an approximately 15 kDa protein, consistent with the apparent molecular weight of Bim short (Bim_S). To affirm equal protein loading, the blot was then stripped and reprobed for the anti-apoptotic Bcl-2 family member, $BclX_L$, which did not demonstrate any significant change in expression under the conditions of this experiment. The blots shown are representative of three separate experiments. *B*, Quantification of Bim_S expression observed under the conditions described in *A* was performed by computer-assisted imaging densitometry. Values represent the means±S.E.M. for three independent experiments and are expressed relative to the densitometry of Bim_S observed in control CGNs (set to 1.0). *Significantly different from the 25K+Ser control ($p<0.01$).

Figure 6. Inhibition of c-Jun signaling attenuates induction of Bim: IGF-I does not block c-Jun activation in trophic factor-deprived CGNs. *A*, CGNs were incubated for 4 hr in either control (25K+Ser) or apoptotic (5K-Ser) medium in the absence or presence of the JNK/p38 inhibitor SB203580 (SB, 20 μM). Following incubation, cells were fixed and c-Jun phosphorylated on Ser63 was detected exclusively in the nuclear compartment using a phospho-specific polyclonal antibody. The images shown are representative of results obtained in three independent experiments. Scale bar=10 microns. *B*, CGNs were incubated for 4 hr in either control

(25K+Ser) or apoptotic (5K-Ser) medium in the presence of either DMSO vehicle (0.2%, VEH) or SB (20 μM) and cell lysates were subjected to SDS-PAGE on 10% polyacrylamide gels. Proteins were transferred to PVDF membranes and immunoblotted (IB) with a polyclonal antibody to c-Jun. The blot shown is representative of three separate experiments. *C*, CGNs were incubated as described in *B*, but for 6 hr, and cell lysates were electrophoresed on 15% polyacrylamide gels and probed for Bim_S. *D*, Densitometric analysis of Bim_S from three independent experiments performed as described in *C*. The densitometry of Bim_S detected in control (25K+Ser) CGNs was set at 1.0 and all other values were calculated relative to the control. *Significantly different from the 25K+Ser control ($p<0.01$). *E*, CGNs were incubated for 4 hr in either control (25K+Ser) or apoptotic (5K-Ser) medium in the presence of either PBS vehicle (VEH) or IGF-I (200 ng/ml). Following incubation, nuclear c-Jun phosphorylated on Ser63 was detected using a phospho-specific polyclonal antibody. The images shown are representative of three experiments. Scale bar=10 microns. *F*, CGNs incubated as described in *E* were lysed and extracted proteins were immunoblotted for c-Jun. The blot shown is illustrative of results obtained from three separate experiments.

Figure 7. IGF-I sustains the phosphorylation of AKT and FKHRL1 and prevents the nuclear localization of FKHRL1 in CGNs deprived of trophic support. *A*, CGNs were incubated for 4 hr in either control (25K+Ser) or apoptotic (5K-Ser) medium containing either PBS vehicle (VEH) or IGF-I (200 ng/ml) ± wortmannin (WORT, 100 nM). Following incubation, cell lysates were subjected to SDS-PAGE on 10% polyacrylamide gels and proteins were transferred to PVDF membranes. Membranes were probed with a phospho-specific antibody that detects *active* AKT phosphorylated on Ser473 (p-AKT). Blots were then stripped and reprobed for total AKT to

demonstrate equal loading. The blots shown are typical of results obtained in three separate experiments. *B*, CGNs were treated exactly as described in *A* and cell lysates were immunoblotted for *inactive* FKHRL1 phosphorylated on Ser253 (p-FKHRL1) using a phospho-specific antibody. Membranes were then stripped and reprobed for total FKHRL1 to verify equal loading. The blots shown are illustrative of three independent experiments. *C*, CGNs incubated as described in *A* were fixed and then incubated with a polyclonal antibody to FKHRL1 followed by a Cy3-conjugated secondary antibody. Fluorescent, digitally deconvolved images were acquired using a 63X oil objective. The arrowheads indicate nuclei that are relatively devoid of FKHRL1 immunoreactivity. The images shown are representative of three separate experiments. Scale bar=10 microns.

Figure 8. Adenoviral dominant-negative AKT induces dephosphorylation of FKHRL1 and increases Bim expression. On day 5 in culture, CGNs were infected with either a negative control adenovirus (Ad-CMV) or adenovirus expressing kinase dead (dominant-negative) AKT (Ad-DN-AKT), each at a multiplicity of infection of 50. Forty-eight hours post-infection, cell lysates were subjected to SDS-PAGE on either 7.5% (p-FKHRL1) or 15% (Bim_S) polyacrylamide gels and proteins were transferred to PVDF membranes. *A*, The membrane was probed with a phospho-specific antibody to *inactive* FKHRL1 phosphorylated on Ser253 (p-FKHRL1). *B*, The blot was probed with a polyclonal antibody that detects the short isoform of Bim (Bim_S).

A

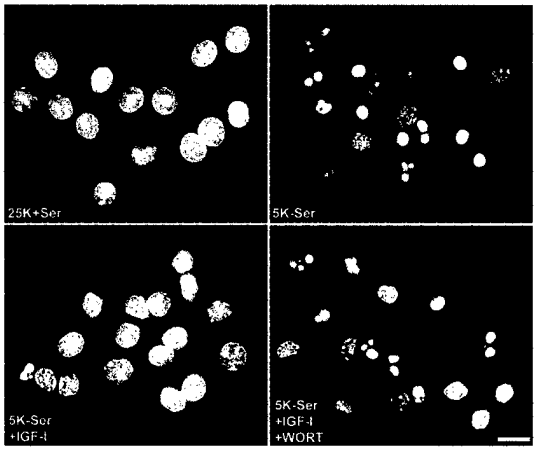
25K+Ser
5K-Ser
5K-Ser
+IGF-I
5K-Ser
+IGF-I
+WORT

B

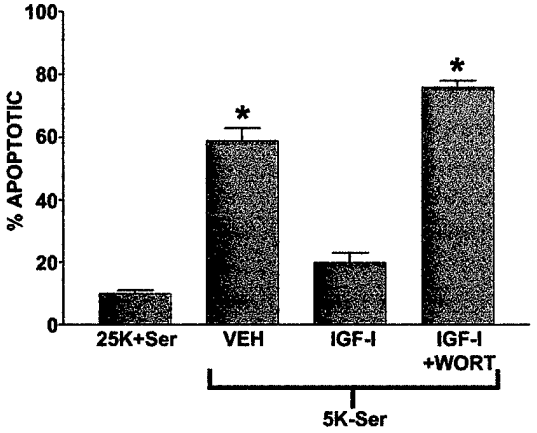
% APOPTOTIC
100
80
60
40
20
0
*
*
25K+Ser
VEH
IGF-I
IGF-I
+WORT
5K-Ser

C

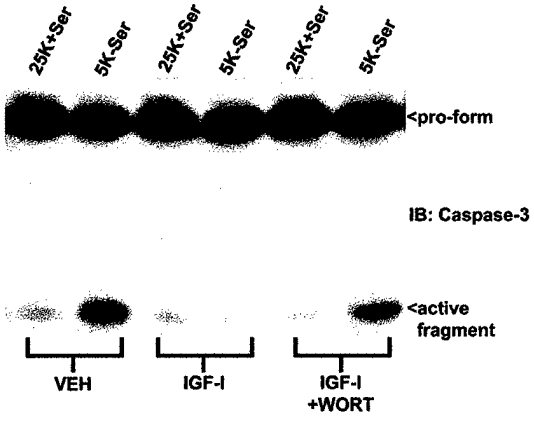
25K+Ser
5K-Ser
25K+Ser
5K-Ser
25K+Ser
5K-Ser
<pro-form
IB: Caspase-3
<active
fragment
VEH
IGF-I
IGF-I
+WORT

D

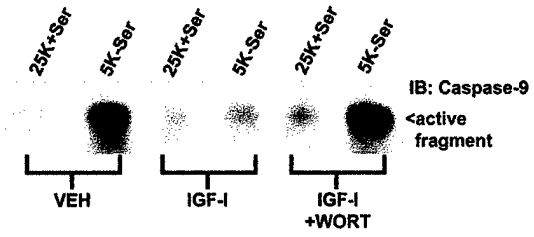
25K+Ser
5K-Ser
25K+Ser
5K-Ser
25K+Ser
5K-Ser
IB: Caspase-9
<active
fragment
VEH
IGF-I
IGF-I
+WORT

Linseman, et al
Fig. 1

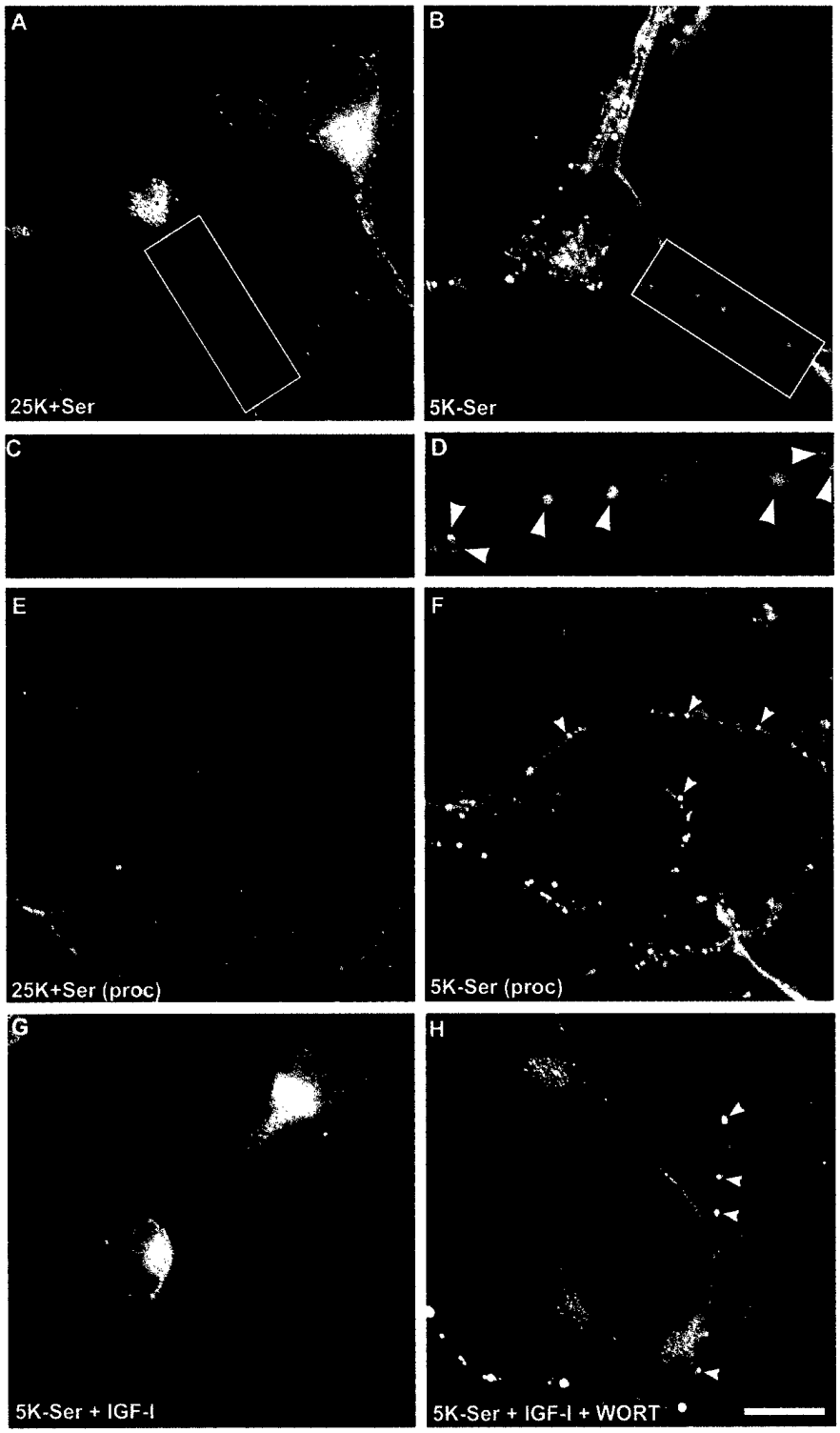
A
25K+Ser
B
5K-Ser
C
D
E
25K+Ser (proc)
F
5K-Ser (proc)
G
5K-Ser + IGF-I
H
5K-Ser + IGF-I + WORT

Linseman, et al
Fig. 2

0804 82

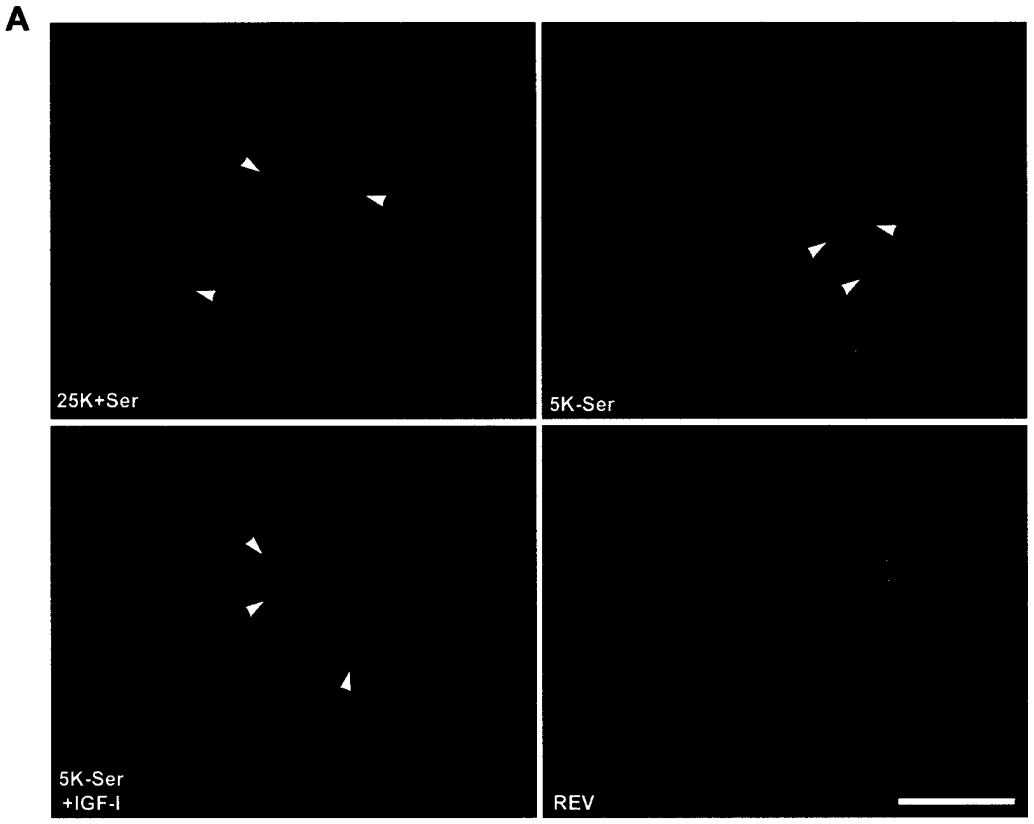
A
25K+Ser
5K-Ser
5K-Ser
+IGF-I
REV
B
% of Total Mitochondria
40
30
20
10
0
25K+Ser
5K-Ser
5K-Ser+IGF-I
<0.3
0.3-0.5
0.5-0.7
0.7-0.9
0.9-1.1
1.1-1.3
1.3-1.5
1.5-1.7
1.7-1.9
>1.9
Mitochondrial Diameter (microns)
C
Mitochondrial Diameter (microns)
1.2
1.0
0.8
0.6
0.4
*
*
25K+Ser
VEH
IGF-I
REV
5K-Ser

0760L-05

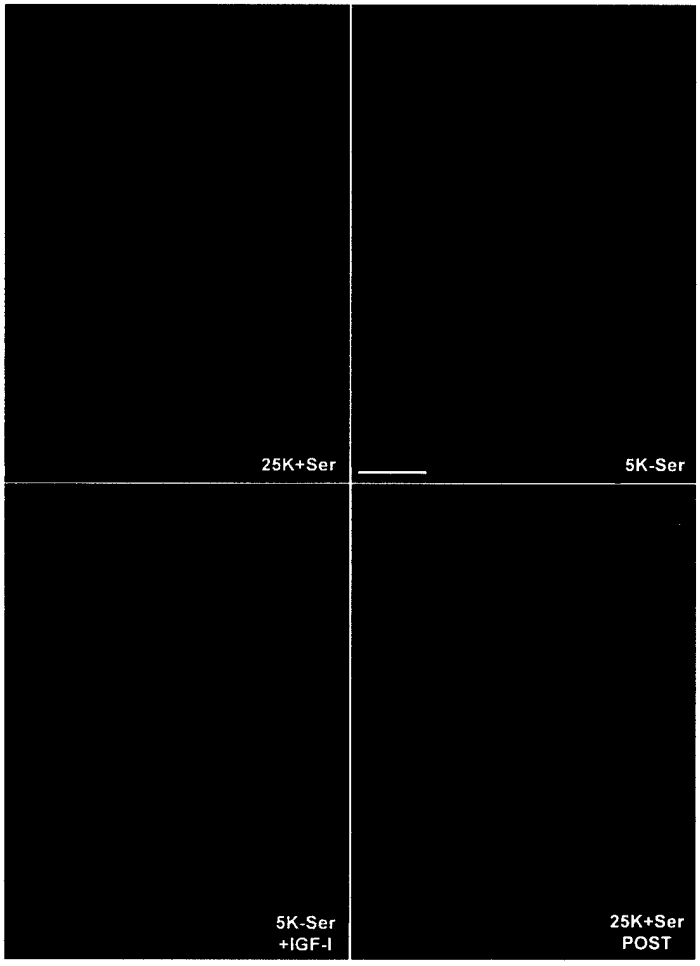
25K+Ser
5K-Ser
5K-Ser
+IGF-I
25K+Ser
POST

Linseman, et al
Fig. 4

0804-05

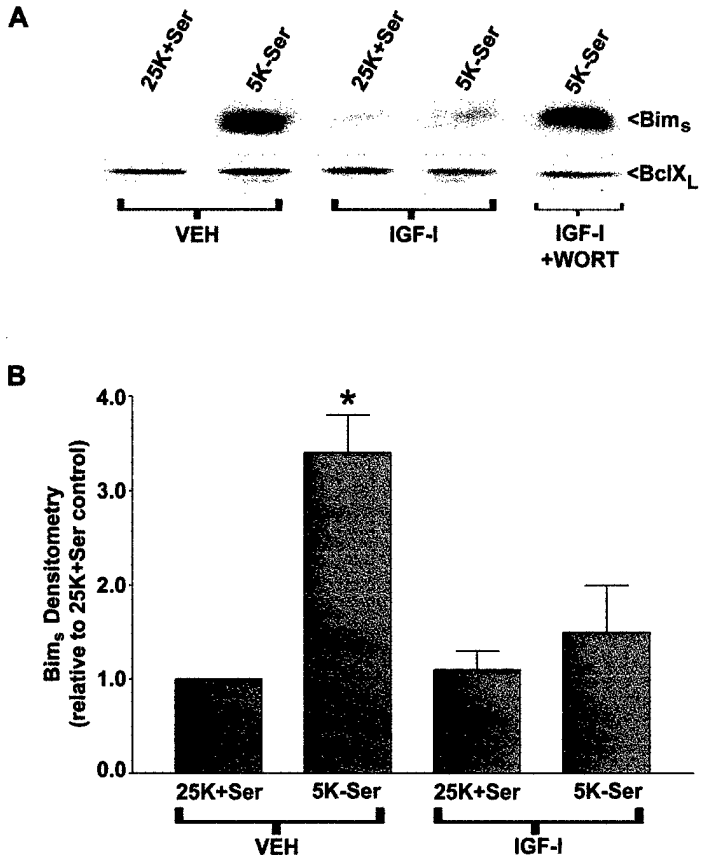
A
25K+Ser
5K-Ser
25K+Ser
5K-Ser
5K-Ser
<Bim$_S$
<BclX$_L$
VEH
IGF-I
IGF-I
+WORT
B
Bim$_S$ Densitometry
(relative to 25K+Ser control)
4.0
3.0
2.0
1.0
0.0
*
25K+Ser
5K-Ser
25K+Ser
5K-Ser
VEH
IGF-I

Linseman, et al
Fig. 5

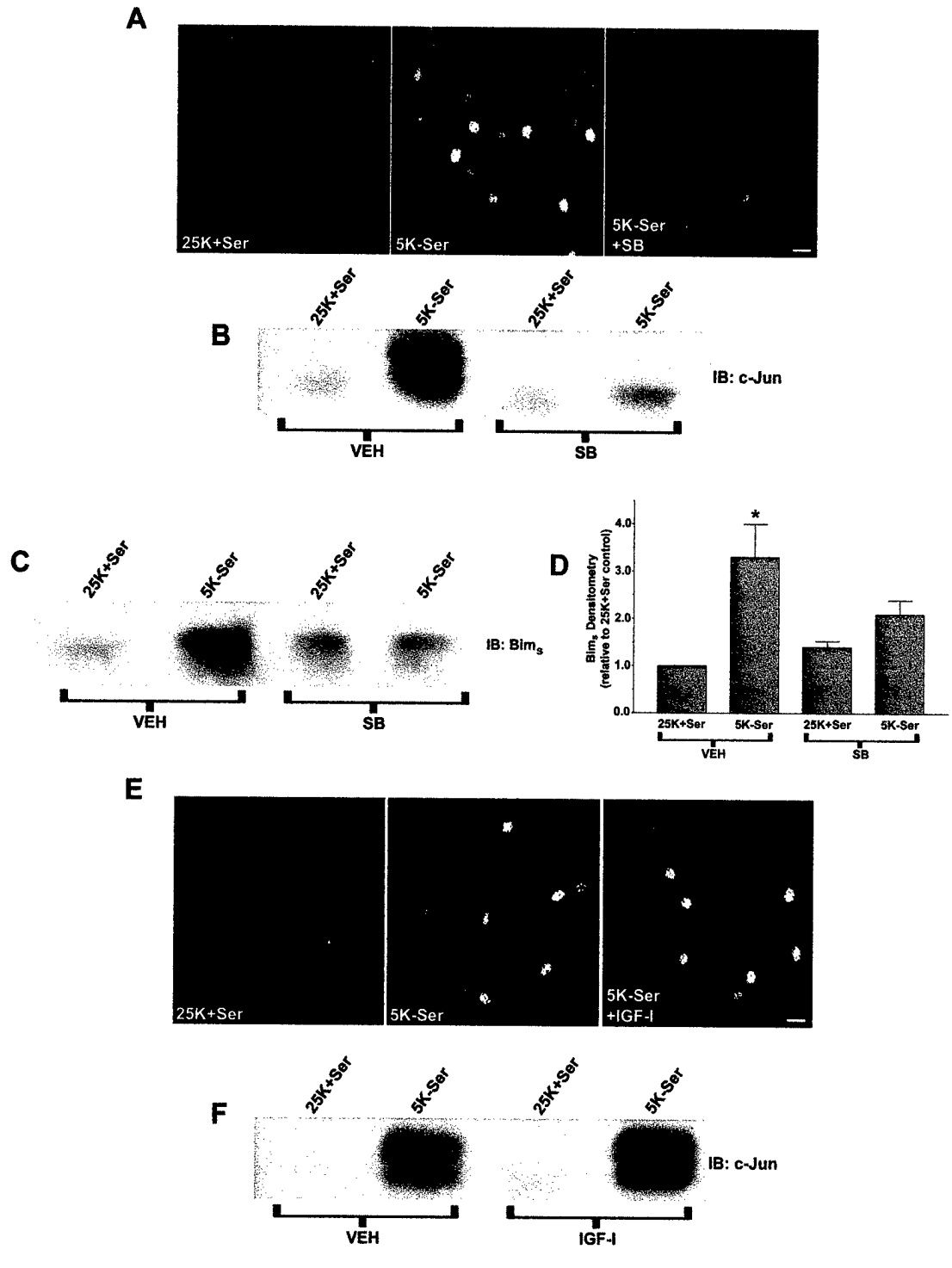
A
25K+Ser
5K-Ser
5K-Ser
+SB
B
25K+Ser
5K-Ser
25K+Ser
5K-Ser
IB: c-Jun
VEH
SB
C
25K+Ser
5K-Ser
25K+Ser
5K-Ser
IB: Bim$_S$
VEH
SB
D
Bim$_S$ Densitometry
(relative to 25K+Ser control)
4.0
3.0
2.0
1.0
0.0
*
25K+Ser
5K-Ser
25K+Ser
5K-Ser
VEH
SB
E
25K+Ser
5K-Ser
5K-Ser
+IGF-I
F
25K+Ser
5K-Ser
25K+Ser
5K-Ser
IB: c-Jun
VEH
IGF-I

Linseman, et al
Fig. 6

A

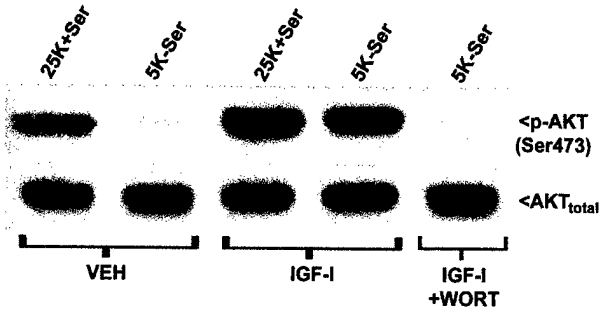
25K+Ser
5K-Ser
25K+Ser
5K-Ser
5K-Ser
<p-AKT (Ser473)
<AKT total
VEH
IGF-I
IGF-I +WORT

B

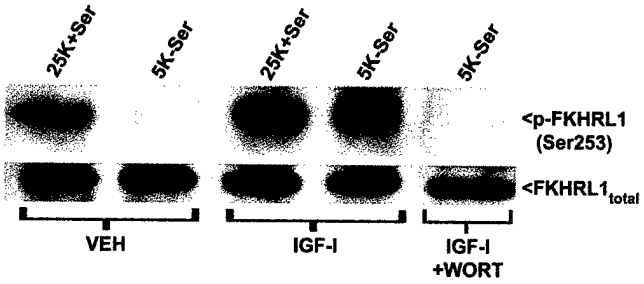
25K+Ser
5K-Ser
25K+Ser
5K-Ser
5K-Ser
<p-FKHRL1 (Ser253)
<FKHRL1 total
VEH
IGF-I
IGF-I +WORT

C

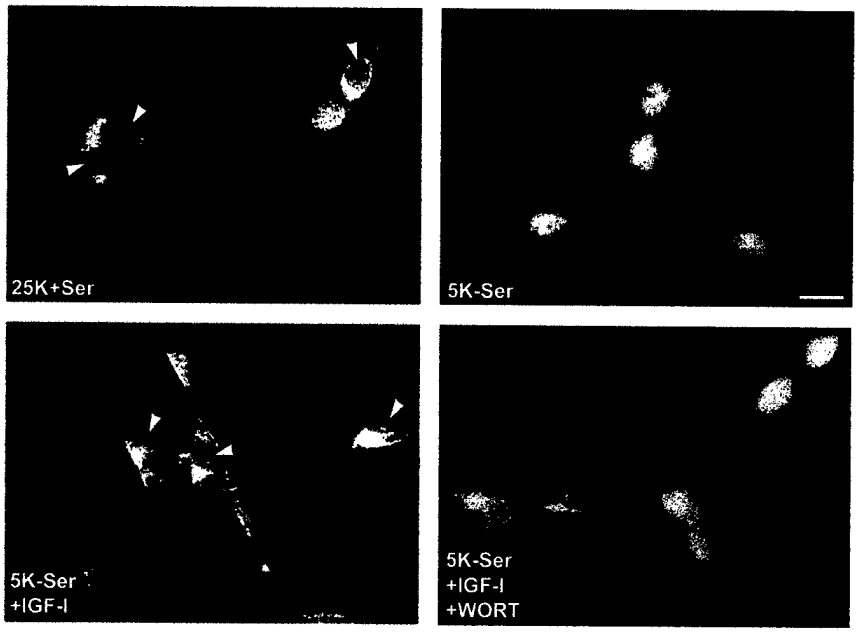
25K+Ser
5K-Ser
5K-Ser +IGF-I
5K-Ser +IGF-I +WORT

Linseman, et al
Fig. 7

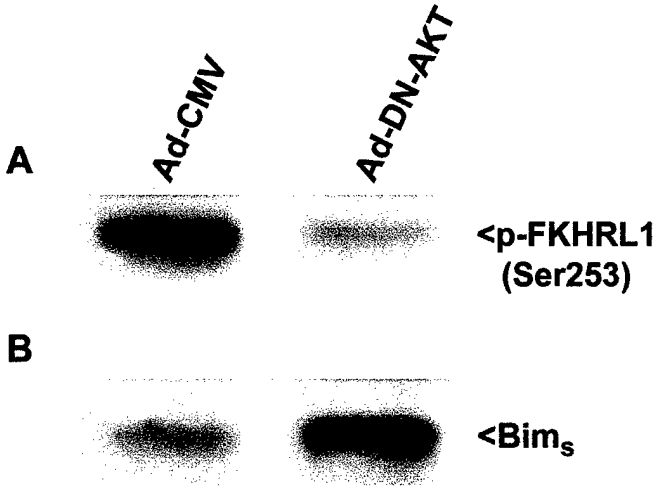
A
Ad-CMV
Ad-DN-AKT
<p-FKHRL1
(Ser253)
B
<Bim$_S$

Linseman, et al
Fig. 8

1: J Biol Chem 2002 Jul 22; [epub ahead of print]

Adhesion related kinase (ARK) repression of gonadotropin releasing hormone(GnRH) gene expression requires RAC activation of the extracellular signal-regulated kinase (ERK) pathway.

Allen MP, Xu M, Linseman DA, Pawlowski JE, Bokoch GM, Heidenreich KA, Wierman ME.

Dept. of Medicine, University of Colorado Health Sciences Center/VAMC, Denver, CO 80220.

Recent studies suggest that adhesion related kinase (Ark) plays a role in gonadotropin releasing hormone (GnRH) neuronal physiology. Ark promotes migration of GnRH neurons via Rac GTPase and concomitantly suppresses GnRH gene expression via homeodomain and myocyte enhancer factor-2 (MEF2) transcription factors. Here, we investigated the signaling cascade required for Ark inhibition of the GnRH promoter in GT1-7 GnRH neuronal cells. Ark repression was blocked by the MEK/ERK pathway inhibitor, PD98059, and dominant negative (DN) MEK1 but was unaffected by DN-Ras. Inhibitors of the Rho family GTPases, C. difficile toxin B (Rho/Rac/Cdc42 inhibitor) and C. sordellii lethal toxin (Rac/Cdc42 inhibitor), blocked Ark inhibition of GnRH transcription. Moreover, DN-Rac blunted both Ark activation of ERK and repression of the GnRH promoter, demonstrating an essential role for Rac in coupling Ark to ERK activation. Like Ark, a constitutively active (CA) mutant of Rac suppressed GnRH transcription in an ERK dependent manner. Finally, Ark-mediated repression was significantly attenuated by a DN-MEF2C, whereas repression induced by CA-Rac was unaffected, indicating that MEF2 proteins are not targets of the Ark-Rac-MEK-ERK cascade. The data suggest that Ark suppresses GnRH gene expression via the coordinated activation of a Rac-ERK signaling pathway and a distinct MEF2-dependent mechanism.

PMID: 12138087 [PubMed - as supplied by publisher]

8th International Conference on Neural Transplantation and Repair, Keystone, CO (2002)

EXTRINSIC AND INTRINSIC DEATH SIGNALING IN CEREBELLAR NEURONAL APOPTOSIS: THE IGF-I CONNECTION

Linseman DA, McClure ML, Phelps RA, Bouchard RJ, Laessig TA, Le SS, Ahmadi F, Heidenreich KA
University of Colorado Health Sciences Center, Department of Pharmacology, 4200 East Ninth Avenue, Denver CO 80262 and Denver Veterans Affairs Medical Center

Primary cerebellar granule neurons die by apoptosis when deprived of serum and depolarizing potassium. Here, we investigated the role of extrinsic (death receptor-mediated) and intrinsic (mitochondrial-dependent) death signals in cerebellar neuron apoptosis. Expression of adenoviral, epitope-tagged, dominant-negative Fas-associated death domain protein (ΔFADD) decreased granule neuron apoptosis by approximately 75%. Immunocytochemical staining for the epitope tag revealed that <5% of granule neurons expressed ΔFADD. In contrast, ΔFADD expression was observed in >95% of Purkinje neurons. Purkinje neurons were calbindin-positive and made up ~2% of the cerebellar neuron culture. Granule neuron survival was dependent on proximity to ΔFADD-expressing Purkinje neurons and was inhibited by an insulin-like growth factor-I (IGF-I) receptor blocking antibody. Utilizing exogenous IGF-I, we identified the intrinsic death pathway as a principal target of IGF-I action in granule neurons. IGF-I blocked activation of both the executioner caspase-3 and the intrinsic initiator caspase-9. Upstream of caspase-9, IGF-I inhibited release of cytochrome C from mitochondria and prevented its redistribution to focal complexes localized in neuronal processes. Finally, IGF-I blocked nuclear translocation of the forkhead transcription factor, FKHRL1, and attenuated induction of its transcriptional target, the BH3-only Bcl-2 family member Bim. The results indicate that blockade of extrinsic death signaling in Purkinje neurons rescues neighboring granule neurons by sustaining the secretion of Purkinje-derived IGF-I. In turn, IGF-I exerts its neuroprotective effect in granule neurons by suppressing the intrinsic death cascade. Thus, IGF-I acts as a key intercellular mediator between cerebellar Purkinje neurons and granule neurons to promote neuron survival. *Supported by a United States Army Medical Research Grant DAMD17-99-1-9481 (K.A.H.), a Veterans Affairs Merit Award (K.A.H.), and a Veterans Affairs Research Enhancement Award Program (K.A.H. and D.A.L.).*

Keystone Symposium, Mitochondria and Pathogenesis
Copper Mountain, CO (2002)

Insulin-like Growth Factor-I Inhibits Bim Induction and the Intrinsic Death Signaling Cascade in Cerebellar Granule Neurons

Daniel A. Linseman, Reid A. Phelps, Ron J. Bouchard, Tracey A. Laessig, Shoshona S. Le, and Kim A. Heidenreich
Department of Pharmacology, University of Colorado Health Sciences Center and Denver Veterans Affairs Medical Center, Denver, Colorado 80220, USA

Cerebellar granule neurons (CGNs) die by apoptosis when deprived of serum and depolarizing potassium. Insulin-like growth factor-I (IGF-I) rescues CGNs from apoptosis, but the mechanism of IGF-I neuroprotection is unclear. In the current study, we identified the intrinsic (mitochondrial) death pathway as a principal target of IGF-I action. In CGNs undergoing apoptosis, IGF-I blocked activation of both the executioner caspase-3 and the intrinsic initiator caspase-9. Upstream of caspase-9, IGF-I inhibited release of cytochrome C from mitochondria and its redistribution to focal complexes localized in neuronal processes. IGF-I had no effect on mitochondrial swelling or membrane depolarization, but significantly attenuated induction of the pro-apoptotic Bcl-2 family member Bim. Although the transcription factor c-Jun has previously been shown to regulate Bim, IGF-I did not block c-Jun phosphorylation in trophic factor-deprived CGNs. In contrast, IGF-I significantly inhibited dephosphorylation and nuclear localization of the forkhead transcription factor, FKHRL1, previously implicated in the regulation of Bim expression in T lymphocytes. Moreover, Bim induction, cytochrome C release and caspase activation were also blocked by cycloheximide, further indicating that *de novo* synthesis of Bim is required for CGN apoptosis. Thus, IGF-I rescues CGNs from apoptosis by blocking intrinsic death signaling at the level of FKHRL1 regulation of Bim. *Supported by a VA Merit Award (K.A.H.) and a VA Research Enhancement Award Program (K.A.H. and D.A.L.).*

Please select Print from the file menu to print your Abstract.

The Endocrine Society's 84th Annual Meeting

Filename: 851395
Contact Author Maria L McClure, BS
Department/Institution: Pharmacology, University of Colorado Health Sciences Center
Address: 4200 East Ninth Ave
City/State/Zip/Country: Denver, Colorado, 80262, United States
Phone: (303) 399-8020 x4418 **Fax:** (303) 393-5271 **E-mail:** maria.mcclure@uchsc.edu

Abstract Format and Category:
Session Type : Regular Abstract Session
Presentation Type: Consider for Oral Presentation
Basic Science Category: 14. Insulin-like Growth Factors
Awards: Travel Grant Awards.
Do you consider yourself a member of one of the following U.S. underrepresented groups?
Hispanic -- Other
Is the subject matter of your abstract related to the Human Genome? No

Title: Suppression of Death Receptor Signaling in Cerebellar Purkinje Neurons Protects Neighboring Granule Neurons from Apoptosis via an IGF-I Dependent Mechanism

Maria L McClure [1]*, Daniel A Linseman [1], Ron J Bouchard [2], Tracey A Laessig [2], Ferough A Ahmadi [1] and Kim A Heidenreich [1]. [1]Pharmacology, University of Colorado Health Sciences Center, Denver, Colorado, 80262 and [2]Research, Denver Veterans Affairs Medical Center, Denver, Colorado, 80220.

Primary cerebellar granule neurons undergo apoptosis when deprived of serum and depolarizing potassium. Here, we investigated a role for death receptor signaling in cerebellar granule neuron apoptosis by expression of adenoviral AU1-tagged dominant-negative Fas-associated death domain protein (Ad-AU1-ΔFADD). Ad-AU1-ΔFADD decreased apoptosis of cerebellar granule neurons from 69±6% to 30±2% ($n=5$, $p<0.01$); however, the protection was not uniformly distributed. Immunocytochemical AU1 staining revealed that <5% of granule neurons expressed ΔFADD. In contrast, ΔFADD expression was observed in >95% of Purkinje neurons. Purkinje neurons were calbindin-positive and made up ~2% of the culture. The uneven distribution of protected granule neurons was associated with proximity to ΔFADD-expressing Purkinje cells. Both Purkinje neurons and granule neurons expressed IGF-I receptors on their cell surfaces and ΔFADD-mediated granule neuron survival was inhibited by an IGF-I receptor blocking antibody. These results indicate that blockade of death receptor signaling in Purkinje neurons rescues neighboring granule neurons that require Purkinje-derived IGF-I. The dependence of cerebellar granule neurons on Purkinje trophic support mimics that found in vivo during cerebellar development.

Keyword 1: Apoptosis
Keyword 2: Insulin-like growth factor-I (IGF-I)
Keyword 3: Cerebellum

The Endocrine Society's 84th Annual Meeting, San Francisco, CA (2002)

Insulin-like Growth Factor-I Rescues Cerebellar Granule Neurons from Apoptosis by Blocking Bim Induction and Mitochondrial Death Signaling

Daniel A. Linseman, Reid A. Phelps, Ron J. Bouchard, Tracey A. Laessig, Shoshona S. Le, and Kim A. Heidenreich
Department of Pharmacology, University of Colorado Health Sciences Center and Denver Veterans Affairs Medical Center, Denver, Colorado 80220, USA

Cerebellar granule neurons (CGNs) die by apoptosis when deprived of serum and depolarizing potassium. Insulin-like growth factor-I (IGF-I) rescues CGNs from apoptosis, but the mechanism of IGF-I neuroprotection is unclear. In the current study, we identified the intrinsic (mitochondrial) death pathway as a principal target of IGF-I action. In CGNs undergoing apoptosis, IGF-I blocked activation of both the executioner caspase-3 and the intrinsic initiator caspase-9. Upstream of caspase-9, IGF-I inhibited release of cytochrome C from mitochondria and its redistribution to focal complexes localized in neuronal processes. IGF-I had no effect on mitochondrial swelling or depolarization, but significantly attenuated induction of the pro-apoptotic Bcl-2 family member Bim. Although the transcription factor c-Jun has been shown to regulate Bim, IGF-I did not block c-Jun phosphorylation in trophic factor-deprived CGNs. In contrast, IGF-I significantly inhibited dephosphorylation and nuclear localization of the forkhead transcription factor, FKHRL1, also recently implicated in the regulation of Bim expression. Bim induction, cytochrome C release and caspase activation were also blocked by cycloheximide, suggesting that de novo synthesis of Bim is required for CGN apoptosis. We conclude that IGF-I rescues CGNs from apoptosis by blocking intrinsic death signaling at the level of FKHRL1 regulation of Bim. This work was supported by grants from the USAMRC (DAMD17-99-1-9481), NIH (NS38619-01A1) and VA (Merit Award and REAP Award) to K.A.H.

IDENTIFICATION OF AN AUTOPHAGIC DEATH PATHWAY IN CEREBELLAR PURKINJE NEURONS DOWNSTREAM OF DEATH RECEPTOR SIGNALING

M.L. McClure[1*]; D.A. Linseman[1,2]; R.J. Bouchard[2]; T.A. Laessig[2]; M.K. Meintzer[1]; S.S. Le[2]; K.A. Heidenreich[1,2]

1. Pharmacology, University of Colorado Health Sciences Center, Denver, CO, USA

2. Denver Veterans Affairs Medical Center, Denver, CO, USA

Cerebellar neuronal cultures obtained from early postnatal rats are recognized as a model system to investigate the regulation of neuronal survival and death. Cerebellar granule neurons make up ~95% of the cerebellar cell culture and undergo classical apoptosis following the removal of serum and depolarizing potassium. In contrast, Purkinje neurons, which make up 3% of the culture, die by an unknown mechanism following serum withdrawal. Here, we show that Purkinje neurons undergo autophagy in response to serum withdrawal. The Purkinje cell death was characterized morphologically by extensive cytoplasmic vacuolation and by a notable lack of nuclear condensation. The vacuoles stained with the acidic pH-sensitive dye, lysosensor blue, and monodansylcadaverine, a marker of autophagolysosomes. An inhibitor of autophagy, 3-methyladenine, blunted the vacuolation and death of Purkinje neurons. Purkinje vacuolation and death were also attenuated by overexpression of a dominant-negative Fas-associated death domain protein (dnFADD), suggesting the involvement of death receptor activation. The autophagic death of Purkinje neurons required new macromolecular synthesis but was independent of caspase activation. These results demonstrate that two interdependent neuronal populations undergo distinct mechanisms of death in response to trophic factor withdrawal. These data are the first to implicate death receptor-mediated autophagy as a potential mechanism of neurodegeneration.

ROTENONE INDUCES DEATH OF PRIMARY DOPAMINE NEURONS BY A CASPASE-DEPENDENT MECHANISM

F.A. Ahmadi[1,3*]; D. Linseman[2,4]; R. Bouchard[2,4]; S. Jones[1]; C.R. Freed[1,2,3]; K.A. Heidenreich[2,3,4]; W.M. Zawada[1,3]

1. Clin Pharmacol, 2. Pharmacol, 3. Neuroscience Program, Univ Colorado Hlth Sci Ctr , Denver, CO, USA

4. VA Hospital, Denver, CO, USA

In rats, pesticide rotenone induces degeneration of dopamine neurons and parkinsonian-like pathology. To understand the mechanism of rotenone-induced toxicity in dopamine neurons, we have established an in vitro model in the primary ventral mesencephalic (VM) cultures from E15 rats. After 11 hrs of exposure to 30nM rotenone, the number of dopamine neurons identified by tyrosine hydroxylase Ab (TH+) declined rapidly with only 23% of the neurons surviving. By contrast, 73% of total cells survived rotenone treatment indicating that TH+ neurons are more sensitive to rotenone. Rotenone's inhibition of mitochondrial complex I reduced ATP levels by 64% (10nM) and 77% (30nM). The more severe loss of ATP induced by 30nM rotenone correlated with a 159% increase in propidium iodide (PI) staining of the VM cells, predicting raise in necrotic cell death. By contrast, 10nM rotenone, which induced a less severe ATP loss, had no effect on PI staining. To examine the role of apoptosis in TH+ neuron death, cultures were stained with Hoechst DNA dye. At 3 and 10nM rotenone, the number of TH+ neurons with apoptotic morphology increased by 26% and 38%, respectively and correlated with a raise in active caspase-3 immunostaining inside TH+ neurons. Increasing the ATP levels with glucose and creatine or caspase inhibition with YVAD-CMK rescued a subset of TH+ neurons from rotenone-induced death. Our results demonstrate that rotenone at low concentrations induces caspase-3 mediated apoptosis, while necrosis becomes an important cell death mechanism at high concentrations of this pesticide.

Supported by: NS39105, NS48711

Ca^{2+}/calmodulin-dependent protein kinase II promotes neuronal survival by inhibiting HDAC repression of MEF2D

Daniel A. Linseman, Christopher M. Bartley, Mary Kay Meintzer, Shoshona S. Le, Tracey A. Laessig, Ron J. Bouchard, and Kim A. Heidenreich

Department of Pharmacology, University of Colorado Health Sciences Center and the Denver Veterans Affairs Medical Center, Denver, Colorado 80220

Ca^{2+}/calmodulin-dependent protein kinase II (CaMKII) function is required for synaptic plasticity and activity-dependent neuronal survival, but the mechanism underlying its neuroprotective effects is unclear. Here, we investigate the effects of CaMKII on the survival of primary cerebellar granule neurons. Granule neuron survival depends on the activity of myocyte enhancer factor 2D (MEF2D), a transcription factor that is regulated in a Ca^{2+}-dependent manner. Induction of granule neuron apoptosis by removal of depolarizing potassium induced rapid cytoplasm-to-nuclear translocation of the MEF2 repressor, histone deacetylase 5 (HDAC5). This effect was mimicked by addition of the CaMK inhibitor KN93, consistent with a mechanism by which CaMK phosphorylation of HDAC5 prevents its nuclear localization. Induction of HDAC5 nuclear translocation by KN93 was associated with a marked loss of MEF2-dependent transcriptional activity, activation of caspase-3, and chromatin condensation and fragmentation. As an alternative approach to selectively decrease CaMKII activity, granule neurons were incubated with a fluorescein-labeled, phosphorothioate antisense oligonucleotide to CaMKIIα. Antisense to CaMKIIα decreased CaMKII protein expression and induced shuttling of HDAC5 to the nucleus. The antisense also induced caspase-3 activation and apoptosis, whereas a missense control oligonucleotide had no effect on neuronal survival. These results suggest that CaMKII promotes the activity-dependent survival of cerebellar granule neurons by preventing HDAC5 localization to the nucleus. In this manner, CaMKII sustains the activity of MEF2D by blocking HDAC-mediated repression of this critical pro-survival transcription factor.

Supported by a VA merit award (KAH), a VA research enhancement award program (DAL and KAH), and (in part) by research grants from the NCI Cancer Education Grant R25 CA49981 and the ACS Colorado Division, Brooks Trust (CMB).